Development and Characterisation of a Colorimetric Binding Phase for the Diffusive Gradients in Thin Films Technique

Russell William McGifford

B.Sc. (Hons)

Submitted in fulfilment of the requirements

for the Degree of

Doctor of Philosophy

University of Tasmania

July, 2011

Declaration

This thesis contains no material which has been accepted for a degree or diploma by the University or any other institution, except by way of background information and duly acknowledged in the thesis, and to the best of the my knowledge and belief no material previously published or written by another person except where due acknowledgement is made in the text of the thesis, nor does the thesis contain any material that infringes copyright.

Russell William McGifford

November, 2010

Authority of Access

Russell William McGifford

November, 2010

Abstract

Passive sampling is a useful method for contaminant analysis and monitoring, and of the techniques available the Diffusive Gradients in Thin Films (DGT) technique is particularly applicable for use in transition metal studies. However, analysis of the metal-accumulating DGT 'binding phase' is typically expensive and time-consuming, which limits the technique's application. In order to improve on the cost and speed of analysis, and to allow in-field analysis, a colorimetric binding phase was developed. By employing metallochromic reagents adsorbed onto ion-exchange resins a colour change was obtained as a result of the binding of metal ions, with the degree of change being proportional to the quantity of complexed metal. This reagent-adsorbed resin was immobilised on adhesive paper labels to provide a robust, cheap and effective colorimetric binding phase.

Quantification of metal loading on these binding phases was undertaken through use of UV-Vis reflectance or Computer Imaging Densitometry (CID), the latter employing a flat-bed scanner for improved ease of analysis. Analytically robust metal quantification was found to be achievable using these methods, with the CID method equivalent in performance to the reflectance method. The use of a variety of metallochromic reagents was explored, with different reagents noted to provide colorimetric responses for different metal ions.

A typical detection limit, provided by Methylthymol Blue adsorbed to Dowex 1x8 resin, was 10 ng Cu(II) per cm^{-2} of disc area. Linear response was seen up to a

stoichiometrically defined metal loading, typically providing a linear response from the detection limit to 2 μg of Cu(II) per cm^{-2}. Selectivity was reagent dependant, in particular Zincon was seen to provide a selective response to Cu(II) at neutral pHs and is a promising candidate for deployment of these colorimetric DGT binding phases.

Acknowledgements

The author would like to acknowledge the help and assistance provided by the following people and groups;

Dr. Andrew Seen for his invaluable assistance, guidance and patience throughout the length of the project. Andrew's supervision has allowed me enough room to plumb the depths of research. The understanding and knowledge of how to perform research and run a project has been, personally, far more valuable than the content of the reasrch itself, and Andrew's supervision style has allowed me to fully explore the nooks and crannies therein. Combined with a sharp eye for detail which has given (some would say hammered in!) me appreciation for the necessity of careful work, from planning to reporting results, and the benefits of precise work, Andrew's help has been genuinely appreciated. My sincere thanks!

Prof. Don McWilliams' help for his assistance during the initial studies into C18 immobilisation during my brief foray into organic synthesis.

Assoc/Prof. Dominic Geraghty for the use of, and guidance with, the microscope photography suite.

Prof. Paul Haddad and Prof. Pavel Nesterenko for their tuition and assistance, particularly with the dye studies involved in the project. Prof. Haddad's assistance with the thesis was invaluable, as was his extensive research experience for early guidance. Prof. Nesterenko's depth of knowledge on the colorimetric agents involved in this work were a terrific boon.

Ms. Tahlia Watts for her assistance in the laboratory during the end of 2009 and for the invaluable help since then. Words could never be thanks enough.

The staff and students of UTas' Newnham Chemistry department, particularly Mr. Barclay Sayer and Mrs. Kym Knights, for support and coping with hundreds of small requests at the worst times without complaint.

The staff and students at the Australian Centre for Research on Separation Science and the School of Chemistry in Sandy Bay for their support and feedback. Thanks for making me feel welcome in Hobart regardless of the time since the last visit, it still felt like coming home in many ways.

Lastly, thanks must be given for the support from DEH/Australian Antarctic Science for funding used during this research (Project number 2665).

Glossary and Abbreviations

AAS – *Atomic Absorption Spectroscopy*

ANZECC – The *Australian and New Zealand Environment Conservation Council*

APDTC – Ammonium pyrrolidine dithiocarbamate

ARMCANZ – The *Agriculture and Resource Management Council of Australia and New Zealand*

BPhen – Bathophenanthroline

CAS – *Chrome azurol S*

Chelex 100 – A transition-metal chelating resin that is commercially available and widely used in typical DGT deployments.

Channel – Either the red (R), green (G) or blue (B) colour of a single pixel when an image is scanned.

Chromogenic Chelating Agent – a colorimetric reagent with the ability to strongly bind metal analytes.

CID – *Computer Imaging Densitometry*, a technique where colour density is measured through the use of imaging software and a luminosity scale.

Colorimetric Reagent – A compound capable of providing a colour change on interaction with an analyte of interest, particularly a divalent metal cation. Includes 'Chromogenic Chelating Agents'.

DeDTC – Diethyl dithiocarbamate

DGT – *Diffusive Gradients in Thin Films*, a passive sampling technique where analyte is collected in a binding phase and the rate of analyte collection is controlled by the use of a known diffusion distance and the analyte's coefficient of diffusion.

Disc – a circular piece of paper label, typically 1 inch in diameter.

DMG – *Dimethyl glyoxime*

DPCI – *Diphenyl carbazide*

DPCO – *Diphenyl carbazone*

DT - *Dithizone*

DTC - *Dithiocarbamate*

Dye – A shorthand notation for an Indicator dye, sim. 'Colorimetric Reagent'.

EBT – *Eriochrome black T*

Equilibration – the process of exposing a resin-dye to the solution matrix providing the associated resin swelling.

Immobilisation – the process of confining a dye or resin such that it is held stationary with regards to physical movement and diffusion.

LED – *Light Emitting Diode*

Loading – quantity of dye on resin, or metal on resin-dye, expressed as μmol g^{-1} or μg cm^{-2}, respectively.

Matrix – The chemical compound of which a resin is made, with consideration of the cross-linking and porosity properties.

MTB – *Methylthymol blue*, an indicator dye.

MTB(2) and MTB(10) – referring to Dowex 1x8 with MTB adsorbed from dye solutions buffered to pH 2 and 10, respectively.

NATA – The *National Association of Testing Authorities*, Australia

oCPC – *ortho-cresolphthaline complexone*

PAN – *1-(2-pyridylazo)-naphthol*

PCV – *Pyrocatechol violet*

PSDVB – *Polystyrene divinylbenzene*, a typical resin substrate (matrix).

Resin-disc – disc with resin adhered.

Resin-dye – Shorthand for a resin-adosrbed dye.

RSD – *Relative Standard Deviation*, one standard deviation expressed as a percentage of the value it is associated with.

Scanner – Refers to a commercially available flat-bed document scanner.

TAN – *1-(2-thiazolylazo)-2-naphthol*

UHQ – *Ultra-High Quality water*, resistivity of 18 ± 1 MΩ cm.

XO – *Xylenol orange*

Table of Contents

Synopsis and Direction – More Simple Metal Monitoring

As living beings our interactions with the world around us are our life, and our waste can have negative impacts on the world and, therefore, ourselves. In *Cradle to Cradle* Braungart and McDonough [1] discuss the waste produced as a result of the industrialisation of the world we live in, and its impact on ourselves. Of this waste, a portion causes further damage when released beyond its source – into the greater world, generally referred to as the 'environment'. Stopping the release of this damaging waste is a key priority for developed countries, however it is no easy task to find the damaging components of this waste; let alone stop the production of them. The extent of this waste is hinted at in the 1970 Report of the Study of Critical Environmental Problems (SCEP) [2], which in the space of a single month compiled more than 300 pages concisely detailing known issues and recommendations for the monitoring and control of these issues. This was done in order to prevent significant damage to industries, populations, and the environment at large. Since this time many issues have expanded further; for example climate change, which is given a total of 10 pages in the SCEP report but is currently the focus of significant world-wide study, as evidenced by the 4th Intergovernmental Panel on Climate Change report of 2007 [3].

The SCEP report highlighted many significant issues and, nearly forty years later, many of these are still of concern. As outlined in the 1972 Stockholm Declaration [4], the presence of harmful substances is of major concern to the quality of the environment, which is in turn of major concern for the quality of human life. Large

quantities of potentially harmful substances exist in the modern environment ('contamination'), many from anthropogenic sources, and the release of these substances continues. Preventing these substances from reaching a level in which significant harm can be inflicted ('pollution') requires the monitoring of areas at risk. Prevention, however, has not always been successful, and in polluted areas remediation must be performed accompanied by monitoring to ensure recovery. Monitoring is therefore a key element in prevention and remediation, and an essential part of the monitoring process is the representative sampling of the environment to enable quantification of these contaminating substances [2].

1.1 – Monitoring Contaminant Concentrations

Sampling processes are complicated by the variable nature of the environment and the wide variety of contaminants potentially present. Aerial, waterborne, and solid contaminants all pose separate sampling challenges, and the variation within each of these environmental phases poses yet more complications, with the impact of pollutants on the biota itself the final point of concern [5]. Water poses a key monitoring phase, both due to its ubiquity in the environment and its role as the primary interface between the biota and the environment [6]. As such, the sampling of water is of utmost importance for monitoring contaminants and managing the effects they have on the environment.

Current water sampling techniques are mostly based on removing physical water samples from the environment for analysis, either through manual 'grab' sampling or auto sampling. In both cases the collected sample is typically taken to a

laboratory and analysed there, using the appropriate technique for the analyte of interest. This technique provides, at best, a measure of the analyte's concentration in the sampled water at the time of analysis [7]. At issue here is that the concentration of most analytes in the water body will fluctuate temporally depending on natural occurrences, such as periods of heavy rain [8], or from intermittent human activities, such as herbicide application [9]. Obtaining a representative sample can therefore be difficult, and while auto (grab) samplers provide a reasonable solution to acquiring samples over an extended period of time their expense and reliability limit their application, plus processing the samples required for the necessary temporal resolution adds significant expense.

In addition to issues with collecting representative samples, current sampling techniques do not provide expedient answers, and their accuracy can be heavily affected by handling techniques. Guidelines have been developed in many countries to minimise these affects by standardised sample handling techniques, such as the ANZECC (Australian and New Zealand Environment and Conservation Council) water quality guidelines [10]. However application of the guidelines may be difficult, and in situations with large times between sampling and analysis, such as remote sampling in Antarctica, application of the guidelines may not be possible.

As well as these problems, laboratory handling and analysis pose further issues. Time consuming laboratory standardisation may be required via inter-laboratory comparison of results, for instance NATA (National Association of Testing Authorities) accreditation and inter-laboratory studies [11], along with the use of standard analyte-specific methods, representative sample standards, and guidelines.

Thus the multiple steps in sample collection, storage, and analysis result in a significant amount of time expended, with the potential for significant financial cost in order to obtain results for a single, small portion of a water body at an instant in time. This expense can result in the abandonment of monitoring programs, or more likely programs not being adopted in the first place.

1.2 - Passive Sampling

The issues associated with grab sampling and handling of samples have resulted in work on developing alternative methods for environmental sampling. Passive sampling has been one of the more important technologies to have come out of this work, and currently provides a variety of methods for sampling organic and inorganic contaminants [13]. A passive sampling device is placed in the environment and accumulates analyte, based on the interaction of the bulk solution with the collection medium of the device. Research on water-based passive sampling has grown substantially since 1987, with nearly 50 journal publications a year as of 2005 [7]. Two general sampling regimes determine analyte uptake in passive samplers, equilibrium-based and kinetic-based passive samplers [7]. Equilibrium-based samplers rely on the partitioning of analytes into a collecting medium, the extent of which is determined by the partition coefficient of the analyte between the collecting medium and bulk solution. The ability of analyte to penetrate the membrane containing the medium provides some selectivity. Ultimately equilibrium is obtained between the collecting medium and bulk solution, and the collecting

medium is removed and analysed [12]. Kinetic samplers typically contain a solid or liquid sorbent for analyte collection with highly favourable thermodynamics for analyte collection, and use a known diffusion distance to maintain the analyte collection rate as proportional to solution concentration [7]. The second method, therefore, provides accumulation of analytes, while allowing for the rate of accumulation to be controlled proportional to the bulk concentration.

Under the kinetic regime a passive sampler provides the time-weighted average concentration of that analyte in the sampled environment, over the sampling period. An advantage of kinetic based passive sampling is *in-situ* preconcentration of the analyte, improving the detection limit of the method used for analysis. When a non-polar organic phase is used, such as a C18 derivitised membrane or oil, organic analyte preconcentration can be readily achieved [13]. In the case of inorganic sampling this can be achieved but a smaller range of mediums are available. It is typically achieved with a solid chelating resin such as Chelex 100 [7]. With the analyte collection rate controlled by diffusion from the bulk solution, through a diffusive medium with similar properties to the solution, calculation of the analyte's time-weighted average concentration can be achieved. Of these techniques, one of the more flexible and accurate ones for aqueous metal sampling is the Diffusive Gradients in Thin-Films technique [14].

The Diffusive Gradients in Thin-films (DGT, schematic representation shown in Figure 1.1) technique is a diffusion-based inorganic sampling method [15]. It uses a polyacrylamide gel providing similar analyte diffusion coefficients to water (see [17]), and collection of analytes in a Chelex 100 'binding phase' which readily accumulates trace metal cations, especially transition metals [18].

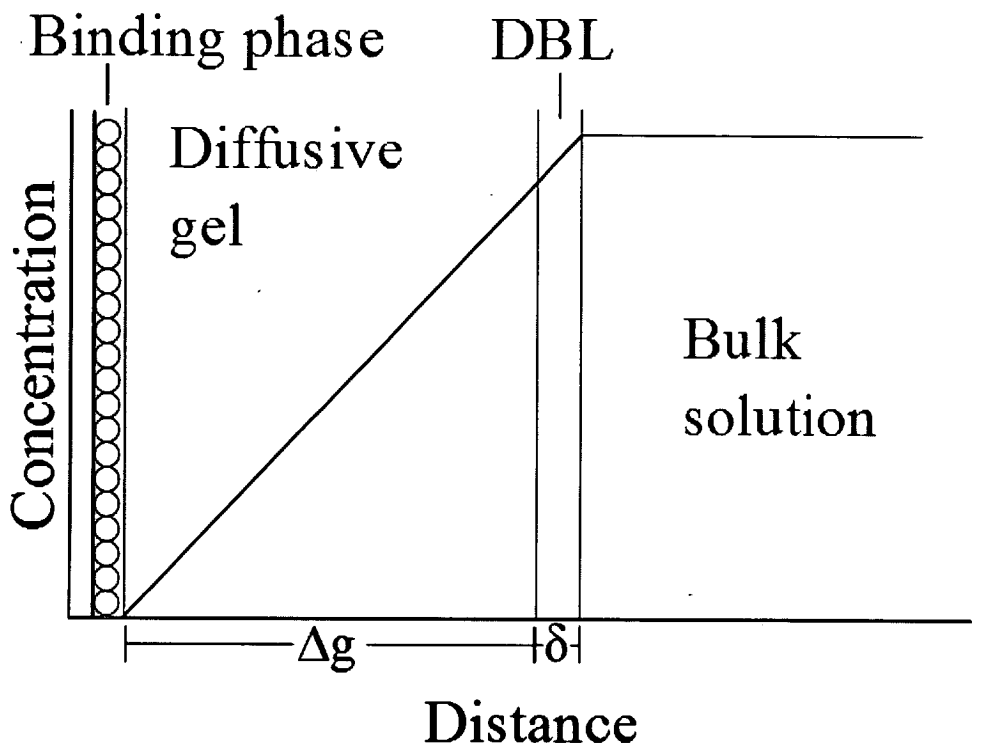

Figure 1.1 – A schematic representation of DGT theory and device structure adapted from [16]. Used with permission from Macmillan Publishers Ltd: NATURE [15], copyright 1994.

Since the metal uptake into the binding phase is driven by the analyte concentration gradient across the polyacrylamide diffusive gel, and with the metal being bound by the binding phase such that the metal ion concentration in solution at the binding phase is effectively zero, the concentration of the analyte in the bulk solution (C_b) can be determined according to the DGT equation [19];

$$C_b = \frac{M.\Delta g}{D.a.t}$$

where M is the mass accumulated in the binding phase, Δg is the thickness of the diffusion layer, D the analyte-specific diffusion coefficient, a the sampling window area and t the time of sampler deployment. This equation is derived from Fick's first law of diffusion [15]. Accordingly, deployment of the device results in a metal loading proportional to both solution concentration and deployment time.

The use of a metal chelating resin as a binding phase results in a deployment device that readily preconcentrates metal analytes, requiring only extraction for analysis [19]. This preconcentration ability allows for short deployment times to accumulate detectable quantities of analytes from solutions of relatively low concentration, for instance it is possible to detect some analytes in pmol L^{-1} solutions after deployments of a single day [7].

The DGT sampling method has been used for a number of marine [20,21], fresh [22,23] and sediment or soil pore-water [24,25] studies of labile metal contaminants, as well as more exotic matrices such as acid mine drainage [26]. The DGT methods can also be used to provide some indication of the bio-available fraction of metals [27], which is difficult to achieve with other methods (see page 78, [28]).

1.3 – Colorimetric Application

The use of Chelex 100 resin, as is typical for DGT, still necessitates that the sampler be stored and transported to a laboratory, and then extracted for analysis, with the associated expenses and time delays. If it were possible to avoid the extraction step and obtain a result directly from the binding phase these costs and delays would be alleviated, as well as removing the potential for error introduced by storage and

extraction. The design of a binding phase which produces a colour change on metal adsorption, and which is proportional to the amount of metal adsorbed, would enable quantification by examination of the binding phase using photometric techniques, or even by comparing to a colour chart. This has been shown in passive sampling for sulfide and iron(II) [29,30], although the iron(II) technique used required post-deployment chemical processing. If colour change could be obtained *in-situ*, post-deployment laboratory work would be essentially removed.

A current commercial example of this is the Merckoquant® Test Strips, which provide measurement of a selection of common inorganic ions through the use of 'dip sticks', in which colour intensity is dependent on analyte concentration. When combined with a hand-held reflectance spectrophotometer, accurate results can be obtained to low mg L^{-1} levels [31]. A combination of this type of technique with DGT's preconcentration ability has the potential to significantly improve detection limits and to allow accurate in-field analysis of time-weighted average metal concentrations, without the expense and time involved in laboratory analysis.

A colorimetric technique would also involve a further change to the general DGT system, in that metal response would be largely dye-specific. This is similar to the application of DGT samplers for sampling sulfide, where sulfide reacts with impregnated AgI to provide a colour change selective for sulfur species [30]. A wide variety of colour-responding metal dyes is available, as discussed in the essential *Handbook of Organic Analytical Reagents* [32], most of which show colour response to only a few metals. For instance bathophenanthroline may be employed for its well-known coloured Fe(II) and Cu(I) reaction, or dimethyl glyoxime's coloured Ni(II), Pd(II) and Pt(II) reactions could be of use. In this manner the

selection of metal-specific dyes may allow the development of specific binding phases.

This would, however, require analytes of interest to be known before hand, and that the dyes deployed are chosen to suit those analytes. While this limits the device's use for exploratory studies, in a monitoring situation it provides an easier method for collecting the relevant data. A colorimetric system would allow immediate visual confirmation of bound metals, avoiding the costly removal, extraction and analysis of samplers yet to accumulate sufficient metal to reach their limit of detection. As well as this, any system for quantifying colour change or intensity allows for a quantitative metal response to be obtained. Commercially available hand-held reflectance spectrophotometers, scanners, digital cameras, or even a comparative colour chart, may therefore give simple and quick metal quantification. Quantification would be available within hours of sampler removal rather than taking days to weeks, avoiding the need for storage and associated issues, as well as extraction and expensive instrumentation. A further advantage of such a system would be that a deployed sampler could be analysed periodically to provide a temporal profile of metal uptake into the DGT sampler. An analyte-specific binding phase would also minimise the remote chance of a binding phase becoming saturated with non-analyte metal species to the exclusion of the analyte itself.

1.4 – Study summary

The aim of this study was to immobilise a colorimetric agent for specific metal species onto a solid substrate, and to use this device as a DGT binding phase.

Primary objectives were the finding of a suitable method for retaining a colorimetric agent; testing of a prototype system utilising a colorimetric agent; and finally expanding the system to a range of dyes in order to explore the potential for selectivity and expand the analyte range.

Retaining a colorimetric agent was considered achievable and a variety of methods were available in literature (Chapter 2). Further to this, immobilised colorimetric agents have been explored in the past as a method to improve UV-Vis spectrophotometry sensitivity, where the adsorption of the reagent onto a solid surface had significantly improved analytical sensitivity [33]. The use of immobilised, non-colorimetric, chelating agents has also been studied in depth (see [34,35]) leading to current uses, such as that of chelation ion chromatography [36]. This range of potential metal chelating agents allows for flexibility in the application of the overall sampler design, but for the purposes of this project a more focused method was needed. The potential methods that could be used to develop this device were examined under the criteria of: metal binding capacity of the immobilised dye; the suitability of the solid substrate as a DGT binding phase; the method of analysis; and the interaction of the binding phase with water and the analyte metal(s).

To this end it was found that the immobilisation of colorimetric chelating agents, referred to synonymously as 'dyes', was the most practical method. Indeed, the adsorption of these dyes onto a stable matrix of high surface area allows for a physically robust colorimetric material. Immobilisation of the resin was then achieved in an inexpensive fashion to provide a stable and useable sampling device that could be easily integrated into the DGT system.

Once immobilised and formed into a suitable binding phase a single dye (methylthymol blue), seen to be promising in preliminary trials, was tested both for DGT sampler functionality, in terms of metal uptake in relation to time and bulk concentration, and to assess whether metal loadings were quantifiable by colour response (Chapter 3). Visibly responding binding phases for use in DGT have been reported for sulfide measurement [30], as have metal-selective binding phases [37,38], with success. For sulfide, Davison et al. [30] developed a binding phase with immobilised AgI, providing a colour change proportional to Ag_2S, and quantified the grayscale change with a desktop scanner. For this study it was proposed that UV-Vis reflectance would be used as a primary analysis technique, and the coloured response obtained from a desktop scanner would also be assessed due to its potential to provide an easier and less expensive method of analysis.

This use of a desktop scanner proved to be an effective and inexpensive alternative to UV-Vis reflectance measurement, with comparable analytical properties seen in the two methods (Chapter 4). Some limitations were observed with scanner use, however a wide range of dyes were still seen to be useable. The relative ease of use and cost of the desktop scanner system meant that it was considered the method of choice.

Once the basic methods for dye immobilisation, DGT function assessment, and analysis were determined with a single dye, the method was extended to explore other dyes (Chapter 5). The wealth of information available on colorimetric chelating agents allows the selection of potential dyes, and many are commercially available. However most dyes require, at minimum, pH buffering for correct function [32] and, therefore, these novel dye-adsorbed binding phases need to be

tested for function under environmental conditions. In order to do this a testing regime was established allowing the rapid quantification of dye response and metal loading. This process has enabled the selection of several metal-specific immobilised dyes providing colorimetric quantification of metal loadings, with a focus on use as a DGT binding phase.

References

[1] W. McDonough, M. Braungart, Cradle to Cradle: Remaking the Way We Make Things, North Point Press, San Fransisco, 2002.

[2] C.L. Wilson, W.H. Matthews, et al., Man's Impact on the Global Environment. Massachusetts Institute of Technology. 1970.

[3] IPCC, Contribution of Working Groups I, II and III to the Fourth Assessment Report of the Intergovernmental Panel on Climate Change. IPCC. 2007.

[4] UNEP, United Nations Conference on the Human Environment, Stockholm, 1972.

[5] D.W. Connell, G.J. Miller, Chemistry and Ecotoxicology of Pollution, John Wiley & Sons, Inc., New York, 1984.

[6] R. Haque, J. Falco, S. Cohen, C. Riordan, in: R. Haque (Ed.), Dynamics, Exposure and Hazard Assessment of Toxic Chemicals, Ann Arbor Science, Ann Arbor, 1980, p. 47.

[7] B. Vrana, et al., Trends in Analytical Chemistry, 24 (2005) 845.

[8] M.C. Gromaire-Mertz, S. Garnaud, A. Gonzalez, G. Chebbo, Water Science & Technology, 39 (1999) 1.

[9] W.A. Battaglin, E.T. Furlong, M.R. Burkhardt, Concentration of Selected Sulphonylurea, Sulphonamide, and Imidazolinone Herbicides, Other Pesticides, and Nutrients in 71 Streams, 5 Reservoir Outflows, and 25 Wells in the Midwestern United States, 1998. U.S. Geological Survey. 2001.

[10] ANZECC and ARMCANZ, Australian and New Zealand guidelines for fresh and marine water quality. Australian and Newzealand Environmental and Conservation Council/Agriculture and Resource Management Council of Anustralian and New Zealand. 2000.

[11] J. Begerow, M. Turfeld, L. Dunemann, Journal of Analytical Atomic Spectrometry, 15 (2000) 347.

[12] P. Mayer, J. Tolls, J.L.M. Hermens, D. Mackay, Environmental Science and Technology, 37 (2003) 185A.

[13] T. Gorecki, J. Namiesnik, Trends in Analytical Chemistry, 21 (2002) 276.

[14] L. Sigg, F. Black, J. Buffle, J. Cao, R. Cleven, W. Davison, J. Galceran, P. Gunkel, E. Kalis, D. Kistler, M. Martin, S. Noel, Y. Nur, N. Odzak, J. Puy, W. van Riemsdjik, E. Temminghoff, M.-L. Tercier-Waeber, S. Toepperwien, R.M. Town, E. Unsworth, K.W. Warnken, L. Weng, H. Xue, H. Zhao, Environmental Science and Technology, 40 (2006) 1934.

[15] W. Davison, H. Zhang, Nature, 367 (1994) 546.

[16] DGT Research, DGT –for measurements in waters, soils and sediments. 2003.

[17] B.L. Larner, A.J. Seen, Analytica Chimica Acta, 539 (2005) 349.

[18] B. McDuffie, P. Figura, Analytical Chemistry, 49 (1977) 1950.

[19] H. Zhang, W. Davison, Analytical Chemistry, 67 (1995) 3391.

[20] M.R. Twiss, J.W. Moffett, Environmental Science and Technology, 36 (2002) 1061.

[21] L. Giusti, H. Zhang, Envionmental Geochemistry and Health, 24 (2002) 47.

[22] K.W. Warnken, Davison, W., Zhang, H., Galceran, J. and Puy, J., Environmental Science and Technology, 41 (2007) 3179–3185.

[23] M. Leermakers, Y. Gao, C. Gabelle, S. Lojen, B. Ouddane, M. Wartel, W. Baeyens, Water, Air and Soil Pollution, 166 (2005) 265.

[24] H. Zhang, F.-J. Zhao, B. Sun, W. Davison, S.P. McGrath, Environmental Science and Technology, 35 (2001) 2602.

[25] H. Zhang, W. Davison, A.M. Tye, N.M.J. Crout, S.D. Young, Environmental Toxicology and Chemistry, 25 (2006) 664.

[26] J. Sondergaard, Analytical Chemistry, 79 (2007) 6419.

[27] M. Camusso, A. Gasparella, Societa Chimica Italiana, 96 (2006).

[28] D.C. Adriano, Trace elements in terrestrial environments: biogeochemistry, bioavailability and risks of metals, Springer, 2001.

[29] D. Jezequel, et al., Estuarine, Coastal and Shelf Science, 72 (2007) 420.

[30] P.R. Teasdale, S. Hayward, W. Davison, Analytical Chemistry, 71 (1999) 2186.

[31] R. Wetselaar, G.D. Smith, J.F. Angus, Communications in Soil Science and Plant Analysis, 29 (1998) 729.

[32] K. Ueno, T. Inamura, K.L. Cheng, Handbook of Organic Analytical Reagents, CRC Press, 1992.

[33] K. Yoshimura, H. Waki, S. Ohashi, Talanta, 23 (1976) 448.

[34] M.L. Marina, V. Gonzalez, A.R. Rodriguez, Mircochemical Journal, 33 (1986) 275.

[35] D. Bilba, D. Bejan, L. Tofan, Croatia Chemica Acta, 71 (1998) 155.

[36] P.N. Nesterenko, P. Jones, Journal of Separation Science, 30 (2007) 1773.

[37] J.M. Pates, M.A. French, H. Zhang, S.E. Bryan, R.C. Wilson, Analytical Chemistry, 77 (2005) 135.

[38] P. Divis, M. Leermakers, H. Docekalova, Y. Gao, Analytical and Bioanalytical Chemistry, 382 (2005) 1715.

Chapter 2

Colorimetric Reagent Immobilisation Methods

Creating the binding phase

2.1 – A Review of Established Colorimetric Reagent Immobilisation Methods

2.1.1 - Rationale

In order to develop a colorimetric DGT technique it is necessary that a method is found to provide a color change upon exposure to metal analytes. From this point the remaining features of the technique can be developed, but the color method will be at the core of the process. In the DGT technique the binding phase is responsible for accumulation of metal ions and therefore is responsible for the final chemical interaction with analytes before extraction. Considering this, altering the binding phase to not only bind metal ions specifically and strongly but to also provide a colorimetric response would provide an effective method for colored metal interaction and could be easily incorporated into the DGT technique. Colorimetric binding phases would therefore entail a method for strongly binding metal analytes, and a method for providing a color change in response to analyte quantities. Ideally, this would involve reagents capable of these interactions immobilised on a solid, robust substrate to provide chemical stability and reliability in use.

Reagents providing these color properties do exist as a wealth of chromogenic chelating agents, many are highlighted by Ueno et al. in the *Handbook of Organic Analytical Reagents* [1]. For instance, the well-known reaction of bathophenanthroline with Fe(II) or Cu(I) may be employed. Other established chromogenic chelating reagents are potentially suitable, such as the transition metal-sensitive dye xylenol orange. The typical use of these reagents, referred to here-on

as 'dyes', is as a metal indicator for wet chemistry techniques, or as a colorimetric spot test for relatively high metal concentrations, typically in the high mg L^{-1} range. As such, the novelty in applying these dyes to DGT deployment is in the method used for the immobilisation of a suitable chromogenic chelating agent.

While dye-based colorimetric spot tests for a variety of analytes have long been common place, methods for improving these tests have been largely neglected in favour of alternative analytical techniques. Modern chromatographic techniques or methods such as inductively coupled plasma, combined with sensitive detection such as mass spectrometry, allow substantially more precise quantification of samples and markedly lower detection limits than visual colorimetric methods. However, these techniques require a substantially larger investment of time and resources, therefore reducing the number of analyses that can be performed under any given budget. For this reason, some research is still performed on colorimetric techniques with relatively simple detection, such as visual observation or UV-Vis spectroscopy. An aim of this project is, therefore, to lower the detection limits of these colorimetric techniques. As there is a pre-concentrating effect with DGT use this should be readily achieved.

A further important characteristic of the binding phase is the capacity for metal ion accumulation, as the DGT binding phase must act as an 'infinite sink'. In short, this means that for correct function it must be possible for the analyte to be accumulated regardless of the amount already accumulated [2]. In practice, limits are set with the typical Chelex 100 binding phases, though they are large enough that they are not typically constraining. In the system hypothesised here, the amount of immobilised dye would determine the metal binding capacity as metal-to-dye interactions would

be expected to be stoichiometric [3]. The use of an immobilised dye system would, therefore, also have an upper limit to the amount of analyte that could be accumulated. This would subsequently lead to an upper limit on the assessable analyte solution concentration.

Ease of fabrication and the cost of the binding phase medium are also of concern in that they make the technique more accessible when compared to conventional techniques, such as current DGT use, but these are secondary to other functional concerns. Chemical stability of the adsorbed dye will be of paramount importance because colorimetric quantification will be dependent on the consistency of the dye response. This is particularly important as the deployment times of a DGT sampler are rarely less than 24 h and, therefore, ample time would be provided for dye loss and degradation. The main additional factors to consider were the robustness of the dye immobilisation method, the cost of the binding phase medium and the ease of fabricating the binding phase into a suitable form. A review of methods employing chelating reagents is undertaken below.

2.1.2 – Reagent Immobilisation

Over the last five decades colorimetric techniques have been largely replaced with direct physical methods such as inductively coupled plasma combined with emission/absorbance spectrophotometry or mass spectrometry. As discussed earlier, these are preferred over colorimetric techniques due to the greater sensitivities and lower detection limits provided. In some situations, though, metal-specific reagents

are still of use. In order to make use of these reagents it is typically necessary to immobilise the reagent, which can be achieved through a variety of techniques.

A wealth of metal-specific chelating agents have been developed and applied to ion-selective electrode (ISE) membranes, where immobilisation is provided through containment in a membrane [4-8]. These reagents can provide highly specific metal interactions, and due to these interactions, only the analyte of interest is able to cross the membrane. However, for ISE, rapid exchange is necessary to allow the analyte to move from the solution, to a complex with the selective reagent, and then on to the inner electrode solution. As such, a strong, permanent binding of the analyte to the reagent was not a property of these chelating agents, and this property is of particular importance for DGT. However, this technique has been modified for use in PVC membranes by placing a proton sensitive chromoionophore along with a metal-selective ionophore, to produce the sensing portion of an optode [9]. While this technique was quite sensitive for lead [5], and could be adapted to a DGT binding phase, the chromoionophores used are quite expensive. Further to this, it was required that the ionic strength and pH be carefully controlled for correct function and this is not easily achievable in natural waters. This last detail in particularly makes ISE-like membranes difficult to apply to environmental DGT situations, otherwise the technique is colorimetric and would allow the use of strongly binding chelating agents.

Immobilisation in the manner described above, or 'capture', of the reagent could also be achieved by using water-insoluble reagents that are impregnated into the binding phase during synthesis. This method has been used for DGT by suspending water-insoluble AgI in the synthesis solution of a poly-acrylamide binding phase

[10]. In this case a layer of insoluble AgI was formed as the gel set, which upon reacting with sulfide in the sample solution caused Ag_2S to form, which is also a highly water insoluble compound. Although this technique was practical, it required that the reagent and product are both water-insoluble. This would greatly limit the colorimetric reagents that could be used with this technique, particularly as many known reagents are water soluble to at least a small degree [1].

The above techniques for immobilisation of colorimetric reagents were effective and could be applied to DGT use but they also have limitations. In order to develop an appropriate method it is necessary to consider what the final form of the device should be. The use of a robust support, or substrate, would be of advantage to DGT and environmental use. Bilba et al. [11] discuss that polymeric supports, such as polymeric resins or cellulose, make ideal substrates for reagent immobilisation and that three main methods exist to obtain immobilisation. Chemical grafting of the reagent to the support has the benefit of forming a particularly stable product, although is time-consuming and potentially expensive. Ionic interactions of the substrate with the reagent were considered to be a simpler but still stable method, and adsorption of the reagent onto the substrate was the simplest form discussed. These adsorption and ionic interaction methods were considered separately by Bilba et al. [11], but as noted by Ordemann and Walton [12] ionic interaction and adsorption typically occur concurrently when reagents such as those discussed above are immobilised using either of these methods. As polymeric substrates would be both inexpensive and physically robust these immobilisation methods are discussed in greater depth below.

2.1.3 – Chemical Grafting

Chemical grafting of the colorimetric reagent on to a fibrous polymeric support, such as cellulose, is a practical method for formation of a binding phase and has resulted in some success. For example, the commercial EXPAPIER product provide preconcentration of ionic analytes [13] using a cellulose acetate disc of 4.7 cm diameter which had been functionalised with either the chelating agent sodium 2-hydroxypropyliminodiacetate, a sulfonate group, or a quarternary ammonium ion-exchange group. In particular, the EXPAPIER product has been used to preconcentrate divalent metal cations for X-Ray fluorescence spectrometry analysis with reasonable accuracy [14]. Non-commercial cellulose applications have also been reported, such as the application of aminoalkyl-derived cellulose to the preconcentration of divalent metal cations as reported by Nakamura et al. [15], where adsorption of metal ions from mildly acidic solutions was readily achieved. Carofiglio [16] reported a potentially DGT-suitable grafting method based on the 'one-pot' synthesis of azo dyes onto a cellulose membrane. In this manner a variety of dyes can be immobilised quickly, allowing for the rapid testing of novel dyes to determine their suitability as colorimetric metal-chelators. As well as cellulose fibres, other fibres such as cotton [17] and polyacrylonitrile [18] have been used for similar applications. Indeed, any substrate which can be chemically modified is potentially of use, which greatly expands the options available for immobilisation of dyes.

Silica gel has been widely examined as a grafted chelating agent support [19-22]. This is of particular interest as silica provides a good contrast for colorimetric agents due to its strong reflectance of visible light. The grafting of chelating agents, such as 8-hydroxyquinoline, onto silica gel has allowed the selective preconcentration of metal analytes for analysis by spectroscopy techniques. In a recent study, silica gel was used to immobilise xylenol orange and the UV-Vis absorption of the silica gel solution was measured to obtain metal loadings directly [23]. This showed that silica gel could be used successfully for colorimetric metal sensing and the use of 'silochrome' gel has been reported to allow colorimetric Cu(II) and Zn(II) determination with PAN as the chelating agent [24]. However, these silica techniques do not allow for the actual fixation of the silica gel, containment was by using a chromatography column packed with the gel. As such, application to a binding phase would require a further method for fixing the silica gel, potentially by 'capture' in a material such as a poly-acrylamide hydrogel, or containment behind the diffusive layer. Glass-fibre filters are a potential solution to this, but are untested as supports in this context.

Similarly, nonporous TiO_2 has been used to provide a suitable solid substrate for grafting of chelating agents. Originally developed with electrical properties in mind, TiO_2 membranes are optically transparent above 380 nm and, as such, are excellent solid supports for colorimetric techniques [25]. TiO_2 has been used as a colorimetric substrate for a technique detecting the hydroxide radical [26], cyanide [27], oxygen [28,29] and mercury [30-32]. Titanium dioxide powder is comparable in cost to ion-exchange resins, in the order of $1 per gram during 2009, and the method for forming films that are potentially suitable for DGT binding phase use is well

understood [30]. As such TiO_2 is a promising support for the chemical grafting of dyes.

Chemical grafting of the colorimetric reagent onto a support suitable for colorimetric applications has been shown for a variety of analytes and substrates. Grafting is an intuitively stable method for colorimetric reagent immobilisation, as a covalent bond is formed between the mechanically robust substrate and the chemically active sensing species. However, chemical grafting is a time-consuming technique and requires further reagents to obtain the product, which raises the cost of grafted materials. In addition to this, the stability of grafted materials is generally not substantially higher than that of many adsorbed reagents [11]. As adsorption is a significantly simpler method for reagent immobilisation, it was thought to be a more appropriate method for obtaining inexpensive binding phases.

2.1.4 – Adsorption

Adsorption of colorimetric reagents onto a substrate has provided suitable colorimetric analyte detection such as for Hg [30]. In this case TiO_2 sensors employed a ruthenium-dye complex, adsorbed onto the TiO_2 surface, to provide a colorimetric response to Hg(II) at 600 nm. This is a promising technique but, long-term stability of the sensor was not assessed and, due to the lack of response of other divalent metal ions to the ruthenium complex, this technique has not been applied to any other analytes. Indeed, many substrates are capable of absorbing substances for colorimetric work. However, the suitability of polymeric resins for the adsorption of colorimetric reagents has been known for more than 50 years [33]. As polymeric

resins are presently employed in binding phases for DGT work, they are a proven substrate and are considered as the preferred substrate for adsorption.

As mentioned, the usefulness of polymeric resins for colorimetric work has been understood for some time. In 1976 Yoshimura et al. [34] proposed a method for providing colorimetric analysis of Cr(III), Fe(III), Cu(II) and Co(II) that was substantially more sensitive than previous aqueous colorimetric techniques through application of resins. This was achieved by adsorption of the dye-analyte mixture to an ion-exchange resin. In this way the colored complex was concentrated on the surface of and, to a lesser extent, within the resin beads. Using UV-Vis absorption spectrophotometry sensitivity was improved by 1 to 3 orders of magnitude over direct measurement of dye-metal solutions. This improvement was all the more significant as the resin method required the use of one tenth the path length typically used for aqueous studies and, therefore, was effectively a further order of magnitude more sensitive than the direct results indicate. This was improved upon over the following decade with new dyes and resins allowing an expansion of the range of analytes to which this method can be applied [35,36].

As adsorption is a promising technique it is worth discussing the method of colorimetric reagent adsorption as understood in the literature. Ordemann and Walton showed that as neutral organic substances were adsorbed on the cation-exchanging Dowex XAD-2 they were more strongly adsorbed in line with increasing aromaticity, as demonstrated by increasing retention times during column chromatography [12]. Interaction between the substance and the polystyrene-divinylbenze polymer of the resin, through the aromatic π-orbitals, was proposed as the primary reason for this. Lundgren and Schilt also observed this effect occurring

with a selection of neutral nitrogen-based chelating dyes [37]. This effect is highlighted by an experiment involving a selection of organic species, all containing a single sulfonate functional group but with increasing aromatic character, being adsorbed to an anion-exchange resin. Adsorption strength was tested by exposure to NaCl solutions in an attempt to elute the adsorbed compounds. As the concentration of NaCl was increased it was seen that the stability of the adsorbed species was proportional to their aromaticity. The least aromatic compounds were completely desorbed at NaCl concentrations of less than 0.1 mol L^{-1}, and the most aromatic compounds remained completely adsorbed at NaCl concentrations of greater than 1 mol L^{-1} [38]. As such it is seen that the aromatic character and the ionic nature of a compound both impact on its stability when adsorbed to an ion-exchange resin.

For neutral compounds, though, Walton [39] postulates that the use of ion-exchange resins for adsorption is still beneficial, in terms of solvent kinetics. This is as greater water permeability is available due to the solvation of the ion-exchange sites. For ionic dyes, of which many contain sulfonic groups and aromatic moieties [40], ion-exchange resins have increased utility due to the beneficial solvent kinetics, ion-exchange processes, and the influence of and π-orbital interactions.

As these compounds are used to interact with cationic metal species it is reasonable to consider the effect this would have on the adsorption strength should the sulfonate group be involved. To examine the sulfonate's interaction with metal ions versus ion-exchange sites, Akaiwa compared the half extraction pH profiles for a variety of metals in a resin-adsorbed 5-sulfo-8-quinolinol system to those in a chloroform dissolved 8-quinolinol system, where the compound was effectively the same but lacking a sulfonate group [3]. This was done with the reasoning that performance of

a dye when adsorbed is similar to performance in non-polar solvents. Good agreement was noted between the values, indicating the sulfonate group in the resin system was not being used for metal interaction, most likely due to an ionic interaction with the fixed cationic sites on the resin. As such it is worth noting that those dyes having sulfonate groups may be favored where adsorption is used for immobilisation and metal interactions are expected.

In some situations ionic sites were noted to be the primary cause of adsorption. For instance, adsorption of Tiron on the anion-exchangers Amberlyst A-26 and Amberlite IR-400 was noted to correspond closely to the capacity of the exchanger, and hence, the number of ionic sites [41]. This indicates that Tiron was not adsorbing using π interactions in the absence of ionic sites, and that the ionic sites were essential. Tiron has two sulfonic acid groups and two hydroxyl groups while its aromatic character is due to a single benzene moiety, resulting in significant ionic character. For DGT functionality where deployment in marine environments is desirable, reliance on ionic interactions may be detrimental due to the presence of counter-ions which could potentially desorb ionic species without significant aromatic character. With the larger aromatic moieties, a combination of ion-exchange and physical adsorption is observed, as discussed, resulting in dyes that are stable at high ionic strengths [42-44]. A further effect on resin adsorption is the resin counter-ion, as discussed by Marina et al. [40]. This can be controlled before dye loading so that a counter-ion with low resin affinity is present to improve dye adsorption. This indicates a necessity to ensure that ions, which the ion-exchange resin will adsorb preferentially to the colorimetric reagent, are not present during deployment.

2.1.5 – Chelating Agent Loaded Resins

During the 1970s, methods for selectively preconcentrating metal ions by using a 'chelating agent-loaded resin' were being developed, such as that by Akaiwa [45]. Here, selections of chelating agents were adsorbed onto a suitable resin for use in the separation and preconcentration of trace elements prior to neutron activation analysis. A chelating agent-loaded resin consists of an anion-exchange resin with a chelating agent adsorbed, such as the colorimetric reagent Zincon. Marina et al. published a review of similar work in 1986 with an exhaustive list of the resin and chelating agent combinations investigated to that point [40]. The majority of these resins were used for selective separation and preconcentration of metal ions, though some colorimetric work is mentioned where a suitable ligand had been immobilised before exposure to the analyte solution. Indeed, much work has been performed employing colorimetric ligands but with non-colorimetric detection methods [46]. The large body of work in this area shows that the adsorption of dyes onto a polymeric resin support is a promising technique to examine.

It has been noted by Bilba et al. that the adsorption of chelating reagents can prove a better choice than chemical grafting as the kinetics of solution interaction are more favorable [11]. As well as this the stability of the reagent on the resin is not less than with grafting when deployed in conditions of near-neutral pH, as would be expected environmentally. The potential stability of adsorbed reagents was highlighted by Paull et al. [47] through the application of commercial resins, modified with adsorbed xylenol orange, to chromatography. Under regular usage, in pH ranges of 0.5 to 11 with 0.5M KNO_3 present, XO was not noticeably desorbed after a year's worth of use in a chromatographic column. This stability is necessary for DGT use

where probes may be deployed for long periods. Deployments of a month in high ionic strength matrices, such as seawater, have been reported [48,49], and even longer deployments have been undertaken [50].

For adsorption, therefore, the choice of resin plays a role in the usefulness of the adsorbed chelating agent. Commercially available resins have been most commonly used [34,35,38,42-44,46,47,51-55] though custom made resins with porous structures have also been used to provide a deeper understanding of the effect of resin cross-linking and porosity on adsorption [41].

In consideration of this, the porosity and composition of the resin plays a role in controlling the rate of analyte uptake, as shown by Egawa et al. [56]. They described a custom highly-porous poly(acrylonitrile-*co*-divinylbenzene) resin with amidioxime for chelation of uranium in a seawater matrix. When compared to other similar preconcentration methods, the amidioxime resin provided a high rate of uranium uptake, which they attributed to the highly porous structure. Larson et al. compared different levels of cross linking in cationic and anionic resin systems noting that as cross linking increases so too does the sorptive capacity of the resin, up to a point where excessive cross linking may sterically hinder dye access to the pores [57]. Variation in cross linking, and hence, porosity [58], is readily available commercially, allowing a suitable off-the-shelf resin to be chosen. Commonly these resins have used a polystyrene divinyl-benzene (PSDVB) matrix, which can result in unfavorable kinetics due to the hydrophobic resin matrix preventing water and any adsorbed species interacting with each other. The inclusion of ion-exchange groups in these resins improves water-resin interaction due to the hydration of the ion-

exchange groups, and for aqueous monitoring deployment only unmodified PSDVB resins are of concern [11].

In regard to neutral resins, Lundgren and Schilt [37] were among the first to study adsorption of a selection of chelating dyes on a commercial PSDVB non-ionic resin, XAD-2. The adsorption was found to be of a type consistent with monolayer Langmuir adsorption, with dye retention proportional to aromaticity. In order to overcome the hydrophobic resin nature it was necessary to wet the resin in methanol before use, but once wetted in this fashion water compatibility was not an issue. Stability of the dye's adsorption on to the resin, once metals were bound, was heavily dependent on solution pH and the presence of anions. A lower pH decreased adsorption stability and the presence of anions was seen to increase the stability of the metal-dye complex on the resin. While this system was used for chromatography, and quantification was not by colorimetry, the suitability and stability of correctly wetted neutral resins as substrates for neutral chelating agents is demonstrated, provided deployment conditions do not contribute to desorption. However this cannot be guaranteed, and the use of ion-exchange resin is preferred.

These PSDVB resins provide a promising set of substrates, due to the structural stability provided by the hydrophobic cross-linked structure [11]. This is useful in marine deployment where the complex matrix of seawater and potential for biological degradation meant structural stability is an important consideration during deployment. As marine deployment is not as chemically harsh as the conditions used for some chromatographic techniques [47], PSDVB matrix resins should be entirely stable. PSDVB resins are not the only commercially available type of polymer resin,

but form the bulk of resin substrates available [59], and due to the factors discussed above were exclusively used for the work reported in this thesis.

Many studies into resin-loaded chelating agents have not been colorimetrically focused, but there have been several studies into this area after Yoshimura's initial work employing PSDVB resins [34]. Colorimetric studies using UV-Vis spectrophotometry have been successful, and a summary of this work is provided by Bilba et al. within their review of general chelating agent-loaded resins [11]. As well as colorimetric detection, fluorometric detection has been reported by Compano et al. [53] using the fluorometric properties of resin-adsorbed 8-(benzenesulfonamido)quinoline. This allowed cadmium(II) and zinc(II) to be detected in a flow-through cell, and provided accurate quantification of the metals at concentrations of less than 2 $\mu g\ L^{-1}$. The demonstrated colorimetric ability of these chelating agent loaded resins, and the compatibility of the PSDVB resin with a wide variety of analytes and matrices, shows suitability for the previously mentioned criteria of colorimetric response, solid binding of the analyte and robustness of the binding phase. Due to the relatively small amount of information available on the colorimetric use of these resins it was necessary to examine these properties in-house.

2.1.6 - Summary

A variety of methods have been discussed for the immobilisation of colorimetric chelating agents. The creation of a robust, stable binding phase was the ultimate goal of this review, and with the wide variety of methods examined adsorption was

considered the most appropriate method for achieving this. Containment of the agent within a membrane, such as in ISE membranes, had buffering concerns and had not been shown to work with strongly chelating agents. Water insoluble agents have been shown to work for DGT, though the limited range of water insoluble colorimetric agents meant this was not a promising method. Chemical grafting was seen to be a robust technique, but more costly than adsorption which was seen to be equally as suitable.

To these ends, a PSDVB based resin method would be most promising. It was, however, considered pertinent to trial a selection of relatively un-tested methods alongside adsorption onto PSDVB resins to find a technique that allowed the inexpensive, stable immobilisation of a colorimetric dye while providing the necessary capacity and kinetics for DGT binding phase use. To this end two containment methods were trialed, C18 functionalised paper and using a PVC membrane, as well as a novel method described by Takahashi et al. [62]. Immobilisation of a modified PSDVB resin was tested using the typical polyacrylamide gel technique, as well as a novel method utilising adhesive label paper.

2.2 – Experimental

2.2.1 – Metal Test Solutions

Metal solutions of Fe(II), Cu(II), Mn(II), Cd(II), Pb(II) and Zn(II) were prepared individually for response tests in acid washed 200.0 mL volumetric flasks. These solutions contained one of the metal salts listed in Table 2.1 at the masses shown, 2.00 mL of a 1.0 M phosphate buffer at a pH of 6.8, prepared from Na_2HPO_4 and NaH_2PO_4 (99%+ puriss. Grade, Riedel-de Haën, Seelze, Germany), and were made to the mark with ultrapure water (17+ MΩ cm^{-1}, Thermo Scientific, Dubuque, USA). Weights were measured on an Ohaus Analytical Plus balance (AP-250D-0, Ohaus Australia, Port Melbourne, Australia).

For storage, acid-washed 250 mL polycarbonate bottles (Sarstedt, Ingle Farm, Australia) were used to avoid metal loss through glass adsorption. Stock solutions of 100 mg L^{-1} were subsequently made by using the weights shown in Table 1 increased by a factor of ten, and these were also stored in 250 mL plastic Sarstedt bottles.

2.2.2 – C18 Functionalised Chromatography Paper

Synthesis of octadecanoyl chloride was undertaken using 9.59 g ($3.38x10^{-2}$ mol) of 99% LR grade octadecanoic (stearic) acid (Ajax, Melbourne, Australia) with addition of 7.6 g ($6.4 x10^{-2}$ mol) of 100% $SOCl_2$ (BDH, Sydney, Australia) and 1 drop of 99% DMF (BDH, Sydney, Australia). After 27 min of gentle refluxing all

Table 2.1 – Metal salts used for metal response test solutions. The weights at right were dissolved in 200 mL to give approximately 10 mg L^{-1} solutions.

Salt	grade	Manufacturer	percentage	Weight (mg)
$CdCl_2.2½H_2O$	AR	Ajax, Sydney, Australia	80	88.8
$FeSO_4.7H_2O$	AR	BDH, Kilsyth, Australia	99.5	40.6
$MnCl_2.4H_2O$	AR	Ajax, Sydney, Australia	98	32.0
$ZnSO_4.7H_2O$	AR	BDH, Kilsyth, Australia	99.5	88.2
$CuSO_4.5H_2O$	AR	Ajax, Sydney, Australia	100	99.6
$Pb(NO_3)_2$	LR	Ajax, Sydney, Australia	99	65.6

octadecanoic acid was consumed and the excess $SOCl_2$ was removed by gentle heating. The light brown oil product was decanted and kept in a desiccator.

A 1 gram quantity of the octadecanoyl chloride was added to a 1 cm^2 piece of Whatman Chr 17 or Whatman P81 chromatography paper. Further tests were performed using 0.25 g of pyridine added pre-reaction to the paper. After the octadecanoyl chloride exposures, a waxy residue was left on the paper surface, which was removed by rising with ethyl acetate (AR grade, Chem Supply, Melbourne, Australia). Dipyridine was absorbed into the C18 phase from aqueous solutions, from MeOH solutions (HiPerSolv, BDH, Sydney, Australia) and from ethyl acetate solution (AR grade, Chem Supply, Melbourne, Australia). Absorption of 1,10-phenanthroline (Reagent grade, Sigma, Milwaukee, USA) into the C18

phase from DMSO (AR grade, BDH, Sydney, Australia) was tested using 1 mL of a 21.8 g L^{-1} dye solution. Absorption of 1,10-phenanthroline from water was also tested using a 2.95 g L^{-1} dye solution.

2.2.3 – Dye Deposition

As described in Takahashi et al. [62], PAN (LR grade, BDH, Poole, England) was immobilised on cellulose acetate filter membranes (0.45 μm pore size, 47 mm diameter, Advantec, Toyo Roshi Kaisha Ltd., Japan) using a stock solution of 50.2 mg of PAN in 100.0 mL acetone (LR grade, Chem Supply, Sydney, Australia). $NaHCO_3$ (LR grade, Ajax, Melbourne, Australia) was used as a buffer in place of TAPS, as in Vogel 3rd edition [60], with 0.0845 g of $NaHCO_3$ in 10.0 mL of ultra-pure water adjusted to a pH of 8.4 using NaOH (AnalaR, BDH, Sydney, Australia) and H_2SO_4 (98% AR grade, BDH, Sydney, Australia). The discs were created by adding 100 μL of the acetone dissolved PAN to a vigorously stirred $NaHCO_3$ buffer solution. This solution was then quickly vacuum filtered through the cellulose acetate discs using a Buchner apparatus, depositing the suspended dye on the filter surface.

Pyrocatechol Violet (90% indicator grade, Aldrich, Milwaukee, USA) was deposited as per PAN. An EBT (Indicator grade, Aldrich, Milwaukee, USA)/1,10-phenanthroline (Reagent grade, Sigma, St. Louis, USA) mixture was created by dissolving 50 mg of each in 100.0 mL of acetone, and depositing as per PAN. To obtain the appropriate dye pH for particle suspension 0.10 M NaOH (AnalaR, BDH, Sydney, Australia) was added into the dye mixture until all dye had completely

dissolved at which point the pH was measured (Orion model 720A pH meter with a GPH Electroder probe) and a pH below complete solubility was used. Dye desorption from the paper was tested by immersion in 100 mL of deionised water for 7 days and observing visually.

2.2.4 – PVC Membrane

PVC membranes were made as per Craggs et al. [63] using PAN (LR grade, BDH, Poole, England) in place of the liquid ion-exchanger. Quantities used were 0.76 g of 'high molecular weight' PVC (Aldrich, Milwaukee, USA) and 0.08 g PAN dissolved in 6 mL THF (AR grade, BDH, Sydney, Australia). The solution was mixed until no particles were visible and then cast using a circular open-ended flask on a glass plate for containment while the solvent evaporated. Discs obtained from this were exposed directly to metal solutions by immersion.

2.2.5 – Polyacrylamide gels

Gels were made as per instructions from DGT Research [61]. The gel solution consisted of 15.0% w/v acrylamide (≥99%, Sigma, St. Louis, USA) and 15 mL of crosslinker (DGT Research, Lancaster, UK) in 100.0 mL of ultrapure water. Polymerisation was initiated in 10.0 mL of gel solution by addition of 20 µL of *N,N,N'N'*-tetramethyethylenediamine and 70 µL of 10% w/v ammonium persulfate (98% SigmaUltra, Sigma, St Louis, USA) in ultrapure water. Gels were cast into

acid-washed polycarbonate or glass holders with commercial vinyl spacers of 0.22 mm used to determine thickness. Gels were set in an oven at 45 ±1 °C.

2.2.6 – Dye immobilisation on resin

For dye immobilisation, vacuum dried resin was suspended in ca. 50 mL of ultrapure water which was then pH adjusted using 65% H_2SO_4 (AnalaR, BDH, Kilsyth, Australia) and 1M NaOH (AnalaR, BDH, Kilsyth, Australia) while monitoring the pH with an Orion model 720A pH meter with a GPH Electroder probe. To this solution the dye was added to provide the necessary resin loading, typically 10.00 mL of 1 mM dye solution was added to 1 g of dried resin for a 10 μmol g^{-1} dye loading on the resin. The resins used were Dowex (Dow Chemicals, Indianapolis, USA) 1x8 (200-400 mesh) and 50W-X8 (400 mesh); Amberlite (Rohm & Hass, Philadelphia, USA) resins CG-400 (100-200 mesh), XAD-2 (20-60 mesh), IR-410 (100-200 mesh) and IR-45 (50-100 mesh); Amberchrom (Rohm & Hass, Philadelphia, USA) CG-300c (bead diameter 120 μm) and a non-commercial unmodified polystyrene divinylbenzene (PSDVB) resin of approximately 100 mesh obtained from the Australian Centre for Research on Separation Science (Hobart, Tasmania, Australia). This solution was shaken for 24 h at or above 100 rpm on a Lab Line Orbit shaker, before the resin was collected by vacuum filtration onto Whatman #54 filter paper and air dried. Uptake was checked by a lack of colour in the supernatant solution, discussed further in Chapter 5.

2.2.7 – Adhesive Labels

Circular discs of 25.4 mm diameter were cut from Esselte Quikstik labels (Stamford, Connecticut, USA) using a metal hole punch. To minimise contamination discs were punched from the plastic-backed side, with up to 4 discs being punched at once. Air-dried resin was added to the discs by removing the backing plastic and pressing the adhesive side into the resin. Resin was then spread around the label by hand, using nitrile gloves. Care was taken not to touch the adhesive surface as this inhibited resin adhesion. Once resin was adhered, discs were equilibrated in a 0.01 mol L^{-1} phosphate (p.a. NaH_2PO_4 and Na_2HPO_4 Riedel-de Haën, Seelze, Germany) buffer solution at a pH of 6.8 to allow the resin to swell and force excess beads off, resulting in even packing.

Microscopy work was performed using an IX71 inverted microscope (Olympus, Pennsylvania, USA) at 100x magnification under fluorescent light. Images were captured with an Optronics DP71 camera using MagnaFIRE software (Optronics, Goleta, California, USA) and stored as .tif files (Adobe, San Jose, California, USA).

For adsorbed metal analysis label discs were extracted using 10% HNO_3 (from 65% w/v Suprapur, Merck, Darnstadt, Germany). Analysis of the extracted solution was performed using ICP-MS (Finnigan Element, Bremen, Germany). Further details can be found in section 3.2.4.

2.3 – Results and Discussion

2.3.1 – C18 Immobilisation

In order to obtain a non-resin binding phase the use of octadecyl groups grafted to paper was trialed as a method for dye immobilisation. If successful, it was thought that this would provide a cheap, easy method for binding phase fabrication in a similar fashion to liquid ion-exchanger membranes, but without the need for plasticisers. After modification with octadecanoyl chloride, the paper was found to have a thick, waxy coating, and to have become brittle. The waxy coating was removed by rinsing with ethyl acetate, though care was needed to not damage the underlying paper.

Bipyridyl and 1,10-phenanthroline were both used to test reagent absorption and Fe(II) response. Dye was seen to have been absorbed into the C18 phase as it was observed that contaminated spots, where steel tweezers had contacted a paper square, were colored and persistent both in and out of water. To further determine if dye had been absorbed qualitatively, the paper was exposed to aqueous Fe(II) solutions; this resulted in patchy colour across the paper surface. This was thought to be due to the hydrophobic nature of the modified paper. As such, it appeared that the dye had been partitioned into the C18 layer, but once there, was not able to interact with aqueous Fe(II). The use of ethanol as a wetting agent to promote water interaction resulted in significant visible dye leaching, which would not be suitable for a DGT technique. Therefore, this method was not considered suitable as it would not allow the interaction with aqueous metal ions necessary for a DGT binding phase.

2.3.2 – Takahashi's Method

Another method of interest for development of inexpensive binding phases was described by Takahashi et al. [62]. The method involved the deposition of dye particles onto a cellulose acetate membrane by vacuum filtration. The dye particles were obtained by addition of a small quantity of water-insoluble dye, dissolved in an organic solvent, to vigorously stirred water which was buffered to ensure that the dye remained water insoluble.

Long-term stability was not reported by Takahashi and co workers and so laboratory work was performed to assess its applicability as a stable DGT binding phase. PAN [1-(2-Pyridylazo)-2-napthol] was deposited onto cellulose acetate filter membranes and used to test Cu(II) and Zn(II) color response. The PAN-impregnated cellulose acetate filter membrane showed a response within 5 min of exposure to separate 100 mg L^{-1} Fe(II), Cu(II) and 10 mg L^{-1} Zn(II) solutions, though exposure to a 10 mg L^{-1} Cu(II) solution required several hours before a response was observed. No response to Fe(II) was observed using a 10 mg L^{-1} solution. Continued solution exposure to metal ions over 5 days did not show visible dye loss to water, indicating that the dye-metal complex had remained water-insoluble.

As aqueous studies had shown qualitative metal color responses with a phenanthroline/EBT (eriochrome black T) solution, an attempt to immobilise a mixture of the dyes in this fashion was made. While dye deposition was visible no metal interactions were observed. PCV (Pyrocatechol violet) was also deposited onto a celluslose acetate membrane in an attempt to observe the response of this

system to Zn(II), a reaction being known between these compounds in aqueous solution [1]. Using diffuse reflectance spectrophotometry, no significant differences were seen between an unexposed disc and a disc immersed for 12 h in 100 mg L^{-1} Zn(II) solution.

A major limitation for this technique was the need to use a dye which was insoluble at neutral pH values, as it appeared to inhibit diffusive interaction with charged species. Takahashi and co workers had used these discs as a filter, drawing the analyte solution through the disc in order to facilitate a colour change. As this technique requires that the dyes are insoluble at the exposure pH, it would appear that interaction with the water sample does not readily occur diffusively. The demonstrated slow colour response times are unsuitable for DGT deployment where a rapid interaction would be necessary to maintain the concentration gradient. This dye restraint also significantly limits the ability of this technique to explore dye responses. As a large range of dyes would be tested, many of which are highly water soluble at environmental (and hence deployment) pHs, it was decided that this technique would not be a suitable method for dye screening or initial work.

2.3.3 – PVC Membrane

A PVC membrane incorporating PAN was trialed using the method described by Craggs and Moody [63]. PAN was employed in place of the ionophore, with casting by evaporation of the THF solvent from a glass plate. The resulting 0.5 mm thick membranes were physically strong and flexible, with a deep red color and slightly transparent. However, immersion in concentrated (100 mg L^{-1}) metal solutions and

solutions of various pHs did not prompt a color change. The highly hydrophobic nature of the membrane, indicated by the fact that water beaded on the surface, was considered to be detriminental to the interaction of solvated charged analytes with PAN. This approach was not studied further.

2.3.4 - DGT resin-gel immobilisation

Resin immobilisation in DGT devices uses the polyacrylamide hydrogel to contain the resin as the gel sets [64]. This allows a single layer of beads to be immobilised and completely hydrated, and by allowing the resin to settle at the bottom of the casting structure the resin is positioned in a sampler in contact with the diffusive gel layer, as shown in Figure 2.1. As this is an established method, its application to novel resin beads would provide as direct a comparison to current DGT techniques as possible.

Several resins were used in an initial study, including Dowex 1x8 and 50W-X8; Amberlite resins CG-400, XAD-2, IR-410, and IR-45; Amberchrom CG-300c; and a non-commercial unmodified polystyrene divinylbenzene (PSDVB) resin. These resins were trialed as obtained, and with one of a selection of dyes adsorbed (see Appendix 1). Dye adsorption was by exposure to a dye solution for 24 h, by which time solution coloration was no longer present and the resin was visibly coloured. Dye adsorption rate was largely dye-specific, and the concentrations of dye used typically resulted in a loading of 10 to 50 μmol of dye per gram of resin.

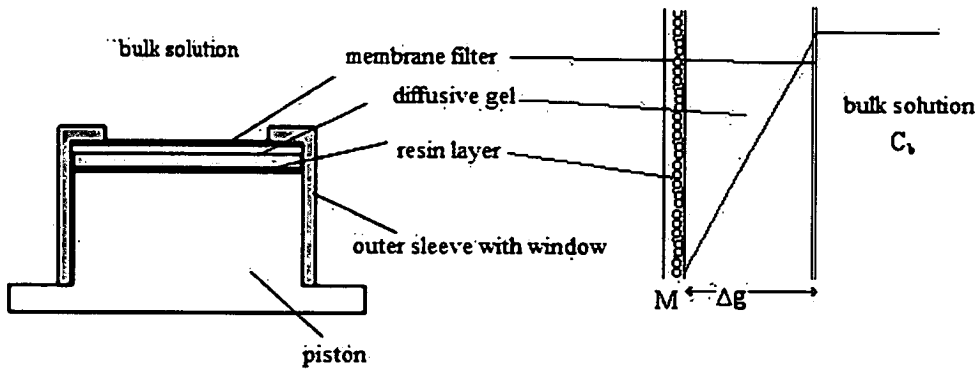

Figure 2.1 – DGT device construction, showing positioning of gel-bound resin beads in relation to the diffusive gel and details relevant to DGT deployment. Modified and reproduced with permission from Zhang and Davison [64]. Copyright 1995 American Chemical Society.

Diffusive gels were prepared as described by Zhang and Davison [61]. Casting was initially performed using glass plates separated by acid-washed vinyl spacers providing a 0.66 or 0.99 mm gap; polycarbonate plates were later used for the majority of castings, with no resulting changes observed in the gels. Gels were set at 45 ±1 °C in an oven. Significant trouble was encountered in obtaining an evenly distributed single layer of resin beads, as resin was seen to aggregate rather than settle to the bottom plate. As well as resin settling issues, gel casting in the presence of Amberlite GC-400 resin was not successful. Only partial polymerisation of the gel was achieved in many cases. No resin was observed to allow 'normal' setting of the gels, with gels being physically weak when compared to Chelex 100 gels in all cases. The actual dye adsorbed was not seen to have an impact on the ability of the gel to set and, due to this, is not specifically discussed. Of the resins mentioned above, Dowex 1x8 resin was observed to have the least interference in gel setting

and provided the fastest observed dye adsorption properties. This resin was therefore selected for use in further testing.

In an attempt to resolve these resin issues, various treatments of the resin before casting were assessed. In most cases dye-adsorbed resin was used, with some exceptions noted. Immobilisation of resin within the gel before dye adsorption did not improve gel stability, and neither did increasing or decreasing the catalyst concentration by 50%. Conversion of resins to the hydroxyl form, before adsorption of the dye and gel casting, improved gel strength but the resulting gels were still significantly more fragile than commercial Chelex 100 gels. Soaking of the resin in acidic, neutral and basic solutions (buffered to pH 1, 6.8 and 10.1) before gel casting did not improve gel setting either, but in the case of the resin soaked at pH 6.8 a white precipitate was noticed. The use of resin soaked in five changes of ultrapure water over two days also resulted in a white precipitate, indicating that it was not due to the phosphate buffer solution. These gel casting difficulties resulted in abandoning this form of resin immobilisation in favor of an alternative technique discovered during resin reflectance testing.

2.3.5 - Adhesive label 'discs'

As the casting of resin gels was proving troublesome, fixing of the resin to the adhesive side of an Esselte Quik-Stik paper label was used for the analysis of adsorbed dyes by UV-Vis reflectance spectrophotometry. This was also found to provide robust immobilisation of the resin when immersed in water over periods of more than a month, and the application of this form of resin immobilisation to a

DGT binding phase was assessed. For negatively charged dyes, Dowex 1x8 anion-exchange resin was chosen for its neutral colour and better adsorption characteristics than GC-400. Amberchrom CG-300c was chosen as a non-ionic resin for neutral dyes, as it was pure white and was available in a consistent 120 μm bead size. No positively charged dyes were considered, thus a cation-exchange resin was not required.

Due to concerns that resin moisture content would impact on reflectance measurements, wet resin was used for initial attempts to adhere resin to the adhesive labels, but it was found that the resin would not adhere to the label. However, air-dried resin could easily be adhered onto a label, and immersion of dry resin-loaded labels in water allowed the resin to swell without loss of adhesion. This 'equilibration' process allowed for the swelling of resin to form a well-packed single layer of beads across the label surface, as shown by the microscopy images in Figure 2.2. Paper labels were cut into 25.4 mm diameter discs, before resin adhesion, to fit aqueous DGT sampling probes. As the dry adhered resin swelled upon wetting a subsequent loss of resin mass was observed due to beads being forced off the disc. In the case of a typical 5.07 cm^2 disc with Dowex 1x8 resin, this loss of mass decreased the resin quantity from 21.3±0.9 mg per disc to 16.3 ±0.6 mg per disc (n=6), or a 23% decrease in resin mass.

Upon drying, resin was seen to contract into clumps, and when re-immersed in water resin once again covered the disc with no visible resin loss occurring. Over 3 drying-wetting cycles this was confirmed by weighing, with disc masses of 16.3 ±0.6 mg, 16.0 ±0.6 mg and16.6 ±0.5 mg (n=6) being observed, showing no significant resin loss. Accordingly, the discs are robust enough to be kept dry if analysis is not

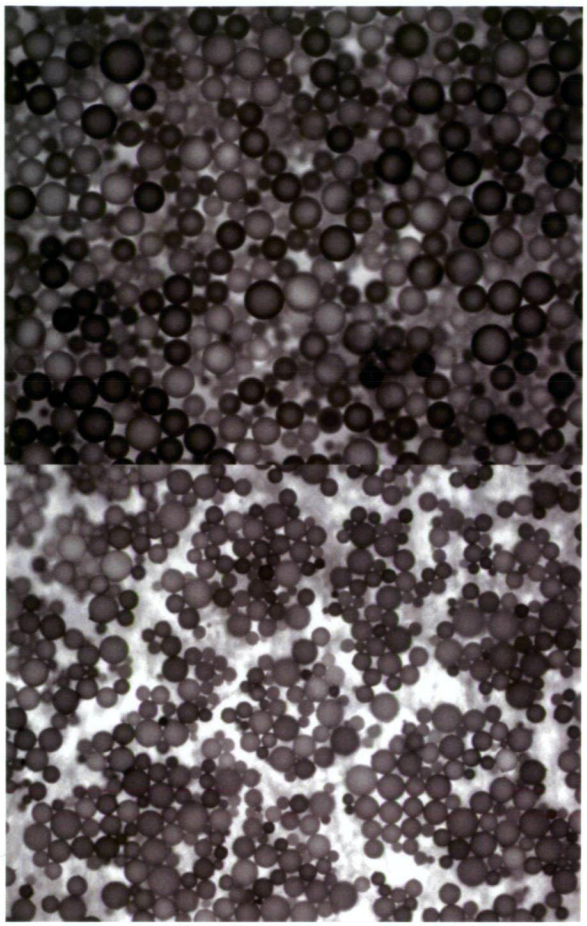

Figure 2.2 - Microscopy of resin-labels. Shown at top are packed beads on a wet label after equilibration, and at bottom the same label is shown after drying. Resin beads are Dowex 1x8 with methylthymol blue adsorbed at 10 μmol of dye per gram of resin, which provides contrast.

immediately possible, without loss of resin when rehydrated for later analysis. No significant loss was observed with the highly cross-linked Amberchrom CG-300c resin, which was understandable as swelling is significantly limited in this resin due to the high degree of cross linking.

Initial wetting was also used to equilibrate the resin and dye to the exposure solution; this allowed ionic and moisture equilibrium to be reached before

deployment. This equilibration step was completed in less than an hour, as observed by the lack of significant change in resin mass between subsequent hour-long equilibrations, as mentioned above. Handling the disc did require care, mainly as resin could be scratched off easily when wet, but during the installation and recovery of the discs from DGT samplers this was not normally an issue.

The strength of the adhesion of resin to the labels was not tested under highly basic conditions as such conditions are not anticipated in the field. However, in an acid extraction solution of pH 1 resin beads were not observed to be lost, although the paper backing would degrade, leaving behind a sheet of adhesive with resin attached. Both anion-exchange and non-ionic resins were found to fix well, with a notably stronger bond for anion-exchange resins, and the immobilisation of dyes onto these resins did not noticeably affect the strength of adhesion. Cation-exchange resins were not tested, as discussed earlier. This method provides an inexpensive, quick and appropriately robust way to fix resin in a single layer for use as a DGT binding phase. The wide variety of label sizes available means the shape of the binding phase could easily be adapted to the sampler in use.

A last concern related to the use of the paper-label based method was contamination from the labels themselves. ICP-MS analysis of acid extractions performed on label discs of 5.07cm^2 diameter, discs with un-modified resin, and discs with resin where methylthymol blue (MTB) had been adsorbed, provided the extractable metal data presented in Table 2.2. A significant amount of calcium can be observed, and as such, calcium-sensitive dyes are not recommended for use unless the dye's formation constants greatly favor other analytes of interest.

Table 2.2 – Mass of metal extracted from Esselette QuikStick labels discs of 5.07 cm^2 without resin, with Dowex 1x8 resin, and with methylthymol blue (MTB) dye adsorbed to Dowex 1x8 resin. Values are the average quantities of the metal observed in a single acid extraction of a disc, ± one standard deviation over triplicate samples.

Metal	Paper only label extract (µg)	Label + resin extract (µg)	Label + MTB extract (µg)
Sr	0.83 ± 0.02	0.83 ± 0.02	0.81 ± 0.03
Na	1.5 ± 1.6	0.1 ± 0.6	0.2 ± 1
Mg	13.1 ± 0.2	13.7 ± 0.3	13.4 ± 0.1
Al	1.35 ± 0.03	1.30 ± 0.07	1.33 ± 0.08
P	1.5 ± 0.1	1.5 ± 0.3	1.58 ± 0.08
S	1.5 ± 0.3	1.5 ± 0.2	2.5 ± 0.3
Ca	$3.30 \pm 0.6 \times 10^3$	$3.30 \pm 1.1 \times 10^3$	$3.21 \pm 1.2 \times 10^3$
Mn	0.183 ± 0.002	0.184 ± 0.01	0.181 ± 0.005
Fe	0.53 ± 0.05	0.50 ± 0.02	0.53 ± 0.02
Cu	0.047 ± 0.009	0.06 ± 0.05	0.044 ± 0.001
Zn	0.10 ± 0.02	0.4 ± 0.1	0.2 ± 0.1
Pb	0.015 ± 0.016	0.011 ± 0.002	0.013 ± 0.002
As	< 0.001	0.4 ± 0.7	<0.001
Cd	<0.0015	<0.0015	<0.0015

2.4 - Conclusion

As the colorimetric reagent used provides the metal-response character of any colorimetric binding phase, the method of colorimetric reagent immobilisation was of primary importance to the physical binding phase. To this end, adsorption of the dye onto a suitable substrate was indicated as the preferred method in the literature. As discussed, this was expected to provide stability equivalent to that of chemical grafting under conditions of moderate pH and low to moderate ionic strength [11]. These conditions are within the range anticipated in environmental deployments, and this method is more efficient and less complicated to perform than grafting. As a substrate for adsorption, the literature had indicated that a PSDVB resin would be ideal.

It was still considered worthwhile to investigate a selection of methods other than adsorption to a PSDVB resin, as it was believed they may offer a yet simpler, more versatile and less expensive alternative. The methods explored, however, were not seen to be effective and the use of PSDVB resins as a substrate for dye adsorption was decided upon. For the immobilisation of the resin, the established DGT polyacrylamide gel technique [61] was not found to be suitable due to the incompatibility of the dye-adsorbed resin with the polymer during gel setting. A method for resin immobilisation, involving adhesion of the resin to a commercial paper label, was developed and this method was shown to provide the necessary robustness and stability for DGT binding phase use. The final physical form of the colorimetric DGT binding phases was, therefore, dye adsorbed to commercially available resin with a PSDVB matrix, which was then adhered to a 1 inch diameter

disc of adhesive paper label for deployment in aqueous DGT probes. These discs were ready for deployment after a single wetting/drying cycle to remove excess resin which also ensured a tight packing of the beads with minimal resin loss.

References

[1] K. Ueno, T. Inamura, K.L. Cheng, Handbook of Organic Analytical Reagents, CRC Press, 1992.

[2] W. Davison, H. Zhang, Nature, 367 (1994) 546.

[3] H. Akaiwa, Journal of Radioanalytical and Nuclear Chemistry, 84 (1984) 165.

[4] E. Bakker, E. Pretsch, P. Buhlmann, Analytical Chemistry, 72 (2000) 1127.

[5] E. Linder, K. Toth, E. Pungor, Analytical Chemistry, 56 (1984) 1127.

[6] M.A. Akl, A.K. Ghoneim, M.H. Abd El-Ziz, Electroanalysis, 18 (2006) 299.

[7] S. Kamata, K. Onoyama, Analytical Chemistry, 63 (2991) 1295.

[8] K.C. Gupta, M.J. D'Arc, Electroanalysis, 12 (2000) 1408.

[9] W. Simon, M. Lerchi, E. Bakker, B. Rusterholz, Analytical Chemistry, 64 (1992) 1534.

[10] P.R. Teasdale, S. Hayward, W. Davison, Analytical Chemistry, 71 (1999) 2186.

[11] D. Bilba, D. Bejan, L. Tofan, Croatia Chemica Acta, 71 (1998) 155.

[12] D.M. Ordemann, H.F. Walton, Analytical Chemistry, 48 (1976) 1728.

[13] M. Aoyagi, M. Hirakawa, T. Matusmoto, T. Chinuki, Kami Parupu Gijutsu Taimusu (1984).

[14] T. Honjo, T. Benya, Fresenius Journal of Analytical Chemistry, 334 (1989) 558.

[15] S. Nakamura, M. Amano, Y. Saegusa, T. Sato, Journal of Applied Polymer Science, 45 (1992) 265.

[16] T. Carofiglio, C. Fregonese, G.J. Mohr, F. Rastrelli, U. Tonellato, Tetrahedron, 62 (2006) 1502.

[17] L.-q. Xu, P. Schramel, Fresenius Journal of Analytical Chemistry, 342 (1992) 179.

[18] X. Chang, Z. Su, G. Zhan, X. Luo, W. Gao, Analyst, 119 (1994).

[19] D. Beauchemin, J.W. McLaren, A.P. Mykytiuk, S.S. Berman, Analytical Chemistry, 59 (1987) 778.

[20] A. Tong, Y. Akama, S. Tanaka, Analytica Chimica Acta, 230 (1990) 179.

[21] R.L. Bruening, B.J. Tarbet, K.E. Krakowiak, M.L. Bruening, R.M. Izatt, J.S. Bradshaw, Analytical Chemistry, 63 (1991) 1014.

[22] R.E. Sturgeon, S.S. Berman, S.N. Willie, J.A.H. Desaulniers, Analytical Chemistry, 53 (1981) 2337.

[23] O.A. Zaporozhets, L.E. Tsyukalo, Journal of Analytical Chemistry, 59 (2004) 386.

[24] S.A. Morozko, V.M. Ivanov, Journal of Analytical Chemistry, 52 (1997) 777.

[25] R. Flood, D. Fitzmaurice, Journal of Physical Chemistry, 99 (1995) 8945.

[26] D. Qinga, W. Deyua, Y. Chunweia, Supramolecular Science, 5 (1998) 469.

[27] E. Palomares, M.V. Martínez-Díaz, T. Torres, E. Coronado, Advanced Functional Materials, 16 (2006) 1166.

[28] S.R. Ricketts, P. Douglas, Sensors and Actuators B: Chemical, 135 (2008) 46.

[29] D. Gutiérrez-Taustea, X. Domènecha, N. Casañ-Pastorb, J.A. Ayllóna, Journal of Photochemistry and Photobiology A: Chemistry, 187 (2007) 45.

[30] E. Coronado, E. Palomares, J.R. Galan-Mascaros, C. Marti-Gastaldo, J.R. Durrant, R. Vilar, M. Gratzel, M.K. Nazeeruddin, Journal of the American Chemical Society, 127 (2005) 12351.

[31] E. Palomares, R. Vilar, J.R. Durrant, Chemical Communications (2004) 362.

[32] M.K. Nazeeruddin, D.D. Censo, R. Humphry-Baker, M. Grätzel, Advanced Functional Materials, 16 (2006) 189.

[33] M. Fujimoto, Bulletin of the Chemical Society of Japan, 27 (1954) 48.

[34] K. Yoshimura, H. Waki, S. Ohashi, Talanta, 23 (1976) 448.

[35] K. Yoshimura, H. Waki, Talanta, 32 (1985) 345.

[36] M.M.A. Shriadah, K. Ohzeki, Analyst, 111 (1986) 555.

[37] J.L. Lundgren, A.A. Schilt, Analytical Chemistry, 49 (1977) 974.

[38] M. Chikuma, M. Nakayama, T. Itoh, H. Tanaka, K. Itoh, Talanta, 27 (1980) 807.

[39] H.F. Walton, Journal of Chromatography, 102 (1974) 57.

[40] M.L. Marina, V. Gonzalez, A.R. Rodriguez, Mircochemical Journal, 33 (1986) 275.

[41] K. Brajter, E. Dabek-Zlotorzynska, Talanta, 27 (1980) 19.

[42] M.L. Marina, V. Gonzalez, A.R. Rodriguez, Bulletin de la Societe Chimique de France, 11 (1984) 339.

[43] M. Chikuma, M. Nakayama, T. Tanaka, H. Tanaka, Talanta, 26 (1979) 911.

[44] H. Tanaka, M. Chikuma, A. Harada, T. Ueda, S. Yube, Talanta, 23 (1976) 489.

[45] M. Leermakers, Y. Gao, C. Gabelle, S. Lojen, B. Ouddane, M. Wartel, W. Baeyens, Water, Air and Soil Pollution, 166 (2005) 265.

[46] Z. Molodovan, L. Vladescu, Talanta, 43 (1996) 1573.

[47] B. Paull, M. Foulkes, P. Jones, Analyst, 119 (1994) 937.

[48] C. Murdock, M. Kelly, L.-Y. Chang, W. Davison, H. Zhang, Environmental Science and Technology, 35 (2001) 4530.

[49] J.M. Pates, M.A. French, H. Zhang, S.E. Bryan, R.C. Wilson, Analytical Chemistry, 77 (2005) 135.

[50] B.L. Larner, A.J. Seen, I. Snape, Chemosphere, 65 (2006) 811.

[51] K. Brajter, Journal of Chromatography, 102 (1974) 385.

[52] K. Bratjer, E. Olbrych-Sleszynska, Talanta, 30 (1983) 355.

[53] R. Compano, R. Ferrer, J. Guiteras, M.D. Prat, Analyst, 119 (1994) 1225.

[54] M. Nakayama, M. Chikuma, H. Tanaka, T. Tanaka, Talanta, 30 (1983) 455.

[55] R.R. Rao, D.G. Goski, A. Chatt, Journal of Radioanalytical and Nuclear Chemistry, 161 (1992) 89.

[56] H. Egawa, N. Kabay, T. Shuto, A. Jyo, Journal of Applied Polymer Science, 46 (1992) 129.

[57] P. Larson, E. Muriga, T.-J. Hsu, H.F. Walton, Analytical Chemistry, 45 (1973) 2306.

[58] H. Deleuzel, X. Schultze, D.C. Sherrington, Polymer Bulletin, 44 (2000) 179.

[59] P. Barbaro, F. Liguori, Chemical Reviews, 109 (2009) 515.

[60] A.I. Vogel, Vogel's Practical Organic Chemistry, Longman, 1962.

[61] H. Zhang, W. Davison, Analytica Chimica Acta, 398 (1999) 329.

[62] Y. Takahashi, H. Kasai, H. Nakanishi, T.M. Suzuki, Angewandte Chemie, 45 (2006) 913.

[63] A. Craggs, G.J. Moody, J.D.R. Thomas, Journal of Chemical Education, 51 (1974) 541.

[64] H. Zhang, W. Davison, Analytical Chemistry, 67 (1995) 3391.

[65] D. Wells, The Penguin Dictionary of Curious and Interesting Numbers, Penguin Books, London, 1986.

[66] C. Song, P. Wang, H.A. Makse, Nature, 453 (2008) 629.

Chapter 3

Methylthymol Blue Binding Phase

Prototyping the colorimetric binding phase system with Ultra Violet-Visible reflectance analysis

3.1 – Colorimetric Binding Phase Development

3.1.1 – Introduction

Over the last decade the development of DGT analysis techniques involving colour has been experimented with; Teasdale et al. [1] first reported on the use of an AgI impregnated polyacrylamide gel for colorimetric analysis of dissolved sulfide in 1999. This gel was used as the binding phase in a DGT device, with the *in-situ* formation of Ag_2S providing a change in colour from faint yellow to black. This colour change could then be used to quantify the accumulated sulfide. The nature of this method also meant it was possible to directly observe the 2-D spatial heterogeneity of sulfide distribution within the sediment layer, without the need to physically divide the gel and analyse individual pieces.

Jezequel et al. reported on a method of DGT measurement of sulfide using a PVC tape simultaneously with an equilibrium (DET) method to measure Fe(II) [2]. Quantification of the Fe(II) was based on the development of colour in a ferrozine-containing gel applied post-sampling to the equilibrated Fe(II) containing gel, which also allowed for 2-D spatial discrimination. However, an issue with this technique is relaxational diffusion of the analyte within the two gel layers during dye application and reaction [3]. This would result in a less precise picture of spatial analyte distribution, and also a time-related reduction in the density which would affect the accuracy, precision, and detection limit of the technique.

In-situ colour development for metal analytes could, alternatively, be obtained by using a binding phase with a completely immobilised colorimetric chelating agent that irreversibly binds the analyte. This would have the advantage of disallowing relaxational diffusion while providing easy 2-D spatial discrimination and quantification. A colorimetric system, as opposed to the colour 'density' (effectively grayscale) systems employed so far, may also improve analysis due to a more specific region of visible light being analysed. This was shown to be a significant gain by Yoshimura and Waki [4]. Lastly, this approach would be more flexible than the AgI system used previously, as novel dyes could be easily included in the system. The use of a suitable dye-resin system, as discussed in Chapter 2, in concert with a colorimetric analysis technique, such as UV-Vis diffuse reflectance spectrophotometry, would provide these characteristics.

3.1.2 - Development

Colorimetric DGT binding phase development began by prototyping the system using a single colorimetric chelating agent (hereto referred to as a 'dye') to assure DGT functionality, and to develop a dye exploration method for future function expansion. These initial steps are the primary focus of this chapter.

In considering the dye it was necessary to examine the required characteristics of a DGT binding phase. Essential to DGT functionality is that metal ions are completely removed from solution at the diffusive layer / binding phase interface, and that the resin does not become saturated. Avoiding this was important, as saturation with an interfering metal ion could lead to a loss of metal binding ability before a

quantifiable amount of metal had been complexed [4]. When considering this, a 'quantifiable amount of metal' was that necessary for a significant colour change to be observed. A second consideration for DGT deployment was that of dye stability. A dye which readily leaches from the resin would affect the metal concentration in the diffusive area of the DGT system and, therefore, the concentration gradient. As well as this, any potential dye/metal leaching loss would lead to the loss of bound analyte. A leaching dye or complex could be lost during deployments and, as deployments are of variable lengths of time, this inconsistency would make analysis difficult. It is essential, therefore, that the dye must remain fixed to the resin to provide adequate function, both before and after metal complexation.

With a physical form for the binding phase decided upon (described in Chapter 2), a dye to develop the system was needed, and from there characterising the prototype system could start [6]. The dye chosen for prototyping, methylthymol blue (MTB), has been used as a chromogenic metal indicator for a variety of metal ions and its structure is found in Figure 3.1 [7]. In particular, it has been noted to form Cu(II), Zn(II), and Co(II) complexes at neutral pHs [8], and these metals are of interest to the work presented here. While MTB itself has not been used in any resin-adsorbed dye studies the author is aware of, it is structurally very similar to xylenol orange, which has been used for metal interaction after adsorption to an ion-exchange resin.

Xylenol orange (abbreviated XO, see Appendix 1 for structure) has been used as a resin-adsorbed metal-chelating dye in a variety of studies [5,9,10]. Bratjer and

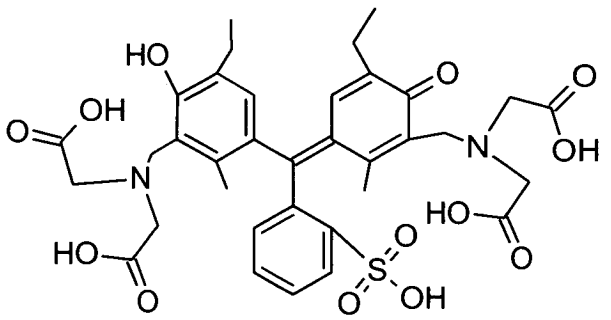

Figure 3.1 – A structural diagram of methylthymol blue. Carboxylic acid pKa values are 0.76, 1.15, 2.58 and 3.23 and the phenol group pKa value is 6.40.

Olbrych-Sleszynska found that XO readily adsorbed to an ion-exchange resin surface and that this adsorption strength was increased when Cu(II) was complexed [5]. In their study XO was adsorbed to the resin Amberlyst A-26 and this was used to separate metal ions during column chromatography. System stability was excellent as XO was observed to bind strongly enough that a 1 mol L^{-1} HCl mobile phase caused only traces of the dye to be observed in the eluent.

Hence it was thought that when the similarly structured MTB was adsorbed to a suitable anion-exchange resin it would provide a stable binding phase, with no significant dye loss. A suitable cationic resin, which is closely related to Amberlyst A-26, is the cross-linked PSDVB based Dowex 1x8. This resin was expected to strongly adsorb MTB, and had been successfully fixed to a substrate for binding phase disc formation (see Chapter 2). Such a system would be anticipated to maintain the concentration gradient necessary for function as a DGT binding phase, without significant dye leaching.

MTB-metal interactions were qualitatively examined and, from this, the dye was confirmed as a prototyping agent. In particular, coloured Cu(II), Fe(II), and Zn(II) interactions were observed when MTB had been adsorbed onto Dowex 1x8. As MTB colour changes have been noted to provide linear colour response to increased metal loadings [8], the adsorbed dye was expected to provide a useful, quantifiable response to these analytes when examined using UV-Vis reflectance spectrophotometry. As such, the MTB based binding phase was considered a suitable system for initial studies into the colorimetric analysis of resin-adsorbed-dye based DGT binding phases.

3.2 – Experimental

3.2.1 – General Chemicals

The metal salts used were all of analytical grade and were (with water of hydration omitted): $CuSO_4$, $CdCl_2$, $MnCl_2$, $PbNO_3$ (Ajax Chemicals, Sydney, Australia); $FeSO_4$ and $ZnSO_4$ (BDH, Kilsyth, Australia). Ultrahigh quality (UHQ) water was sourced from a Barnstead (Thermo Scientific, Waltham, USA) water purifier with a conductivity of 18 ± 1 MΩ cm^{-1}. PO_4^{3-} buffers were made using low-metal PO_4^{3-} salts (p.a. grade Na_2HPO_4 and NaH_2PO_4, Riedel-de Haën, Seelze, Germany). Equipment was acid-washed using a 10% v/v HNO_3 bath.

3.2.2 – Dye Immobilisation

Solutions of MTB were prepared using indicator grade MTB dye (indicator grade, Riedel-de Haën, Seelze, Germany) in ultrapure water and stored at room temperature in the dark as 1 mmol L^{-1} aqueous stock. For dye immobilisation, vacuum dried Dowex 1x8 resin was suspended in ca. 50 mL of ultrapure water, which was then pH adjusted using 30% H_2SO_4 (AnalaR, BDH, Kilsyth, Australia), and 1 M NaOH (AnalaR, BDH, Kilsyth, Australia) while monitoring the pH with an Orion model 720A pH meter with a GPH Electrode probe. Typically a pH of 2 was used, but as discussed in the text a variety of pH values were employed, measured to ± 0.05 pH units. To this solution the 1 mmol L^{-1} MTB stock was added to provide the necessary resin loading, typically 10.0 mL of MTB solution was added to 1.00 g of resin for a loading of 10.0 μmol g^{-1} (expressed as μmol of dye per gram of dry

resin). This solution was shaken for 24 h at, or above, 100 rpm on a Lab Line Orbit shaker before the resin was collected by vacuum filtration onto Whatman #54 filter paper and air dried. Uptake was checked by a lack of colour in the supernatant solution. Air dried resin was adhered to 25.4 mm diameter Esselte 'Quik Stik' adhesive paper label (Stamford, Connecticut, USA) discs by removing the label's backing plastic and pushing the disc's adhesive side into a layer of resin on a glass plate. The accumulated resin was then spread over the disc using nitrile gloves, with light pressing. Discs were then tapped to remove excess resin.

Once resin-discs were made, equilibration of the resin was performed by immersing the discs in ultrapure water containing a 0.01 mol L^{-1} PO_4^{3-} pH buffer. After one or more hour's immersion in the equilibration solution, discs were removed and rinsed with deionised water in order to remove excess resin before being air dried. Resin and disc weights were determined to 0.01 mg using an analytical balance (Ohaus Analytical Plus, AP-250D-0, Ohaus Australia, Port Melbourne). During weight determinations, discs were vacuum-dried between equilibrations for at least 24 h to remove moisture using house vacuum.

3.2.3 – MTB Disc Metal Complexation

Loading of metals into a resin MTB disc was initially performed by exposing discs directly to a 50.0 mL solution containing a known metal quantity, calculated to provide the loading required at 100% uptake. For the typical case of a 10 μmol g^{-1} (μmol of MTB per gram of dry Dowex 1x8) disc, holding 16.3 mg of resin, this was 10.3 μg of Cu(II). Discs were exposed for 24 h with mixing on a Lab Line Orbit

shaker. Supernatant solutions from initial tests were examined using flame AAS (Varian SpectrAA 600, Mulgrave, Australia) to ensure complete uptake, with no Cu(II) detected. After exposure, discs were removed and rinsed with purified water before being colorimetrically analysed. Discs were air dried in a dark environment for long-term storage.

Homogenous coloration of the exposed disc area was achieved by using a polyacrylamide diffusive gel during Cu(II) complexation. DGT sampling devices were assembled in plastic DGT holders (3.14 cm^2 exposed area, DGT Research Ltd., Lancaster, UK), and consisted of a MTB-resin disc covered with a polyacrylamide hydrogel diffusion layer (0.82 mm thick, DGT Research Ltd., Lancaster, UK) and a Pall Tuffryn (Ann Arbor, Michigan, USA) polysulfone membrane (0.45 μm pore size, 145 μm thickness, HT-450 PALL). DGT holders and polyacrylamide hydrogel diffusion layers were acid-washed (1 mol L^{-1} HNO_3) before use. Sampler components were wetted with 0.01 mol L^{-1} PO_4^{3-} buffer during assembly to ensure that assembly could be achieved without trapping air between layers. DGT sampling devices were deployed into 200 mL polycarbonate containers (Sarsteadt, Ingle Farm, Australia), face-up. Exposure solutions consisted of 100 mL of a mixed 0.02 mol L^{-1} PO_4^{3-} buffer and 0.2 mol L^{-1} $NaNO_3$ solution, plus a volume of 10 mg L^{-1} Cu(II) to provide a range of concentrations between 54 and 270 μg L^{-1} of Cu(II) after the sample was diluted with UHQ water to 200 mL. DGT sampling devices were exposed to the uptake solution at 24.9 ± 1.8 °C and agitated at 100 rpm (Lab Line Orbit shaker) for 1, 2 or 3 days. Solutions for multi-day tests were remade on a daily basis with samplers transferred to the new solutions after 24 h. In all cases the

theoretical mass of Cu(II) removed from solution was less than 1%, ensuring no practical decrease in Cu(II) concentration.

3.2.4 – Metal extraction and analysis

Metal extraction was performed by placing dried resin discs, individually, in 70 mL polycarbonate containers (Sarsteadt, Ingle Farm, Australia) and adding 10.00 mL of 1 mol L^{-1} HNO_3 (from 65% w/v Suprapur, Merck, Darnstadt, Germany). Extraction solutions were shaken for 24 h on a Lab Line Orbit shaker before 40.00 mL of ultrapure water was added to the extract solution. This was then syringed-filtered (PALL Acrodisc GHP filters, 0.45 μm) prior to analysis. Weights were recorded at each step to determine the percentage of the extract solution recovered for analysis, using water and acid densities appropriate to the daily environmental temperature. Extraction efficiency tests were performed by repeating this process on extracted discs of the highest metal loading.

Initial analyses were performed at the Central Science Laboratory, University of Tasmania, on a magnetic-sector ICP-MS (Finnigan Element, Bremen, Germany). Further metal analyses were performed using a SpectrAA 800 AAS with GTA-95 graphite furnace attachment and PAL autosampler (Varian, Melbourne, Australia) at a wavelength of 324.8 nm and lamp current of 3 mA. The temperature profile used for Cu(II) analysis was (# indicates no gas flow) 85°C(5s), 95°C(40s), 120°C(10s), 800°C(5s), 800°C(1s)#, 2300°C(1.1s)#, 2300°C(2s)# and 2300°C(2s). Calibration was by a prepared Cu(II) standard solution, automatically diluted by the instrument

with 0.1 mol L^{-1} HNO_3 (from 65% w/v Suprapur, Merck, Darmstadt, Germany) in order to provide a comparable matrix.

3.2.5 – UV-Visible Spectroscopy

A Cary 1E spectrophotometer (Varian, Melbourne, Australia) was employed for all UV-Visible spectrophotometric measurements using Varian SpectrAA software (version 1.3). Resin-dye absorbance spectra were collected using 0.1 mm path length quartz cuvettes (Starna, Ingle Farm, Australia). Packing of the cuvette was achieved by adding resin as a water-slurry with a pipette, and allowing an hour or more to settle. Metal-loaded resin, without disc immobilisation, was obtained by exposing resin to metal stock solutions in ultrapure water with a 0.01 M pH 6.8 PO_4^{3-} buffer, providing amounts of metals equimolar or twice equimolar to the loaded dye as per the calculation in section 3.2.3. Uptake was performed in conical flasks and assumed to be completed 5 min after further colour development was no longer visible. Typically this was observed in less than 10 min.

Diffuse reflectance spectrophotometry was performed on MTB resin discs, prepared as discussed above, using a Labsphere DRA-CA-30I attachment (North Sutton, USA) with the 0° (diffuse) wedge; baselines were taken using either unmodified Dowex 1x8 resin or a Spectrafelct reflectance standard (AS-01158-060, USRS-99-010-0B69A, Labsphere, North Sutton, USA). To avoid variation in spectra caused by resin moisture, discs were analysed wet. Scattering due to water droplets was minimised by blotting discs with lint-free tissue paper, but removal of all moisture was avoided to ensure resin hydration. Discs were supported using a glass plate in

order to maintain a flat surface. Spectra obtained were saved as comma delineated spread sheet files (.csv) for access and analysis in Microsoft excel 2007 or 2004.

3.2.6 – Dye stability

MTB resin-discs were bleached by exposure to a 60 W incandescent bulb at a distance of 1 to 5 cm until the green MTB (without complexed metal) was no longer coloured, typically taking 2 weeks. Exposure to UV light was also tested by containing the discs in a 'black-light' box (containing four Philips TUV 6 W 57 416E/40 bulbs) for a comparable amount of time to the incandescent exposure. Temperature tests were performed by placing discs in a 70°C drying oven, or covered by aluminium foil and placed under an incandescent bulb at a distance of 3 to 5 cm for 2 weeks. LED Z(Light Emitting Diode) exposure was performed in a custom light box with power supplied from a Dick Smith Electronics Q1760 DC power converter, using Z0862A (red), Z0865A (green) and Z0869 (blue) LEDs (Altronics, Perth, Australia).

As NO_3^- was seen to have an effect on dye adsorption, stability tests were performed to confirm this. Dye loss tests for matrices containing $NaNO_3$ (AnalaR, ChemSupply, Sydney, Australia) and PO_4^{3-} were performed with NaCl (AR grade, Univar, Melbourne, Australia) as an accessory ionic buffer. Ion concentrations were set so total ionic strength was equivalent to 1 mol L^{-1} KCl, with $NaNO_3$ concentrations of 0.01, 0.1 and 1 mol L^{-1} and PO_4^{3-} concentrations of 0.001, 0.01 and 0.1 mol L^{-1}. The remaining ionic strength was provided by NaCl, considered to be effectively inert due to the presence of Na^+ ions from MTB and buffer salts, and

the presence of Cl^- ions as the Dowex 1x8 counter ion. Direct exposure of the MTB resin discs to Cu(II) was performed in both cases using 5 μg of Cu(II) per disc with the removal of discs after 5 h. Further PO_4^{3-} tests were performed with DGT assemblies as per homogeneous colouration, Section 3.2.3, with the same NaCl and PO_4^{3-} concentrations as in the direct PO_4^{3-} test and a Cu(II) concentration of 259 μg L^{-1}. The difference in Cu(II) uptake between these solutions was used to determine test results. After exposure all discs were colorimetrically assessed and metal ions subsequently extracted. Average temperature across the exposure during the DGT like test was 25°C.

3.2.7 - Statistics

The statistical tests used were Student's T test and Dixon's Q-test for outliers. Where error/variation in results is discussed the value given for error is ± one standard deviation, unless otherwise mentioned. Relative standard deviations are described by the acronym 'RSD'.

3.3 – Results and Discussion

3.3.1 – Binding Phase Construction

In the initial attempts to adsorb MTB onto Dowex 1x8 resin a gram of wet resin was added to 100 mL of a 5 mmol L^{-1} aqueous solution of the dye. As pH was known to affect the coloration of MTB in solution, and also MTB's chelating properties, an examination of the affect that the adsorption solution's pH had on the MTB binding phase colour was undertaken. This was performed by adjusting the adsorption solution pH to integral values from 1 through to 10. In effect, this range of pH values allowed for observation of the impact that increasing the number of ionised functional groups had on adsorption, with reference to pK_a values (see Figure 3.1). After allowing 24 h for dye adsorption, the resin discs were equilibrated in a pH 6.8 solution. The collected reflectance spectra are shown in Figure 3.2.

Visual observation of fresh discs showed that those with adsorption pH values of 2 and 10 appeared to be the most strongly coloured. This indicated that either a larger quantity of MTB had been adsorbed, or that there were more favorable colour properties due to the adsorption mechanism at these pH values. Spectra differ slightly at the intermediate pH values of 3 and 6, there was concern that a change in metal response may occur if these adsorption pH values were employed. In terms of practical work, adsorption pH values of 3 or 6 were avoided to maintain constant visible light behavior, and tests were performed using adsorption pH values of 2 or 10. When adsorption was carried out at these two pH values the resin with adsorbed MTB was referred to as MTB(2) or MTB(10), respectively.

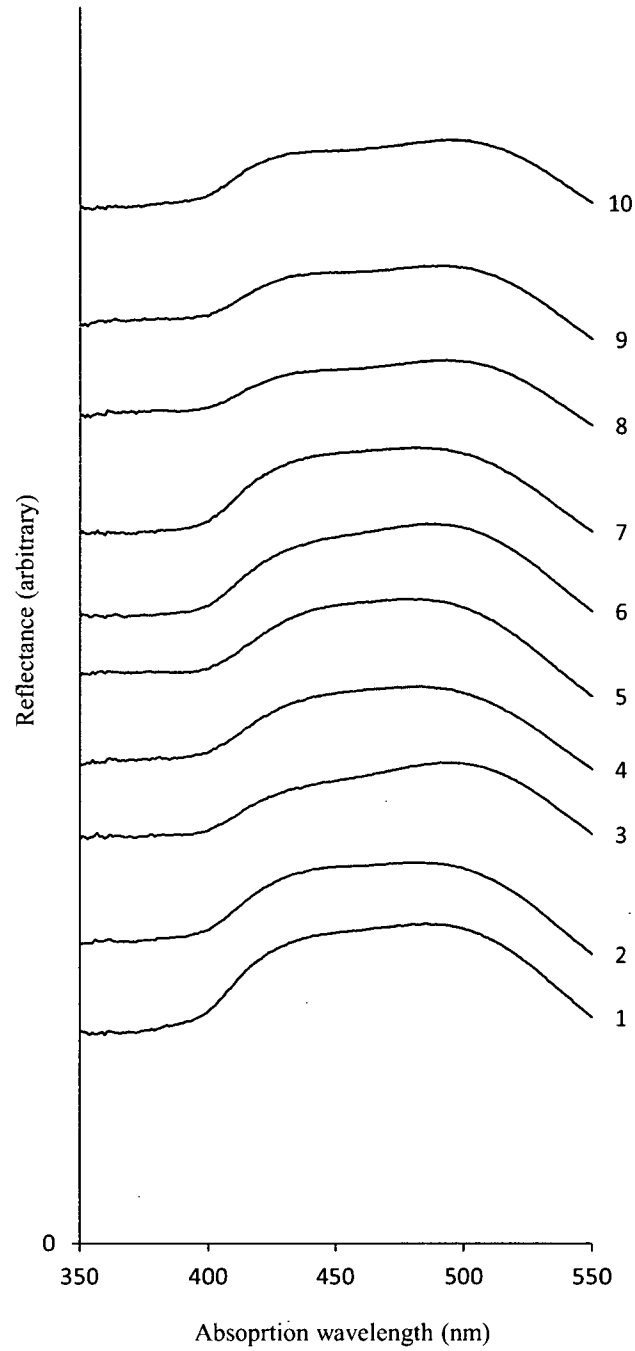

Figure 3.2 – Variable region of UV-Visible spectrum on MTB adsorbed at pHs incremental from 1, shown on right.

MTB(2) and MTB(10) displayed responses to pH changes as expected, showing yellow discs at low pH, moving through green at about pH 5 and turning blue above a pH of 8. Interestingly, this intermediate green colour is not reported by Yoshino et al. [8], but rather a gray colour. Gray colouration was seen on the initial drying of the MTB(10) resin, after dye adsorption but before resin immobilisation. Once the discs were dried from the equilibration step they obtained a permanent green colour for the neutral pH range, even through successive wetting/drying cycles.

With these discs, colour change on metal exposure was observed, but the change upon addition of metals to this resin required greater than μg metal quantities per disc, whereas a sub μg per disc detection limit was desired. As it was known that XO did have a better colorimetric detection limit than MTB had displayed with some transition metals [8], methods for lowering the detection limit were considered.

As the detection limit was the point at which an overall colour change was detectable, the proportion of dye that needed to be complexed for an overall colour change was determined. To this end Cu(II) was used to measure these properties, as it had been seen to provide a strong colour in a short amount of time. Dye loading on these discs was in the order of 1 mmol of dye per gram of dry resin, giving approximately 62.5 μmol of dye per disc. Cu(II) coloration was not observed at this dye loading until more than 10 μg, or 0.16 μmol, of Cu(II) was added. This was stoichiometrically equivalent to approximately 0.3% of the dye present, and it was thought that this represented the minimum percentage of complexed dye to obtain a significant colour change. As such, it was thought that decreasing the total dye quantity would lower the detection limit.

A more precise dye loading of 10.0 μmol of MTB per 1.00 gram of Dowex 1x8 resin was used, with the resin added dry to remove any variation in mass due to moisture content. With these discs a metal quantity as small as 50 ng of Cu(II) could be visually observed on a disc holding 16 mg of resin. In terms of molar quantities this meant that less than 0.8 nmol of Cu(II) was observable with 160 nmol of dye, showing that as little as 0.5% of the dye needed to be complexed for an observable change at this dye loading. To allow comparison between metal loadings in different physical forms (e.g., a sediment vs. aqueous probe), metal loadings were described in terms of the mass of metal per area of resin disc. The above loading of 50 ng of Cu(II) on a 5.07 cm^2 disc was, therefore, described as a Cu(II) loading of 10 ng cm^{-2}. These comparisons require a consistent resin mass and dye loading per area and, as such, are only applicable when comparing binding phases of the same resin type, mesh size and dye loading. For ease of reference, a molar dye loading per mass of resin is expressed henceforth as μmol g^{-1}, whereas metal loadings are expressed as μg cm^{-2}.

Assuming that the Cu(II)- MTB interactions were equimolar, meaning one Cu(II) ion was complexed to a single adsorbed MTB molecule, a theoretical disc capacity can be calculated. A disc loaded at 10 μmol MTB g^{-1} of resin, and with 16.3 ± 0.6 mg of resin adhered to a disc, would be able to complex a maximum of 10.4 ± 0.4 μg of Cu(II), or approximately 2 μg cm^{-2}. As mentioned above, the lower observable limit was 0.01 μg cm^{-2}. While this does not allow a large practical range for metal response compared to Chelex 100-based DGT samplers, it is worth considering this in terms of environmental monitoring work. The ANZECC and ARMCANZ water quality management strategy [11] proposes trigger levels of 0.3 to 8 μg L^{-1} for Cu in

marine water systems. This lower level would be detectable by a disc with a loading of 10 μmol g^{-1} in water at 10°C after a two week deployment time, and the upper level after less than a day, if the DGT equation [12] is followed.

Attempts were made to further decrease this detection time by reducing dye loading, but with dye loadings below 10 μmol g^{-1} the discs suffered from significant instability in colour over a two week immersion. This was determined to be largely due to visible light instability in the MTB discs, as discussed later in this chapter, but for shorter deployment times disc loadings as low as 2 μmol g^{-1} of resin have been seen to provide a coloured Cu(II) response.

As such, for the use of MTB as a binding phase chelating agent it was found that 10 μmol g^{-1} provided a loading that appeared robust and allowed for the desired detection limits to be achieved.

3.3.2 - Metal Interactions

MTB interactions with Cu(II), Fe(II), Zn(II), Mn(II), Cd(II) and Pb(II) were examined in detail using three methods; aqueous UV-Vis absorptivity, resin-adsorbed UV-Vis absorptivity and resin-adsorbed reflectance using paper label disc backings. Examinations of the UV-Vis absorption spectra of MTB-metal solutions were performed at pH 6.8, chosen to permit comparison with the expected deployment conditions. These studies were complicated by the presence of free dye and, in some cases, insoluble metal species. Figure 3.3 shows that a level of interaction was observed with most divalent metal cations, with an increase in the 600 nm absorption band and, typically, a local minimum around 400 nm. These

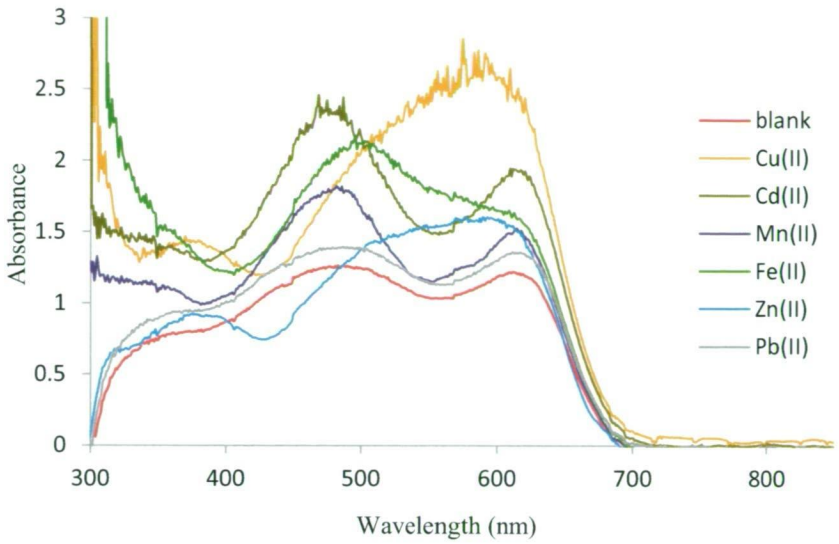

Figure 3.3 – Aqueous UV-Vis absorption of MTB with several divalent metal cations. Strong, unique interactions are observed for Cu(II), Fe(II) and Zn(II). Note absorption is high throughout the region of interest.

observations agree well with the results reported by Yoshino and co-workers for a selection of metal ions [8]. Solution coloration was not visibly varied, with all metal containing solutions appearing a faint yellow-orange. This was understandable as absorbance was high across all sub-650 nm wavelengths.

When adsorbed onto Dowex 1x8, 10 μmol g^{-1} MTB(10) a colour change was seen on exposure to Fe(II) to burgundy, and on exposure to Cu(II) and Zn(II) solutions to purple but the resin remained green for the other metals tested. This was examined through UV-Vis absorbance using 1 mm quartz cuvettes packed with resin (Figure 3.4). It can be seen that the spectra of the blank and of MTB with Pb(II) are similar. Similarities can also be seen between the MTB complexed Mn(II) and Cd(II) spectra, with very similar relative absorbance between the two peaks. Spectral variations of MTB with these four metals present are in the intensity of the overall

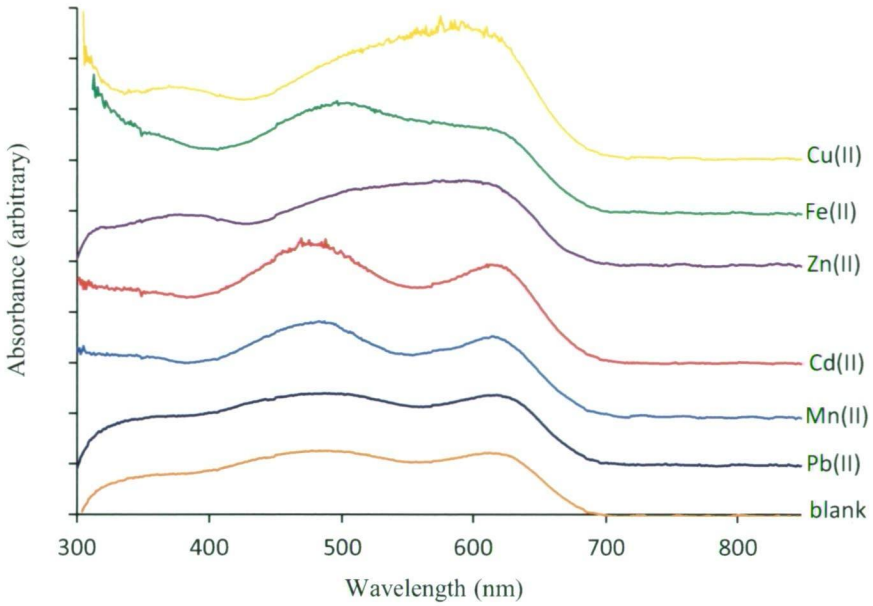

Figure 3.4 – UV-Vis absorption spectra of MTB(10) metal interactions with equimolar metal loadings. Unique spectra are observed with Zn(II), Fe(II) and Cu(II).

spectra, rather than the wavelengths of the two absorbance maxima. The variation in the absorbance of these spectra may have been due to resin packing in the cuvette. Yoshimura and Waki [4] discuss that the absorption of a resin-adsorbed dye system is due to a combination of four light-interacting factors, 3 of which are affected by resin packing. The remaining 3 spectra do provide significant structural differences that cannot be explained by packing, as the absorbance maxima and minima differ substantially from the blank. These spectra show that Zn(II), Fe(II) and Cu(II) interact with the dye in a novel, and potentially quantifiable, way.

For reflectance analysis, discs were made from the same resin samples used for the UV-Vis absorption spectra, shown in Figure 3.4, after drying and equilibrating to

provide an even well-packed resin layer (as discussed in Chapter 2). Large variations were seen between the dry discs, and this was thought to be primarily due to moisture content [13]. As the reflectance response of wet discs was more consistent than air-dried discs, and not substantially weaker, it was decided that wet analysis would provide a more precise method. Reflectance spectra of the resin-adsorbed MTB metal interactions are shown in Figure 3.5, and it can be seen that at equimolar loadings no qualitative differences are observed between the blank spectrum and those for Mn(II), Cd(II) and Pb(II). Examination of the resin in this fashion proved substantially more precise than with the use of resin-packed cuvettes. This was partially due to the swelling of resin during equilibration providing a very tight, consistent packing from this technique. These results support the belief that the variation in the absorbance spectra of these resin-adsorbed MTB metal interactions (Figure 4) differed due to packing rather than resin character.

Taking into account the complementary, but inverse, nature of reflectance and absorption spectroscopy, similarities were observed between Figure 4 and Figure 5, particularly with regard to the novel Cu(II), Zn(II) and Fe(II) responses between 500 and 650 nm. Interestingly, Cu(II) and Zn(II) no longer appeared to share the same reflectance spectrum, but rather Zn(II) showed both maxima and minima at a slightly lower wavelength than Cu(II), with an apparent reflectance minimum at 530 nm rather than 570 nm. This was not considered to be due to a chemical change, as it was unlikely that a different binding mode resulted from the transfer of packed resin beads to a label-immobilised layer. The possibility of this being due to resin drying during immobilisation and analysis was examined, as a solvatochromic shift

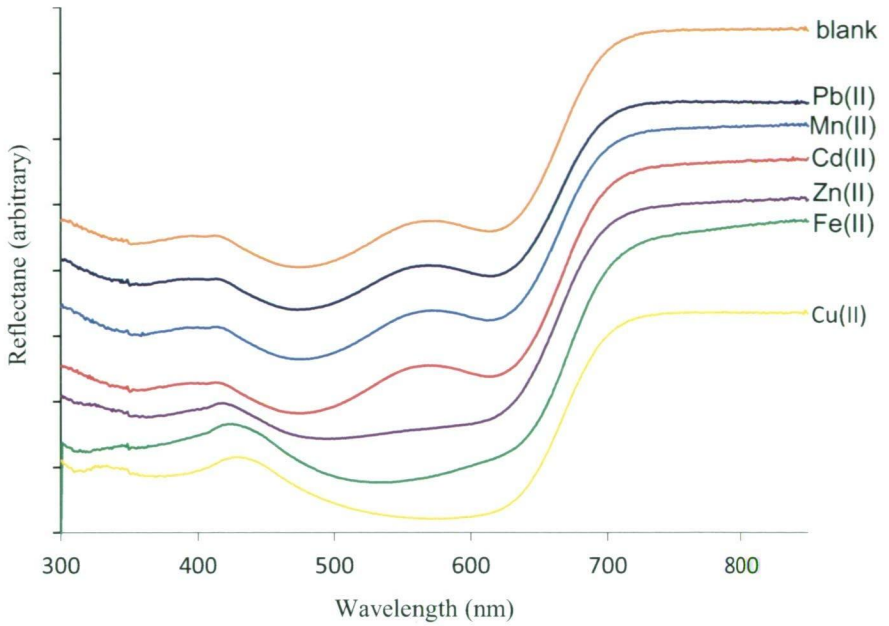

Figure 3.5 – Diffuse reflectance spectra of MTB(10) metal interactions using resin from absorptivity test in Figure 4. Similar spectra for Pb(II), Mn(II) and Cd(II) to the blank indicate no metal interaction.

during drying may have shown significant changes in the wavelength of maximum absorption.

However, variation of less than 5 nm was observed between discs thoroughly wet and those having been blotted and air dried for 15 min, a substantially longer time than would have occurred during normal analysis. Rather, it appears this is a difference that is either not visible using absorbance studies, or is masked by the method in which absorbance studies are carried out. It may also be due to background interference from the paper labels, though this is less likely as it would be expected to impact on the Cu(II) and Zn(II) spectra in the same manner. In either

case, discrimination of the Zn(II) and Cu(II) profiles may be possible using diffuse reflectance spectra.

During the absorbance and reflectance experiments with the MTB resin, Cu(II) was consistently seen to provide the best colorimetric response. To this end, Cu(II) was used to further examine the disc character and suitability for DGT deployment. In order to perform this it was necessary to have an understanding of the interaction of Cu(II) with the adsorbed MTB, in terms of metal-to-dye ratios. Complexed Cu(II) to MTB ratios of 1:1 and 2:1 have been studied in aqueous solutions, with an observable difference in colour between the two complexes. The compounds were seen to readily form when the appropriate amount of Cu(II) was present [8].

However, qualitative observation of the Cu(II) interaction with resin-adsorbed MTB discs had shown the development of only one colour up to stoichiometric metal to dye ratios of 10:1. As such, only one form of dye-to-metal interaction appeared to be occurring. To examine the interaction, Cu(II) was added to solution with the discs at ratios to the adsorbed MTB of 0.1, 0.3, 0.45, 0.6, 0.8, 0.9, 1 and 2. An increase in colour was observed to a maximum at the equimolar (1:1) Cu(II) quantity. As such, the Cu(II) interaction with MTB on these discs was taken to be 1:1, and 2:1 metal complexes did not appear to be formed as readily as in solution. Exposure of the discs to a Cu(II) ratio more than an order of magnitude in excess produced a light blue colour, similar to the aqueous 2:1 Cu(II) complex as reported by Yoshino et al. [8]. Both reported interactions of MTB with Cu(II) have, therefore, been observed but the adsorption of the dye onto a resin has resulted in the 2:1 complex being less easily formed at pH 6.8. This is potentially due to the positive charge being formed on the MTB molecule interacting with the neutral/cationic Dowex 1x8 resin matrix.

In general, UV-Visible work with the MTB resins indicated that Cu(II) would be the best analyte for further work in the system because it showed the best response and the most distinct spectrum, plus the interaction of Cu(II) with the resin-phase MTB was observed to be equimolar. It was also necessary to monitor resin moisture conditions as they were of some importance to analysis, and to avoid this discs were kept wet during analysis.

3.3.3 – Cu(II) Complex Retention and Stability with Adsorbed MTB(10)

DGT deployment times of up to 7 weeks have been reported [14], and consequently the desorption of the Cu(II)-dye complex from the resin was assessed to ensure the Cu(II)-dye complex remained adsorbed during long deployment times. Due to the adsorption of the dye from solutions over a large pH range (Section 3.3.1) resulting in effectively 100% uptake, the retention of the dye on Dowex 1x8 resin over a near-neutral range of pH values was not considered an issue, and was not studied.

Instability of the Cu(II) complexed dye was examined by immersing 2, 4, and 10 $\mu mol\ g^{-1}$ MTB(10) discs, with equimolar Cu(II) loadings, in ultrapure water and observing colour change. After a two week immersion, with minimal light exposure, the spectra in Figure 3.6 were obtained from the average reflectance values of triplicate samples. It can be seen that the Cu(II)-dye complex is not completely stable as a statistically significant difference was observed between the before-and- after discs of the 2 and 4 $\mu mol\ g^{-1}$ loadings at 300 nm ($T_{2\mu mol}$=5.851, $T_{4\ \mu mol}$ =3.398, $T_{95\%C.I.,\ 2D.F.}$=2.78) and 600nm ($T_{2\ \mu mol}$=4.329, $T_{4\ \mu mol}$=2.994), and with the 2 $\mu mol\ g^{-1}$ loadings at 430 nm ($T_{2\ \mu mol}$=7.343). However, this change does not

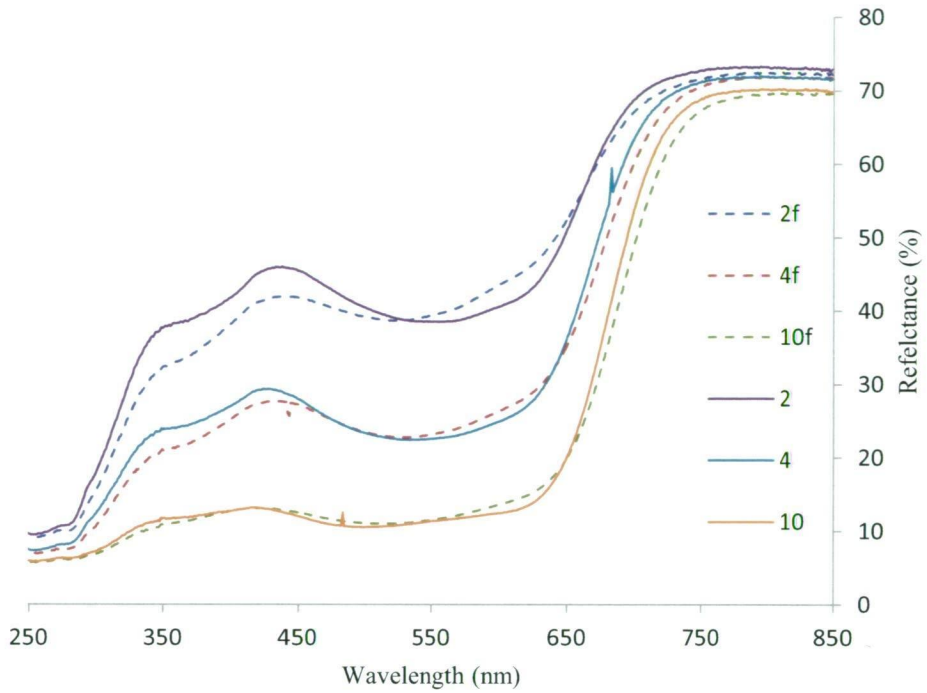

Figure 3.6 – Results of a 2 week immersion of Cu(II) adsorbed MTB discs of 2, 4, or 10 μmol g^{-1} dye loadings. Spectra after the two weeks are identified by a dashed line and 'f' tag in the key. Reflectance pairs are 2, 4 and 10μmol of MTB g^{-1} of Dowex 1x8 resin in descending order. Note dye instability is inversely proportional to loading.

appear to be due to dye desorption as this would result in a higher reflectance across the spectrum due to the decreasing MTB absorption of light. Rather, this indicates the loss of Cu(II) from the dye and a reversion of the molecule to the uncomplexed form (spectra shown in Figure 5).

Loss was more pronounced for the lower dye loadings and, as Cu(II) complexation was equimolar in all cases, this was not proportional to the resin's complexed Cu(II) quantity, indicating that this was not thermodynamic instability. As the 10 μmol g^{-1} discs did not show statistically significant changes (at the 95% confidence interval,

for 300, 430 and 600 nm at 4 degrees of freedom, $t<2.132$), the instability was not deemed significant over the two-week time periods involved here. Hence, a 10 μmol g^{-1} loading was considered the minimum for reliable dye-Cu(II) complex stability over periods of two weeks or less. Alongside using this loading it was considered pertinent to restrict deployment times to several days in order to further prevent Cu(II) loss.

The MTB dye itself appeared to be adsorbed in a stable manner on immersed resin at loadings of 10 μmol g^{-1} and above, with acid extraction conditions (1mol L^{-1} HNO_3 for 24 h) not causing either coloration of the supernatant or noticeable colour loss from the disc. However, in subsequent work it was found that NO_3^- ions in a $NaNO_3$ solution desorbed small, but colorimetrically significant, dye quantities at a pH of 6.8. Why this was not observed with HNO_3 is not clear, although the protonation of ionic sites may have reduced the ability of the NO_3^- ion to interact with the MTB molecule. Combined with a resulting increase in the importance of the π-π adsorption [15], this may have increased stability at low pH.

Observations at a pH of 6.8 were that a NO_3^- concentration of greater than 0.1 mol L^{-1} resulted in lower Cu(II) complexation. This was confirmed by acid extraction and AAS analysis where it was seen that the extracted Cu(II) quantities for NO_3^- concentrations of 0.001, 0.01, 0.1 and 1 mol L^{-1}, were 2.64 ± 0.14, 2.82 ± 0.13, 2.57 ± 0.14 and 1.84 ± 0.06 μg, respectively. This leaching of resin-adsorbed MTB was not observed with seawater, PO_4^{3-} buffer, or high NaCl concentrations.

The cause of this desorption may be due to the anion-exchange site having a higher affinity for NO_3^- than for MTB, leading to MTB loss as a result of ion-exchange.

This is analogous to the impact of Cl^- and CH_3COO^- counter ions on Tiron immobilisation, where the presence of these ions had a negative impact on Tiron stability due to their affinity for the resin matrix [16]. The impact of this on DGT deployment is discussed later, along with a more detailed analysis of the ion affinity concerns, but it is worth noting here that UV-Vis analysis indicated dye loss from the resin, rather than Cu(II) loss from the MTB-Cu(II) complex, in the presence of NO_3^-.

Under the course of regular work MTB(2) and MTB(10) were seen to 'bleach' when left exposed to ambient laboratory light. In order to ascertain the cause of the bleaching discs were exposed to UV light from a fluorescent 'black light', to visible light using an incandescent bulb, and to LEDs of three colours (red, green and blue). Heat exposure was tested at 70°C in a drying oven and by placing aluminium-foil covered discs at approximately 2 cm from an incandescent bulb, in order to provide heat comparable to that during bleaching with visible light. After exposure for two weeks, the UV light and heat tests did not have an appreciable effect on disc coloration, but exposure to a 60 W incandescent light source at 2 cm resulted in the loss of colour from 10 μmol g^{-1} discs without complexed Cu(II). Coloured LEDs also caused significant bleaching over 48 h, but the point-source nature of the light did not provide even bleaching across the disc. Bleached discs were visually off-white and visibly identical to un-absorbed Dowex 1x8 resin discs and, as such, visible light was believed to be degrading the chromophore of the MTB.

It was also noticed that the time since dye adsorption had an impact on dye degradation and desorption. For resin where the dye had been adsorbed less than 2 months before use no dye loss was observed visually in 1 mol L^{-1} NO_3^- solutions and

no light bleaching was apparent after 24 h. Dye adsorbed more than 6 months prior to testing with MTB loadings of 20 μmol g^{-1} showed substantial colour loss in 1 mol L^{-1} $NaNO_3$ solutions after a few hours, though loss to ultrapure water or 0.1 mol L^{-1} phosphate solutions was not observed from the same discs over this time period. Increased time since adsorption also resulted in substantially higher sensitivity to visible light bleaching, with 6 month old 10 μmol g^{-1} discs completely bleached within 24 h. Cu(II) complexed discs older than 6 months also bleached readily, with the metal exposed areas losing all colour over a 48 hour period.

The stability concerns in the presence of NO_3^-, in visible light, and at low dye loadings, set practical limits on the use of MTB(2) and MTB(10) samplers. The low light stability necessitated that binding phases be shielded from light, and that exposure to light during handling was kept to a minimum. The increased impact of light with the disc age implies that adsorption in the weeks prior to use is the best method for consistent results. Other than these concerns, binding phases were physically robust, wet or dry, and chemically stable at low NO_3^- concentrations. They were considered suitable for use in the month following dye adsorption at a loading of 10 μmol g^{-1}, for deployments of up to 2 weeks.

3.3.4 – Cu(II) Uptake by MTB Binding Phase Discs

3.3.4.1 – ICP-MS Results

As the Cu(II) interaction with a MTB(10) system was understood to be 1:1 for Cu(II) levels up to, and marginally beyond, equimolar, a calibration was performed with discs of a 10 μmol g^{-1} loading up to an equimolar Cu(II) to MTB ratio. This

was justified as DGT deployment in waters contaminated with Cu(II) at the ANZECC lower trigger concentration (0.3 μg L^{-1} [17]) would be expected to obtain equimolar Cu(II) at this loading after several weeks of deployment. A quantifiable result could be obtained after a day at that concentration and a 10 μmol g^{-1} loading would, therefore, be appropriate for monitoring deployment. Calibration was performed by loading discs with Cu(II) amounts up to equimolar as a '100%' maximum. As typical discs held $1.63x10^{-2}$ g of resin, 0.163 μmol of MTB would be expected on a disc at a 10μmol g^{-1} loading, equating to 10.4 μg of Cu(II) at 100% loading. For simplicity's sake, and to allow for variation in disc resin levels (an RSD of 5%, see Chapter 2), 10 μg of Cu(II) was used as a theoretical 100% loading, expressed as 2 μg cm^{-2} as discussed earlier.

For accurate calibration it was necessary to complex Cu(II) via a diffusive gel using a DGT sampling device, the reasons for which are discussed in Section 3.3.4.3. Using this uptake method the accumulated Cu(II) was extracted and analysed using ICP-MS to determine the quantities loaded. These values were then compared to those predicted using the DGT equation [12] in order to determine whether the discs were functioning correctly as binding phases. Figure 3.7 shows metal loading as a function of bulk solution concentration (a) and time (b).

Linear uptake is observed in both cases and a zero-intercept linear relationship is seen to have a strong fit using regression (R^2 values of 0.9945 for [a], and 0.9779 for [b]). As it has been noted that a 50% loading could be regarded as a theoretical maximum for passive sampling [18], the maximum loading observed of 28% was thought to be suitable as it represented a large portion of the expected useful range for DGT analysis.

However, this loading was lower than that expected from an initial calculation of the accumulated mass, performed using the bulk solution concentrations shown in Figure 3.7 along with the following constants: $D = 5.42 \times 10^{-6}$ mol cm^{-2} (appropriate for the test temperature), $a = 3.14$ cm^2, and $\Delta g = 0.08$ cm. In all, an accumulated mass 28% of that expected was observed. Extraction efficiency was measured by performing a second extraction on discs which, when analysed for Cu(II) content, did not show significant levels indicating an extraction efficiency greater than 99%. This 28% loading, therefore, represented the total Cu(II) accumulation.

The case of incomplete complexation, which would reduce the concentration gradient and consequently the Cu(II) flux across the diffusive layer, was not a likely explanation for this lower than expected Cu(II) loading due to MTB discs having been observed to completely bind equimolar quantities of metal in 24 h. Increases in the diffusive boundary layer thickness were also unlikely as the Cu(II) uptake solutions were shaken during the experimental time period in an effort to minimise the boundary layer. Whilst it can be expected that the boundary layer might vary from that reported by Camusso and Gasparella of 0.24 mm for a well shaken flask [19], for the boundary layer to account for the lower than expected Cu(II) uptake observed it would have needed to be an unreasonably thick 1.6 mm. To confirm this, diffusive boundary layer (DBL) tests of the type performed by Warnken et al. [20] were undertaken using Δg values of 0.56, 0.96 and 1.78 mm to check this assumption, with shaking at 100 rpm, providing a DBL thickness measurement of 0.3 ± 0.1 mm. As such, increased DBL was not considered a primary cause of the lower than expected uptake.

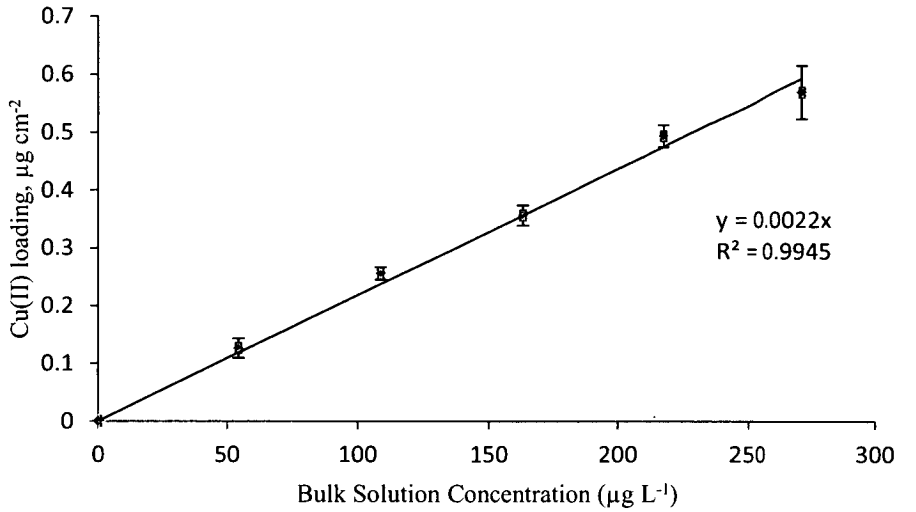

a) 24 hour exposures

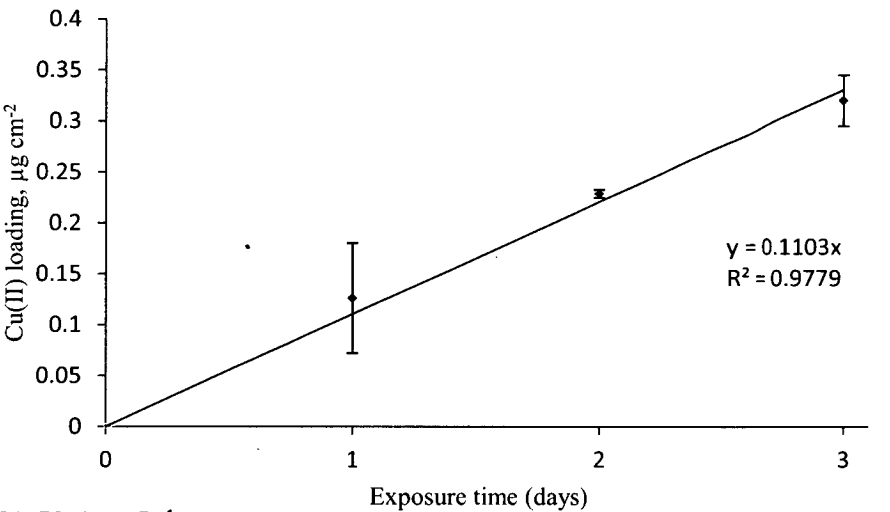

b) 53.4 µg L^{-1} exposures

Figure 3.7 – At top, (a) shows Cu(II) accumulation is linear to bulk solution concentration over a 24 h deployment time. At bottom, (b) shows Cu(II) uptake is linear with time. This shows DGT function with MTB binding phases.

Ionic effects were considered possible causes, with the paper label or exchange resin perhaps acting as a source for excess ions. This was supported by an observed bulging of the diffusion gels when the polysulfone or cellulose acetate protecting membrane was not used in previous tests, although in the case of the above DGT uptake experiments a protective membrane was used which precluded bulging. Alongside the membrane an ionic buffer was used to counter osmotic effects, as it had been seen to minimise the effects of this bulging without a membrane present, and this buffer was examined as a potential source of interfering species.

As the buffer contents were $NaNO_3$ and Na_2HPO_4/NaH_2PO_4, these were considered potential interferences that may have led to either lower available metal concentrations, or direct inhibition of the ability of MTB to complex Cu(II). As PO_4^{3-} is known to complex Cu(II) ions [21], the effect of PO_4^{3-} was tested in the absence of NO_3^- and compared to the DGT calibration results. In order to maintain comparable ionic strength to the DGT tests NaCl was added, which was not considered likely to interfere as both Na^+ and Cl^- are ubiquitous in all tests due to the use of Na^+ in dye and buffer salts and Cl^- as the resin counter-ion. After 24 h of exposure to 259 $\mu g\ L^{-1}$ of Cu(II), the samplers were extracted and the absorbed metal quantified to calculate diffusion coefficients. For PO_4^{3-} concentrations of 1 $x10^{-1}$, 1 $x10^{-2}$ and 0 mol L^{-1} diffusion coefficients of $6.5 \pm 0.3\ x10^{-6}$, $6.4 \pm 0.1\ x10^{-6}$ and $6.8 \pm 0.5\ x10^{-6}\ cm^2\ s^{-1}$ were calculated, respectively. These compare favorably with the anticipated value of $6.23\ x10^{-6}\ cm^2\ s^{-1}$ [20]. These results indicated that PO_4^{3-} was not responsible for the observed decrease in Cu(II) uptake during DGT tests, with the 0 M PO_4^{3-} 'blank' (containing solely NaCl) results also confirming that Na^+ and Cl^- were not interfering.

As PO_4^{3-} was not seen to cause a decrease in Cu(II) uptake, NO_3^- was considered next. Since a new pH buffer would be needed for a comparable test, which would introduce more ionic complexity, it was decided that testing of the effect of NO_3^- on the MTB binding phases directly, i.e. without a diffusive layer, would be a more prudent course. In this test, triplicate discs were immersed in $NaNO_3$ solutions of 0, 0.01, 0.1 and 1 mol L^{-1}, with NaCl used to maintain ionic strength. The discs were exposed to 2.5 μg of Cu(II) for 3 h before being removed, extracted and analysed using GF-AAS analysis. Extracted metal quantities were 2.6 ± 0.1, 2.8 ± 0.1, 2.6 ± 0.1 and 1.84 ± 0.06 μg per disc, respectively, for increasing NO_3^- concentrations. It can be seen that the highest NO_3^- concentration caused a distinct decrease in adsorbed Cu(II). This decrease shows that NO_3^- was having an effect on the Cu(II) uptake by the resin, and when considered alongside the previously observed dye desorption it was believed that NO_3^- was causing the loss of MTB from the resin.

In explanation, NO_3^- has been noted to have a high affinity for strongly basic ion-exchange systems such as Dowex 1x8, with the quaternary ammonium Amberlite IRN-78 resin showing significantly higher affinity for NO_3^- than Cl^-. The Cl^- ion is, in turn, similar to sulfonate-like (HSO_3^-) anions, such as the primary ionic moiety in MTB [22]. If ion-exchange was the cause of this desorption then I^-, Br^-, ClO_4^-, NO_2^- and SCN^- are also of concern as they have higher affinities for quaternary ammonium resins than chloride. These ions are typically not present in significant concentrations environmentally, however these factors are important to consider.

3.3.4.2– UV-Vis Analysis of Directly Exposed Discs

Colorimetric analysis of Cu(II) exposed discs was performed by using diffuse reflectance UV-Vis spectrophotometry. For calibration it was thought that analysis of discs exposed directly to controlled quantities of Cu(II), without diffusive gels, would provide the best method for assessing colour response. Before analysis the discs were immersed in water until the paper label was thoroughly wet, and excess water was gently blotted away. This was to ensure that resin hydration was maintained at a consistent level, and avoided hypsochromic issues. Testing showed that analysis following this procedure was reproducible, with RSDs of less than 1% provided that measurements were taken within 5 min. The highest sensitivity was provided at a wavelength of 560 nm, as seen for MTB(10) in Figure 3.8. A comparison of MTB(2) and MTB(10) disc calibrations, under the same conditions, is shown below in Figure 3.9a. A similar response was obtained for both MTB-resins, but lower standard deviations show that MTB(10) was more precise. As such, MTB(10) was used in further tests. A separate calibration of the MTB(10) discs, with higher resolution in the sub-equimolar range, is shown in Figure 3.9b.

A linear reflectance response to Cu(II) was obtained using MTB(10), with the highest sensitivity at a wavelength of 560 nm and linear regime ending around 1.2 μg Cu(II) cm^{-2}. Relatively large variation can be seen, in some cases 30% of the total response, with an average of ± 0.8% reflectance. As an approximately 1:1 loading of 2 μg cm^{-2} is approached the response decreases substantially.

To explore the cause of this non-linearity absorbance studies were performed using MTB(10) where the Cu(II) complexation had been undertaken with the resin free in

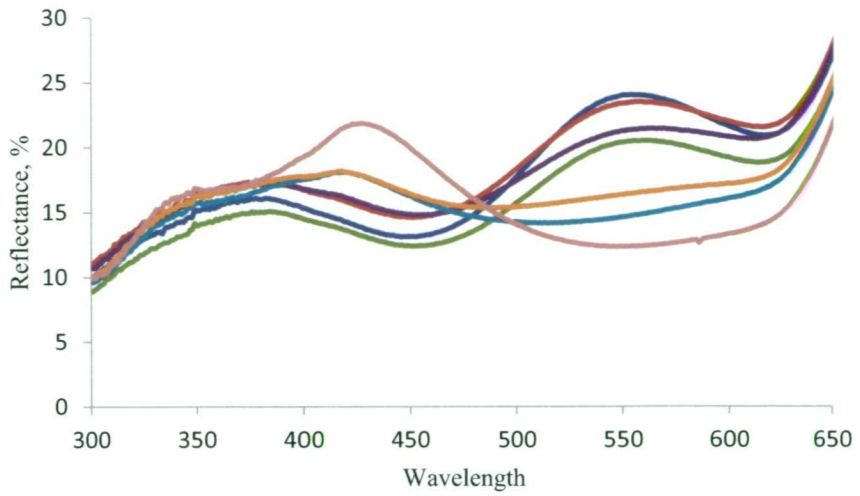

Figure 3.8 – Reflectance spectra for MTB(10) discs showing the highest colorimetric response at 560 nm. Loadings are, from top to bottom at 550 nm, 0, 0.01, 0.1, 0.2, 0.6, 1 and 1.4, in μg cm^{-2} of Cu(II).

solution, rather than immobilised on discs. In this way any source of heterogeneity from the disc-bound resin and reflectance system would be negated, and an even colouration across resin bead surfaces was seen. This resin was then analysed using UV-Vis absorbance in 1 mm path length quartz cuvettes. In Figure 3.10a it can be seen that as copper loading increases a bathochromic shift is seen, with the 560 nm feature moving approximately 3-5 nm towards the red end of the spectrum for every 10% increase in Cu(II) loading. This is more pronounced at higher loadings, and if the maximum absorbance of around 550 nm is considered independently of wavelength, rather than reflectance at 560 nm as shown in Figures 3.9a and 3.9b, the MTB-resin shows a linear response past 80% Cu(II) loading as seen in Figure 3.10b.

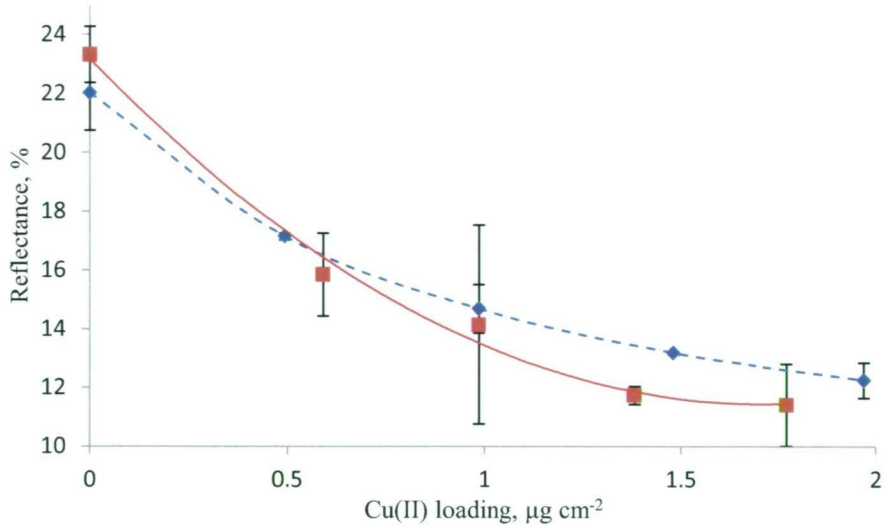

Figure 3.9a – Calibration of MTB(10) (dashed) and MTB(2) with Cu(II) (solid) using UV-Vis diffuse reflectance at 560 nm.

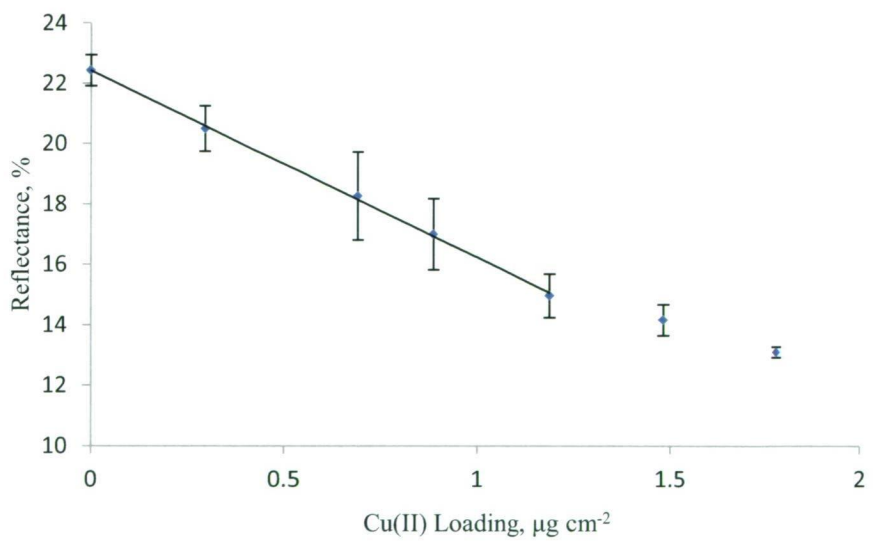

Figure 3.9b – Higher resolution calibration of MTB(10) discs using direct Cu(II) uptake by immersion in Cu(II) solution. Analysis was via UV-Vis reflectance spectrophotometry.

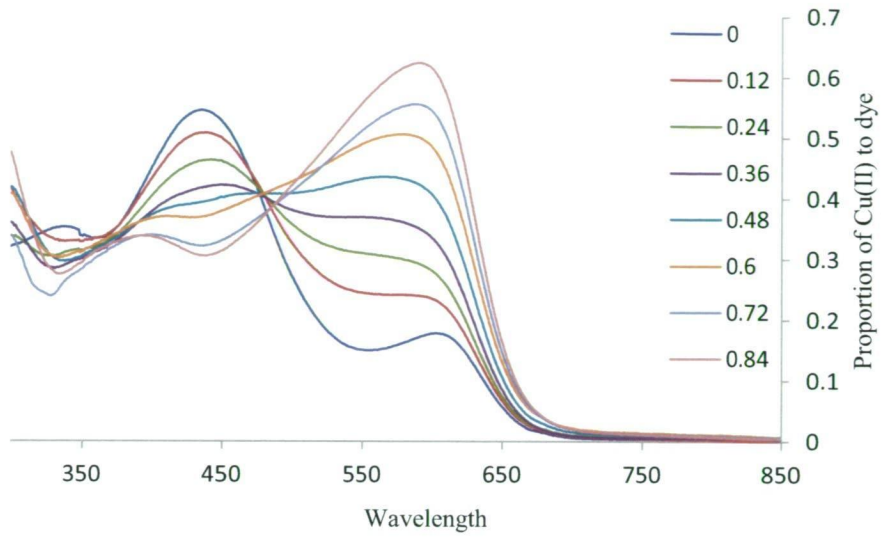

Fig 3.10a – The absorbance spectra of MTB(10) with Cu(II) complexed onto resin by exposure to a stirred solution. Note the chromatic shift as Cu(II) loading increases.

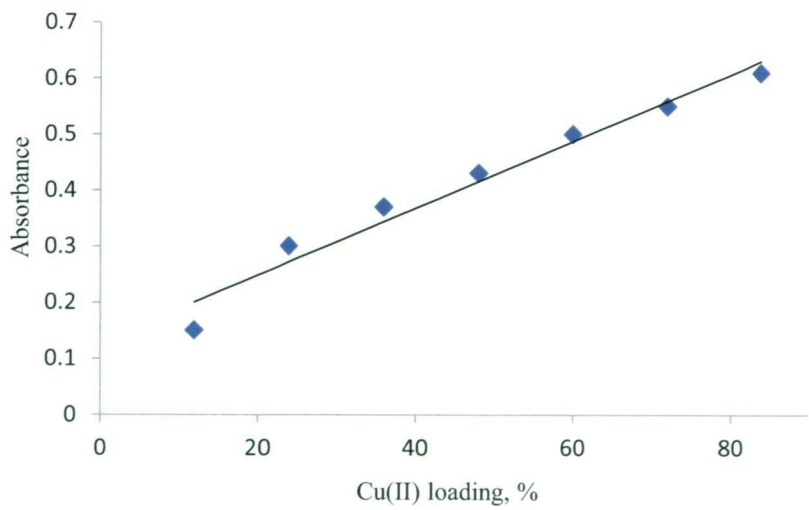

Fig 3.10b – Maximum absorbance values in the 550 nm range rather than values at 550 nm specifically, plotted against Cu(II) loading.

This evenly coloured resin was adhered to paper label discs, with tripicates prepared for each Cu(II) loading, to assess whether this shift could be corrected for during reflectance work. An analysis was performed by assessing the blank at 560 nm and increasing this wavelength by 4 nm per increase in Cu(II) loading of 0.2 μg cm^{-2}, in an attempt to account for the observed shift. Using this increase did not improve the analysis with reflectance, as linearity was lost at a Cu(II) loading of approximately 1.0 μg cm^{-2}, or 50%. As such, this bathochromic shift was not seen to occur in the same manner with reflectance analysis, and analysis at a single wavelength was used.

To avoid the non-linearity issues with analysis at high loading a 50% loading (1.0 μg cm^{-2}) was used as a maximum loading for binding phase quantification. This also fits with consideration of the work by Ouyang and Pawliszyn regarding a maximum of 50% loading with passive sampling to ensure that sampling remains in the kinetic regime [18].

While reflectance analysis of Cu(II) adsorbed MTB(10) provided adequate results, the relative standard deviation of 5 to 10% gives an error in Cu(II) loading of up to 0.2 μg cm^{-2}, and it was hoped that the total response may be improved. Three potential causes of this error were considered: disc manufacture, variation in reflectance measurement, and inhomogeneous coloration of the disc surface.

Variation in reflectance measurement was shown to be less than 0.1% RSD, with this variation decreasing at higher wavelengths. This was performed using dry discs to avoid hypsochromacy issues. At 560 nm, standard deviations for replicate measurements of uncomplexed MTB discs were from 0.01 to 0.05 % reflectance;

this was lower at 750 nm and about twice as much at 350 nm. These reflectance errors were therefore insignificant compared to the error of up to 1.5% reflectance observed during calibration runs at 560 nm. Disc manufacture was a significantly larger source of error, with the standard deviation of triplicates up to 1% reflectance within a batch of prepared discs. As the analytical range of the system is typically below 20% reflectance, this represents approximately 5% of the total response. To determine the impact that disc position had on reflectance measurements, analysis of a disc with shifting of the observed area was compared to repeat measurements of a stationary disc over an hour. The standard deviations of these tests were 0.19% and 0.16%, respectively. These results show that the variation between individual discs is a significant source of error, and accounted for the majority of error in UV-Vis analysis.

A variation of 1% reflectance response between discs in a batch accounts for the lesser quantities of error in the calibration presented in Figure 3.9b, with the larger variations thought to be due to the heterogeneous nature of the Cu(II) adsorption. Figure 3.11a shows the tendency for colour to appear initially at the extremities of the disc and to then move inwards, as maximum colour develops at the perimeter. This can be seen in Figure 9b, where the variation decreases as a maximum loading is approached. The cause of this uptake at extremities is not understood; it was initially thought to be due to the larger volume of water a resin bead would have access to at the edge of a sampler when compared to central beads. To restrict the resin's exposure to the water directly above the discs, they were placed in a DGT

Figure 3.11a – From left to right 0, 25, 45, 60 and 90% Cu(II) loading obtained using direct Cu(II) complexation, i.e. discs were exposed directly to Cu(II) solution. Note the heterogeneous colouration of the resin layer, with homogenous colouration only becoming apparent as 100% loading is approached.

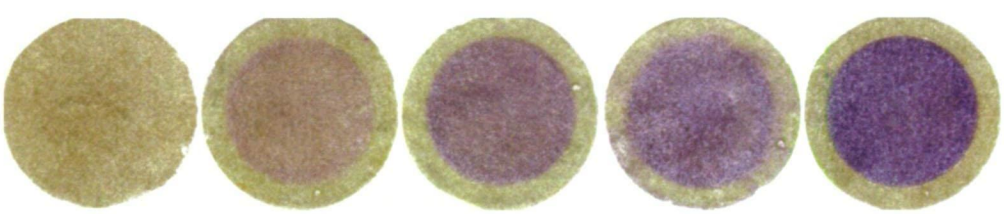

Figure 3.11b – From left to right 0, 15, 45, 80 and 100% loading obtained from DGT calibration exposure employing sample holders and diffusive gels. The unexposed outer ring is due to cover from DGT sample holders. A difference in coloration is apparent between Figures 11a and 11b and is due primarily to resin hydration, with the resin in Figure 11b being dry.

sampler probe body without diffusive gels. The uptake pattern observed with direct exposure was still present, with beads towards the outside of the exposed area complexing Cu(II) first. The cause of this heterogeneity was not clear, but its affect on variation was assessable.

Ten repeat scans of a 50% Cu(II) loaded MTB(2) disc showing inhomogeneous colouration were performed with movement of these discs to analyse a new area between each measurement. A standard deviation of 0.5% reflectance was observed for these scans which, when combined with the variation seen in blank discs of a single batch, accounts for the upper end of variation seen during calibration (Figure 9b). This suggests that this inhomogeneous colouration is a primary cause of the low precision seen in the calibration of this technique, and along with the variation in disc manufacture these sources account for the majority of the error in this technique. Due to the uniform bead packing on equilibration, disc manufacture was as consistent as possible with the 200-400 mesh resin. Improvements may be obtained by using a finer mesh size, however, this mesh size is the finest commercially available for Dowex 1x8. As no clear method for improving manufacture was available, a method for reducing the colour heterogeneity was explored.

3.3.4.3 – Homogenous Colouration From DGT Cu(II) Uptake

Exposure of the MTB(10) discs in DGT devices with polyacrylamide diffusive gels provided a more uniform colouration of the disc surface, with no observable difference between the centre and perimeter, as shown in Figure 3.11b. The

calibrations performed in section 3.3.4.1 were assessed by reflectance spectrophotometry to obtain suitable colorimetric calibration curves. Figure 3.12 shows the average reflectance response and standard deviation of triplicate discs over a range of loadings to 28% of equimolar.

When the smaller scale of this calibration is considered, it can be seen that much greater precision is obtained. This error is approximately ± 1% reflectance and is, therefore, likely due to the variation in disc manufacture seen by reflectance as discussed above. Accordingly, this was thought to be the most precise result obtainable using UV-Vis reflectance on these MTB discs. It can be seen that the blank measurement is substantially displaced from the linear fit of the remaining calibration points and is a significant outlier at the 99% confidence interval ($Q=0.966 > Q_{99\%}= 0.740$, n=6, values calculated from the difference of the sample's mean to extrapolated line of best fit value). Examination of these discs showed that resin without Cu(II) complexed was lighter in colour, such as in the blanks and around the edges of the discs. These edges were not exposed to Cu(II) due to the nature of DGT sampling devices, but were exposed to the bulk solution matrix via lateral diffusion. Accordingly, this colour loss was thought to be due to the previously mentioned desorption of MTB by NO_3^-. Using the data in Figure 3.12, a relationship can be established between % reflectance and mass of Cu(II) accumulated in the MTB-resin binding phase with the Cu(II) loading being equal to

$$\mu gCu.cm^{-2} = \frac{(R-24.8)}{-8.61}$$

where R is the % reflectance value.

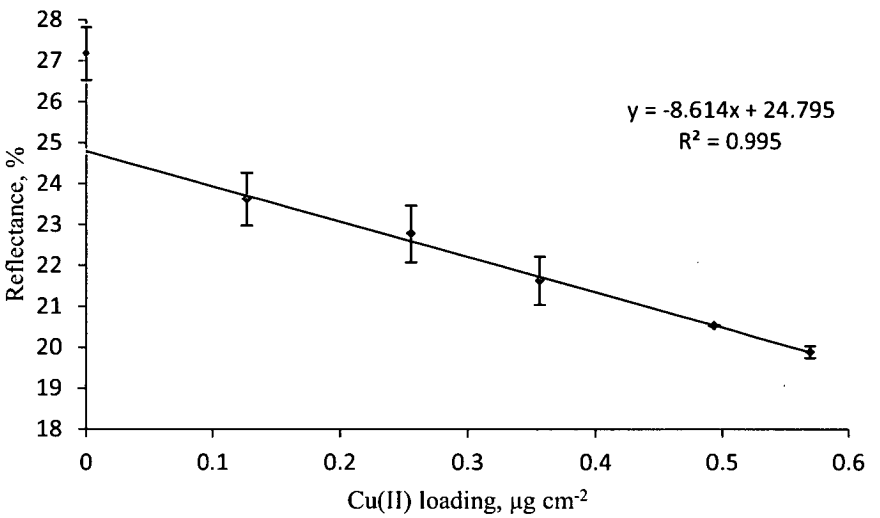

Figure 3.12 – Calibration of homogeneously coloured MTB binding phases. Trend line omits the blank value.

3.3.5 – Dye Bleaching and Analytical Use

Bleaching was first noticed during the direct uptake calibration tests. Discs left uncovered on benches lost colour over several weeks, though those with complexed metal retained colour in complexed areas, as shown in Figure 3.13. The cause of bleaching was determined to be visible light, as discussed in Section 3.3.3, and exposure to an incandescent source was found to be the best method for accelerating bleaching. On recently made discs the red colour attributed to Cu(II) complexed MTB appeared stable, with continued exposure to an incandescent light source over a week providing little visible change to the metal complexed area. However, it was

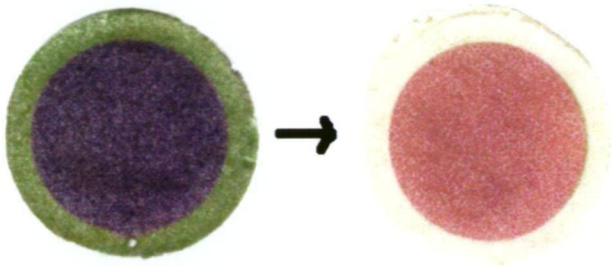

Figure 3.13 – The bleaching process resulted in the loss of colour in the un-complexed green MTB, while Cu(II) complexed MTB initially retained a red colour.

found that older Cu(II) complexed resin bleached past the red stage to off-white in 48 h, indicating that the red Cu(II) complex may not be stable on fresh resin.

Initially, though, it was seen that bleaching of Cu(II) loaded resin disc selectively bleached the uncomplexed MTB. It was thought that the removal of the uncomplexed MTB would improve the sensitivity of the technique as the background reflectance of the resin would be higher. Discs previously measured by reflectance were bleached to assess spectral properties. The change in spectrum between such discs, after 48 h of bleaching under a 60 watt globe, is shown in Figure 3.14. The near-IR range remains largely unchanged, as is the general case with the MTB-resin discs, but significant changes are observed among the remaining portions of the spectrum. The bleached Cu(II) exposed resin retains significant features and has a lower average reflectance, supporting the belief that the retained red colour is due to the removal of the uncomplexed MTB.

Discs used for previous calibration runs were bleached before being re-assessed with reflectance to determine if an improvement to the response, or precision, was obtained. A wavelength of 515 nm was found to provide the highest reflectance

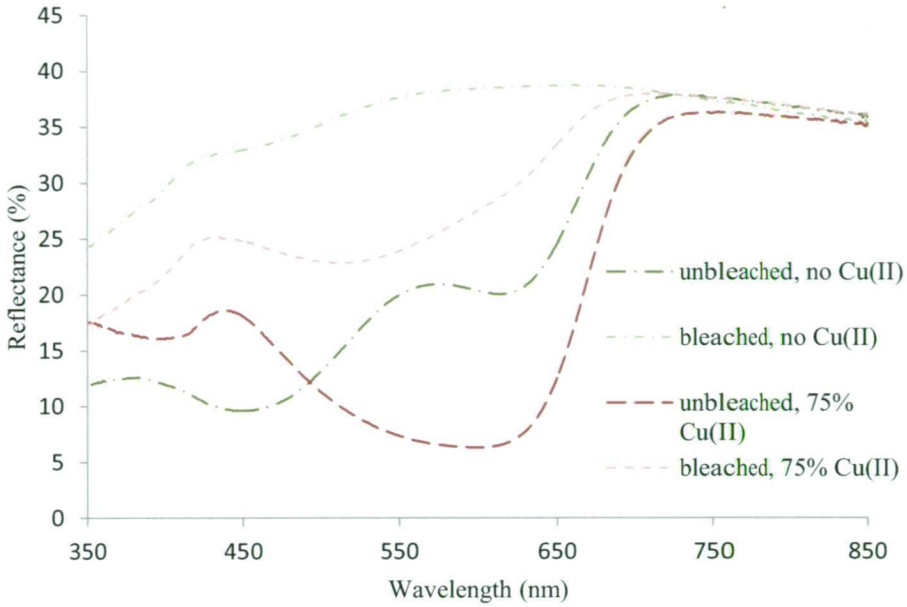

Figure 3.14 – Comparison of diffuse reflectance spectra of 6 month old MTB(10) before and after bleaching: the -·- traces show uncomplexed dye, complexed dye is shown by the --- traces. Fainter traces (upper) show bleached spectra of the same discs after 48 h. Cu(II) percentages refer to complexed Cu(II) quantity in proportion to dye present.

response for Cu(II) analysis after bleaching and, as such, this was the wavelength measured. Figure 3.15 shows the response of these discs, which are seen to have a substantially better response in terms of % reflectance per μg of Cu(II) complexed. The variation amongst these measurements was substantially greater than pre-bleached samples though, with average error being ± 3.0% reflectance for bleached MTB(10) and ± 4.4% reflectance for bleached MTB(2), as compared to ± 1.5% reflectance for unbleached MTB discs when Cu(II) was complexed directly.

As this error was more substantial than that obtained before bleaching, the Cu(II) bound dye was most likely affected. As mentioned earlier, bleaching of the Cu(II)

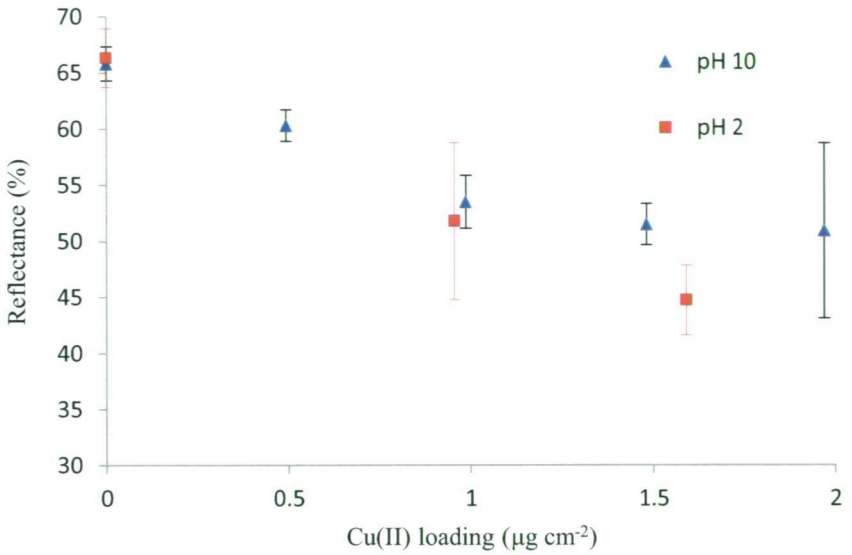

Fig 3.15 – Calibration of MTB(2) and MTB(10) discs using inhomogeneous uptake and bleaching, measured at 515 nm. Note that the error associated with the triplicates is greater than that observed in Figure 7a. Also, note that the dynamic range of response is significantly larger, but RSD values are proportionally larger.

complexed dye was observed in resin where MTB had been adsorbed more than 6 months prior to light exposure. Uncomplexed dye on this resin still bleached, though substantially faster. In these discs, uncomplexed MTB colour was lost in less than 24 h, and metal complexed colour was seen to bleach completely after 48 h, such that no colour remained on the disc. Thus although the intention with fresh discs was to bleach the uncomplexed MTB only, it is unlikely that this would have been achieved without also bleaching some of the Cu(II)-MTB complex over the week-long exposure times.

The error due to disc manufacture results in a variation of ± 1% reflectance, if the bleaching process can be performed in a manner that does not increase this uncertainty it should be possible to use it to improve analytical performance due to

the greater reflectance response of a bleached disc (due to a reflectance response of 10% reflectance per μg cm^{-2} compared to 5% reflectance per μg cm^{-2}). However, the bleaching of the Cu(II) complex makes this somewhat unlikely.

However, as the complexed dye had greater light stability it may be possible to use highly dye-loaded discs and remove interfering uncomplexed dye, allowing lower detection limits for high dye loadings. It may also be possible to isolate the wavelengths responsible for the bleaching of the 2 compounds, and if different this would allow selective removal. As such, bleaching has the potential for improvement if a UV-Vis reflectance method is used, but without substantial further work it highlights the light stability of the discs and the necessity to avoid light exposure where possible with the MTB-resin system.

3.4 Conclusion

The MTB-Dowex 1x8 system has been shown to successfully act as a DGT binding phase and provide quantification of complexed Cu(II) from pH neutral solutions. The use of UV-Vis reflectance as an analytical technique has been shown to be successful and the method has demonstrated that *in-situ*, stable colour development can be achieved.

While Cu(II) quantification was successful, the complexities of the MTB system, particularly with regard to light and NO_3^- sensitivity, reduce the system's robustness and limit its use for field deployment. However, this approach has developed techniques for using resin-adsorbed dyes during metal complexation and analysis and has provided an understanding of the details to be explored when other dyes are used in this manner. As well as this, it has been shown that dye character, with respect to metal complexation and the colour of the metal complex, is substantially different from aqueous character when adsorbed on resin. As such, examination of other dyes for application to this method must be done after resin adsorption

The development of the MTB system, while not ideal for environmental deployments, has shown that the colorimetric DGT binding phase is possible and suitable for Cu(II) analysis. The development of this binding phase also provides a structured way to undertake examination of other dyes being employed in a similar manner.

References

[1] P.R. Teasdale, S. Hayward, W. Davison, Analytical Chemistry, 71 (1999) 2186.

[2] D. Jezequel, etal., Estuarine, Coastal and Shelf Science, 72 (2007) 420.

[3] D. Robertson, P.R. Teasdale, D.T. Welsh, Limnology and Oceanography: Methods, 6 (2008) 502.

[4] K. Yoshimura, H. Waki, Talanta, 32 (1985) 345.

[5] K. Bratjer, E. Olbrych-Sleszynska, Talanta, 30 (1983) 355.

[6] T. Kelley, J. Littman, The art of innovation: Lessons in creativity from IDEO, America's leading design firm, Random House, Inc., New York, 2001.

[7] K. Ueno, T. Inamura, K.L. Cheng, Handbook of Organic Analytical Reagents, CRC Press, 1992.

[8] T. Yoshino, H. Imada, S. MurakamiI, M. Kagawa, Talanta, 21 (1974) 211.

[9] H. Chao, N. Suzuki, Analytica Chimica Acta, 125 (1981).

[10] Z. Zhou, X. Mao, Gaodeng. Xuexiao Huaxue Xuebao, 3 (1982) 181.

[11] National water quality management strategy ; no. 4a. Australian and New Zealand Environment and Conservation Council and Agriculture and Resource Management Council of Australia and New Zealand. 2000.

[12] W. Davison, H. Zhang, Nature, 367 (1994) 546.

[13] J. Inczedy, Journal of Thermal Analysis, 13 (1978) 257.

[14] B.L. Larner, A.J. Seen, Analytica Chimica Acta, 539 (2005) 349.

[15] M.L. Marina, V. Gonzalez, A.R. Rodriguez, Mircochemical Journal, 33 (1986) 275.

[16] M.L. Marina, V. Gonzalez, A.R. Rodriguez, Bulletin de la Societe Chimique de France, 11 (1984) 339.

[17] ANZECC and ARMCANZ, Australian and New Zealand guidelines for fresh and marine water quality. Australian and Newzealand Environmental and Conservation Council/Agriculture and Resource Management Council of Anustralian and New Zealand. 2000.

[18] G. Ouyang, J. Pawliszyn, Journal of Chromatography A, 1168 (2007) 226.

[19] M. Camusso, A. Gasparella, Societa Chimica Italiana, 96 (2006).

[20] K.W. Warnken, H. Zhang, W. Davison, Analytical Chemistry, 78 (2006) 3780.

[21] M.S. Sastry, M.D. Sastry, Journal of Chemical Sciences, 97 (1986) 587.

[22] E.O. Skogley, A. Dobermann, Journal of Environmental Quality, 25 (1996) 13.

Chapter 4

Computer Imaging Densitometry Analysis

Application of a flat-bed scanner to the quantification of colour change

4.1 – Colour Quantification Using Consumer Flat-bed Scanners

4.1.1 – Digital Colorimetric Analysis

The term 'Computer Imaging Densitometry' (CID) was first used by Davison et al. [1] to describe the use of a computer-imaging system for analysis of colour 'density'. In this case 'density' referred to the amount of 'colour' in a system, for instance a grey scale range would be said to have no density at white and maximum density when black. The inverse of this concept is luminosity, the quantifying value for CID work, where a white sample provides maximum luminosity. The computer-imaging system used by Davison et al. was a desktop scanner with colour quantified in NIH (National Institute of Health) Image, by using the luminosity value obtained when the image was examined [2]. Using this technique, S^{2-} levels were quickly quantified in sediments through the use of a DGT binding phase consisting of AgI-impregnated gel. Colorimetric response was provided by a colour change from pale yellow to black upon the binding of S^{2-} to the Ag^{+}.

Digital quantification of visual data is not a new concept and has been used for more than 40 years [3]. In earlier cases density was quantified as being inversely proportional to the incident light divided by the transmitted light, as with electromagnetic radiation transmission and such that a more weakly transmitting image has a higher density. The technique was used to obtain quantification of radiographs, particularly x-ray crystallography [4], but has been used for a variety of other purposes where quantification of visible monochrome data was required (for

example see [5]). However, for most of the last 40 years the primary use of computer densitometric systems has been for the direct quantification of coloured gel areas, such as in electrophoresis gels [6]. Early computing techniques for analysis of these images suffered from high cost and, compared to modern techniques, required long analysis and sample preparation times. Commercial electrophoresis scanners reduced the time required for analysis, but were a significant monetary investment.

The introduction of affordable consumer scanners in the early 1990s allowed densitometric data to be obtained less expensively [7,8]. Combined with readily available image manipulation software, scanners provide a simple, flexible, and effective way to analyse colour intensity. The application of consumer scanners to generic measurements became more widely used in the late 1990s, with the ISI Web of Knowledge database returning 12 hits in total for 'flat-bed scanner' up to 1995 and nearly 200 in the 14 years since. Flat-bed scanners do not represent the entire extent of the application of consumer-based technology to quantitative analysis, with many consumer image-reproduction items being applied, including video cameras [9] and digital still cameras [10]. In this latter case, Byrne et al. [10] highlighted the growing trend for use of the colour data obtained from such analyses to be used in quantification, in place of the general colour density. Indeed, a comparison of a colour analysing flat-bed scanner technique to a conventional 'slit' densitometry technique [11] has shown that the consumer techniques can provide superior results to more established methods by employing the greater fidelity of information available when colour is considered. However, in current consumer systems, the theoretical considerations and methods of collection of information are not as well

documented as in earlier commercial densitometer/scanner systems. Even so, some understanding of these systems is available and is necessary for the application of such a system.

4.1.2 – Consumer Hardware and Function

Of the current methods for colour quantification using consumer hardware, the most common employ either digital cameras or flat-bed scanners. In general, digital cameras operate on similar principles to one of the two major flat-bed scanner types and, as flat-bed scanners are to be used for the work in this thesis, discussion particular to cameras will be omitted, but can be considered to be a similar case to the 'CCD' scanner type.

The visible light information, i.e. colour, collected in a consumer flat-bed scanner is determined primarily by the data necessary for display and storage of the image on the computer. In its most simple conventional form these data are stored as a raster image, or 'bitmap', where the image is defined as a field of square, uniform 'pixels', each being the smallest spatial division of the image. These pixels are organised as the cells of a grid, with the relative position and colour information of each pixel stored in a file for display and reproduction [12]. Colour data can be stored at any number of levels with the simplest being 1 bit of data per pixel, representing the presence or absence of a single 'colour' (e.g., black or white – 'monochromatic'). For general human observation, the minimum colour data generally accepted for a realistic representation of a real-world image, and therefore the smallest acceptable image file in terms of colour data stored, is the 24 bit system. This colour

description system employs 3 separate colours per pixel, typically red, green and blue, and each colour is described by 8 bits of data per colour.

For each colour, 8 bits per pixel describes 2^8 or 256 levels of colour – from none of the respective colour (0) to the maximum (255). As mentioned, the three colours are typically red, green and blue (R, G and B, or RGB), with the actual colour described in the 'Red', 'Green' or 'Blue' value depending on the display equipment, for instance, the emission spectrum of LEDs in a contemporary flat-screen monitor, or the reflectance profile of a dye used by a printer. It is worth noting that as this is an additive colour system, colours other than the three stored ('R, G, B') can be described by combinations of the three, with black described as the absence of any and white as the maximum of each. As such, each pixel can have one of 256 x 256 x 256, or 16,777,216 individual colours.

Collection of visible light in a consumer digital imaging system therefore depends on the collection of 'Red', 'Green' and 'Blue' components. Modern consumer flat-bed scanners are of two types, the Charge-Coupled Device (CCD) type and Contact Image Sensor (CIS) type. The method for separating out the RGB components of visible light is the primary distinction between the two scanner types.

In a CCD scanner, light is provided from a source giving a good approximation of the normal solar visible light spectrum, such as a cold-cathode or xenon fluorescent tube. RGB discrimination is achieved by the use of physical sensing unit pixels, each formed from several sensors, with separate filters for red, green, and blue light over individual sensors, similar to the method described by Farrell et al. [13]. The number of these physical pixels determines the maximum resolution (number of

pixels) for full fidelity, or native resolution, at which the scanner measures. CIS scanners function by using a photodiode array with sensitivity to all visible light, providing colour discrimination by alternating the illuminating source between red, green and blue LEDs. In this way the light source being used at a given time determines the colour being measured by the photodiode array [14].

In either type the size of the response of the red, green or blue-selective system determines the response of the respective colour 'channel' given to the image handling software. For instance, in a system providing 8 bits per colour, an equivalent of 100% response from the green detection system would provide a green channel 'luminosity' of 2^8. This value is usually described as 255, with the minimum value being 0, such that the luminosity value will lie between 0 and 255. Actual colour resolution may not be this large; Vrehl, Saber and Trussell noted that a commercial '48 bit' scanner with a purported colour resolution of 16 bits per channel has an actual resolution of only 6 bits when assessing grey images, due to the precision of the detector [14].

In general, both systems use a light source to illuminate the object to be scanned, and a light-detecting system to collect the reflected light and interpret it as a digital signal divided into red, green, and blue, for transmission to the computer. As such, the emission properties of the light source are important, as are the reflective properties of the scanned object [10]. Flat-bed scanners are made primarily for image collection from flat, matte sources, such as paper, and the optical and detection systems are oriented to collect the majority of diffusely reflected light as well as the spectral component [14]. A variety of automatic physical and software self-correction techniques are used to account for fluctuations in sensor response,

light source emission, introduced noise, and scanning system movement, as well as for compensation of differing surfaces placed in the scanner. These are referred to as metameric corrections [15]. Perhaps the main limitation of consumer equipment is this metamerism, resulting in a misrepresentation of the visible spectrum. Response of the device will depend heavily on the wavelength of light permitted through the filters of a CCD system, or of the spectrum emitted by the LEDs of a CIS system, in combination with the reflective properties of the object being scanned. The intended use of these devices has resulted in the range of colours collected being biased towards the human visual system. Due to this, much of the visible spectrum has a reduced response compared to maxima roughly correlated with human visual responses, effectively red, green and blue.

4.1.3 – Dye Analysis

This metameric wavelength limitation is also the main drawback of the scanning systems for analytical quantification. Analysis of dyes with maximum absorbance between the peak emission, or transmission, wavelengths of the optical system will have a low signal-to-noise ratio compared to those with a response in the area of the scanner's maximum sensitivity. However, due to the broad nature of most UV-Vis features it is likely that many dyes would be quantifiable. For methylthymol blue (MTB, see Chapter 3) the maximum absorbance of the Cu(II) complex, 560 nm, sits within the width at half-peak-height emission range of most green LEDs [16] and, as such, the quantification of bound Cu(II) should be possible with a CID system. As well as this, due to the width of the LED emission peak (typically about 35 nm), the

shift seen in the Cu(II) absorbance peak during diffuse reflectance work is hoped to have a lesser impact on quantification than was seen using UV-Vis spectrophotometry[17].

For laboratory quantification both CIS and CCD should provide comparable performance, however, the small size and low power usage of the CIS scanning system would prove useful for in-field quantification. As such, quantification of MTB will focus on using an affordable, off-the-shelf consumer CIS scanner. The aim of this chapter is therefore to explore the application of a CIS-based CID technique employing colour channel luminosity values to the quantification of Cu(II) loaded on to a MTB(10) binding phase. Examination of the performance of the scanner for this task will be a key point, as will the ability of the scanner to obtain analytical performance equivalent to the UV-Vis system discussed in Chapter 3. Subsequent comparison of the CID results to those obtained via diffuse reflectance UV-Vis spectrophotometry will be made.

4.2 – Experimental

4.2.1 – Scanner Characterisation

Scanner performance was assessed using the following paint sample swatches from the Berger Interior Bold series – Romantic Zing B52, Flirty B51, Green Guru B41 and Blue Illusion B40 (Orica Australia, Melbourne, Australia). Swatches were cut into 2 x 2 cm pieces to allow comparison of sensor response across the platen with equivalent colours. Colour quantification was via *The Gimp* version 2.4.5 (maintained by Spencer Kimball and Peter Mattis at http://www.gimp.org/) or *ImageJ* (ver. 1.40g, Wayne Rasband, NIH, USA) software with images acquired using Canon *Scangear* software version 12.0.1 (Canon Inc, Tokyo, Japan) and the standard TWAIN protocol (located at http://www.twain.org/, included by default).

Temperature effects were assessed by inserting a -10 to 50°C thermometer (Hg 76 mm immersion N_2 filled, Zeal, England) within the scanner housing, centred under the mobile scanning unit to provide the most accurate measurement of temperature within the unit, with readings of the temperature taken after each run. Calibration was performed using bleached white office paper (EXP800 80sgm white, Corporate Express, Mascot, Australia) as a reference standard. For comparison to UV-Vis reflectance data, swatches were scanned 10 times following a warm up of 3 scans allowing the temperature inside the scanner to stabilise. Scanner calibration was through the internal software option, under the 'settings' pane in the *Scangear* interface and 6 sheets of bleached printer paper (EXP800, 80gsm white, Corporate Express, Melbourne, Australia) were used for this purpose so that the entire platen was covered with an end-to-end jointed, 3-deep layer of the paper during calibration.

UV-Vis analysis of colour swatches was performed using the above 4 cm^2 paint swatch sections on a Cary 1E spectrophotometer (Varian, Melbourne, Australia) with a Labsphere DRA-CA-30I reflectance attachment (USA) employing the 0° (specular) and 8° (diffuse) wedges. Data for comparison to the CID technique was collected from 10 repeat scans of the same swatch squares used in the CID measurements.

4.2.2 – CID Analysis of MTB Discs

MTB discs used for CID analysis were the same discs used for UV-Vis reflectance work in Chapter 3 and, as such, experimental details for the manufacture and exposure of these discs can be found there (Sections 3.2.3 and 3.2.4). As with UV-Vis analysis, MTB disks were measured immediately after wetting and blotting to remove excess water, to ensure complete resin hydration.

A consistent position on the scanner was maintained by marking the inside of the lid to avoid error introduced by disc positioning. Analysis of disks was performed by using the elliptical tool to select the exposed area while avoiding un-exposed resin outside this area. When the 'select contiguous regions' tool was used the location of the selection was chosen by eye, with either the most intense colour or the centre of the disc being selected subjectively. In the case of scratched disks the area without resin was de-selected using the 'select hand-drawn regions' tool, digitally deselecting the portion of the exposed resin removed alongside the scratch, rather than inclusion of some of the damaged area. Mean R, G and B values of the selected area were recorded from the histogram tool and stored in *Microsoft Excel 2003*.

4.3 – Scanner Characterisation

4.3.1 – Software Use

In order to use a computer-based technique effectively, the method of handling the data must be considered. Collection of scanner data and transfer to the image analysis package was performed using the TWAIN protocol and proprietary scanner-specific Canon *Scangear* software, as these were supplied with the equipment used and are standard software for image collection. Image analysis was performed in two programs; *ImageJ* [18] and *The Gimp 2* software. Both are open-source applications, meaning they have the source code published if necessary and are readily available. Further to this they are free to use. *ImageJ* was created for working with digital microscope and digitally acquired electrophoresis images, allowing the user to modify the images as necessary for biological work and to save files in a variety of low-loss formats. *The Gimp 2* software is an image-manipulation program allowing a large range of modifications and analyses to be performed on images. While it is not function-specific like *ImageJ*, it is more flexible, user-friendly, and allows for the saving of data in a greater range of formats with the ability to handle all aspects of the file structure and, therefore, ensure a file which will not compress data to the point of information loss.

Image handling was assessed by comparing image histogram data, which summarizes the colour data for the complete image for 4 different colour swatches. Identical results were obtained for the two packages and due to *The Gimp*'s ease of use, it was chosen as the preferred image handling tool. The use of image storage files was considered as this allows data to be re-examined using different methods at

a later date, provided that a suitable file format is used. For the relatively high 32 and 48 bit colour depths obtainable from the scanner, the RAW file format would be ideal, but it suffers from a lack of consistency in the way programs deal with the file data. As such, the data in a RAW file may not be transferable to another program easily and may also be handled differently after software updates. The TIFF format can handle the same colour depths and is more widely used, being considered a standard for image processing [19]. PNG is also a promising potential file format but does not handle colour data directly as RGB, and the majority of other file formats either do not store high colour-depth data, or cause substantial data loss due to file compression, making them unsuitable. Due to TIFF's wide use as a standard, it was chosen as the data storage format, with the provision that a compression-less method was used to minimise data loss.

4.3.2 – CID Application

Application of the scanner to colour densitometry held a number of concerns. Primary among these was the stability of the colour response of the system, as well as the resolution of colour response. Batch handling of discs was also assessed to see if it was possible to increase the throughput of the system by analysing multiple discs simultaneously. The variability between individual sensing units within the scanner may have an impact on results and was assessed. This was important, as a disc is analysed by many sensors simultaneously, rather than the entire analysed area being integrated into one signal as in UV-Vis analysis. Therefore, variation in results

due to the position on the platen must be assessed which will impact on both single disc handling and batch analysis.

Testing of colour response was performed using paint swatch samples of various colours cut into 4 cm^2 square sections. Red swatches were found to provide the highest response, in terms of luminosity value, in all channels (R, G and B) and were used for the basic characterisation. Data obtained was displayed in the Gimp software as a histogram (see Figure 4.1) for each image, with the number of pixels in each channel and their colour depth in terms of luminosity from 0 to 255. Individual swatches had reproducible luminosity values, with the mean swatch luminosities typically varying by only 0.2% RSD over 6 scans for luminosities of ca. 175. Half of this variation was seen between the first and second scan and was found to be due to the warming of the scanning system during use, which is discussed later. As such, this variation was further reduced by allowing the scanner to warm up before readings were taken, and due to this, three un-recorded scans were typically performed before data acquisition as a 'warm-up'.

Simultaneous scanning of a large number of discs utilising the whole platen was trialed to reduce the time required, as approximately 40 seconds was needed per scan. Batch processing could, therefore, reduce the time to obtain results for 20 samples from nearly half an hour to under 10 min (including image handling and data extraction). Examination of a single swatch square at 12 points distributed over the platen showed variation between the mean luminosity values at these points substantially larger than repeat scans at any one point. Triplicate scans at each point

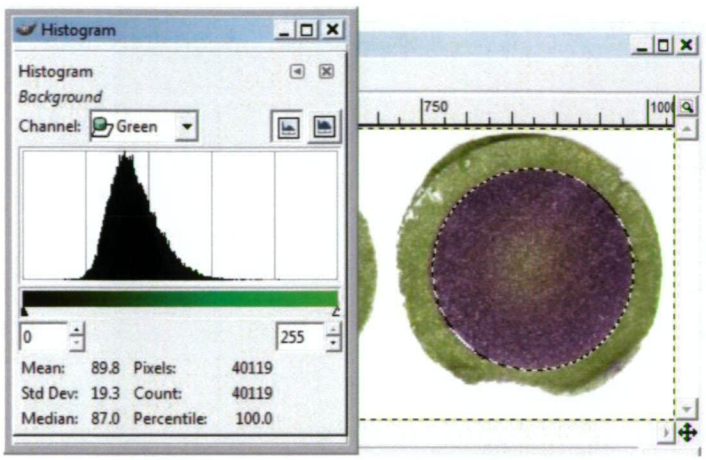

Figure 4.1 – The Gimp histogram showing an example of a Cu(II) adsorbed MTB disc with the metal-bound purple region selected. Data provided in the 'green channel' histogram includes statistical analysis of the G channel data in each of the selected pixels. Note that 'Std Dev' applies only to the spread of colour in the selected area.

showed little variation in luminosity measurements with the greatest range at any point, after warm up, being the lowest reported difference of 0.1 luminosity units. In comparison, the range of mean values across the 12 points was 2.1 luminosity units. Hence, the position of the disc on the platen was seen to have a large impact on the result obtained and a position was marked on the scanner roof to ensure the same platen location was used for each scan.

This variation was not confined to one axis and, therefore, was not due solely to variation within the photodiodes which are arranged as a single row laterally in the detection array. Due to the stability of locations between scans it appears to be a mechanical or software source of error, and it was thought it may be potentially accounted for in batch tests. If a correction was to be found it would need to apply to

all colours, such that each point affected each channel consistently. To test the difference between colour responses at these points, the average histogram red-channel means of triplicate scans were collected at 5 points on the platen using red and yellow swatch squares. If the deviation of the red and yellow swatch luminosities was the same at each point, a platen-wide correction could therefore be applied as the variation would be independent of colour. The means of the red and yellow swatches were zeroed to the reading at the first position, chosen for the lowest luminosity values, and the differences for each of the remaining points compared (Figure 4.2). Changes between the colours were seen to roughly correlate with each other, but not to an extent where a single correction could be applied to the platen to account for error on both the red and yellow swatches. As actual analyses will involve discs of varying colour a platen-wide correction could not be applied effectively, and measurement at a single point on the platen was determined to be the most reliable method.

Besides the improvements in time, ease of use, and portability one of the primary advantages of the scanning technique over UV-Vis reflectance is the software flexibility of being able to choose the area analysed after data collection. This allows the user to define the area included in the histogram analysis and, hence, the pixels used for the statistical analysis of luminosity response. Two primary methods were available for analytical area selection: the 'magic-wand' or 'contiguous regions' method and the 'elliptical/rectangular' (direct) method. The latter allows the user to define the boundary of the area down to individual pixels, whereas the former uses an algorithm to select pixel areas adjacent to the chosen pixel which contain similar colours.

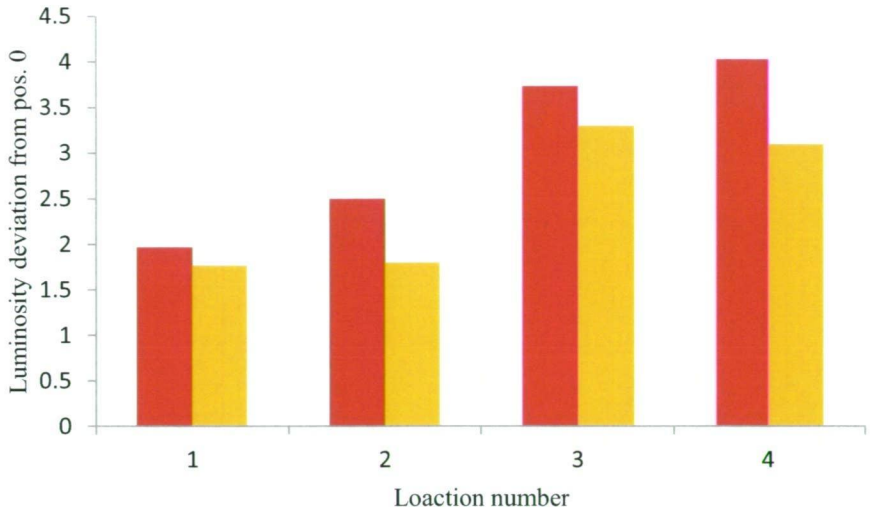

Figure 4.2 – Red (left) vs yellow (right) absolute luminosity deviations at locations '1' through '4' from a single initial location '0'.

Direct selection was more robust for disc application, as it would not exclude potentially relevant pixels due to sharp luminosity borders on the disc. It can, however, introduce errors through the selection of border area which contained blended data from unexposed and exposed disc regions and also requires significantly more user time and concentration. The contiguous method selects areas of similar colour and allows a 'threshold' value to be set, determining the variation between adjacent pixels that can be tolerated to include them in the selection. For this setting a threshold value of 10 to 60, which represents the maximum difference in luminosity between adjacent pixels to allow inclusion, was found to provide 1% relative standard deviation amongst average swatch luminosity means. Threshold values below 10 resulted in a sharp increase in the relative standard deviation. However, the lowest relative standard deviation seen with direct selection was 0.1%

which when compared with contiguous selection's RSD being 1% it can be seen direct selection is a more precise method.

As noted, direct selection also proves more robust when relatively inhomogeneously coloured samples are scanned, such as methylthymol blue discs. The contiguous method results are highly dependent on where the initial selection point is located, as well as selection of the correct threshold value, as shown in Figure 4.3. However, care must still be taken with the direct method as the edge of the exposed area is not clearly defined due to lateral diffusion in the diffusion gel [20] and selection of un-exposed material may impact on the average luminosity reading. For the most accurate result it is important to select the largest area possible without including border zones, though this did not prove difficult as it is possible to select an area just inside the visible exposure border and obtain consistent results.

Scanner settings were explored, particularly the scanning resolution in terms of 'dots-per-inch' (DPI) and colour depth. At high DPI settings, vertical lines of higher luminosity were visible in the final images. Initially this was thought to be due to LED illumination not being sufficiently diffuse, or photodiode response not being even, however, this appeared vertically in both landscape and portrait orientations, and such lines would rotate with the orientation. Due to their vertical orientation in the image regardless of the image orientation, these lines were considered an artifact of image handling rather than due to the optical system. At a setting of 100 DPI lines were not apparent and, therefore, this resolution was used.

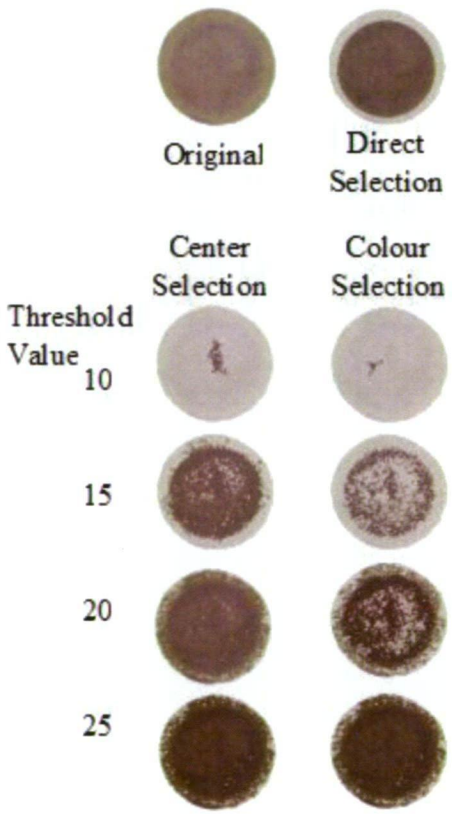

Figure 4.3 –The original disc and direct selection method are shown at the top. Contiguous selection of inhomogenously coloured MTB discs, with the selected area darkened, is shown below. The location of the selection was either, the disc centre (left), or the area of most coloration (right). It can be seen that using contiguous selection, large portions of the disc may not be selected, or uncomplexed regions are, with the amount selected increasing with threshold value.

Colour settings in the older scanner software, used for a few initial studies, allowed choice between 32 bit and 48 bit colour. These two settings vary by the size of the channels for red, green, blue and 'gamma' data, gamma indicating overall lightness and were not relevant to this work, with the 32 bit case containing 8 bits per channel, and the 48 bit case containing 12 bits per channel [17]. This 12 bit data was 'scaled-down' to 8 bit (256 colours) in the image handling software, but did provide a more precise response in terms of lower standard deviations in repeated swatch square scans. However, the updated Scangear software that was used for MTB calibration and the majority of swatch tests only allows for 'Colour' or 'Colour: Documents' to be selected. In this case the latter method provided lower standard deviations, and appears to be a relabeled 48 bit option.

4.3.3 – Temperature Dependence of Scanner Response

Analysis of the commercial paint sample swatch squares, with 24 h between measurements, was performed to determine the stability of the results without calibration. When measurements were taken at this one-day separation little difference was found between results. However, results were noted to vary over the course of a day, in extreme cases by up to 3 luminosity units for G-channel analysis of MTB discs with a luminosity of ca. 170. This was thought to be due to variation in the laboratory temperature, which during summer could be as much as 15°C due to ineffective air conditioning. A plot of luminosity results of the initial scans for a single swatch square relative to temperature is shown in Figure 4.4.

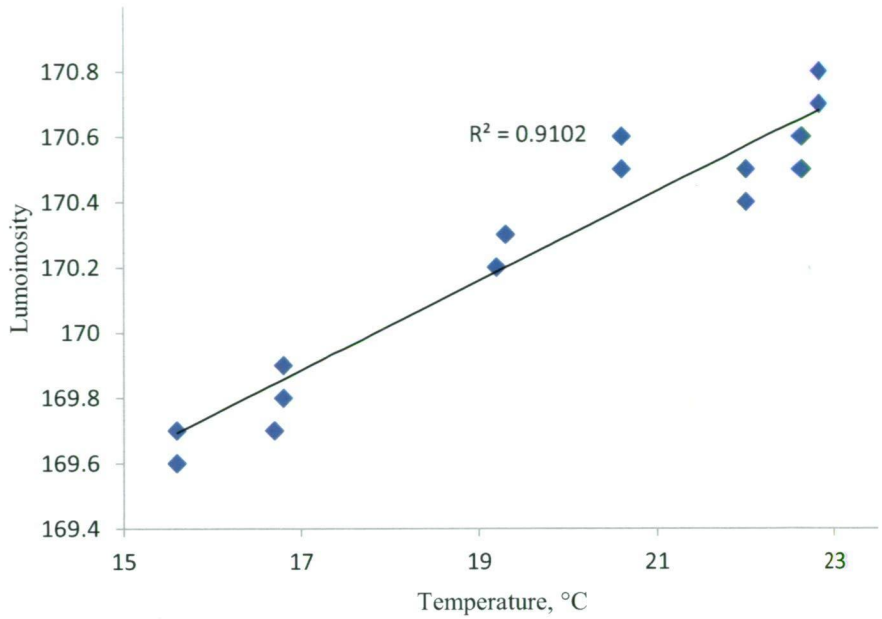

Figure 4.4 – Luminosity values of a single red swatch square measured at varying temperatures, temperature data was recorded from within the scanner housing.

While noisy, a clear increasing trend can be seen in the data. The cause of this is likely to be temperature dependence of the active components of the scanner, particularly the LED and photodiode systems. As both systems rely on the interfaces between different materials to generate electrical signals the effects of temperature can be significant. In the case of a typical high-performance green LED (of the InGaN type) as would be found in a scanning system, a decrease in emitted light intensity is found with increasing temperature [21]. This would be expected to provide an apparent decrease in luminosity assuming that the photodiode response remained the same. As the luminosity is found to increase with temperature, indicating a larger portion of reflected light, a decrease in emission would not explain this observation. For photodiodes, visible light wavelength discrimination is

not readily changed by temperature, but the 'dark current' can be strongly affected. Due to the reverse bias in photodiodes higher temperatures lead to an effective decrease in resistance and hence a higher current [22]. This may account for the higher luminosity readings observed as the current increase from light interaction with the photodiodes will be added to this 'dark current', resulting in a higher overall current for the same reflected light.

When the scanner was calibrated before use at each temperature the results obtained were much more consistent, with no difference in the 'R' channel results between 3 triplicate scans at 17, 20 and 22°C greater than 0.1 luminosity units. Internal calibration of the scanner can be performed under the 'settings' pane of the scan collection window. This calibration can therefore be used to account for these temperature changes, but as the calibration process takes several minutes it is not recommended to be performed before each measurement. However, it is certainly simple to perform this task before each batch. As temperatures are likely to remain stable over the short term this calibration is primarily worth undertaking if the climate of the area in which scans are performed is not tightly controlled or if scans are performed in the field and need to be compared with those performed elsewhere, as usually would be the case to quantify field-exposed discs. Operational limits of temperature effects were not explored, and it is reasonable to expect that significant extremes of temperature may overcome the calibration's ability to account for the effect of temperature on response. In addition to consideration of these factors, a consistent standard should be used for the calibration: in this test 3 sheets of bleached printer paper were employed. This is recommended as the platen roof can become heavily stained with continued use.

4.3.4 - Comparison with UV-Vis Reflectance Analysis

For a direct comparison between the UV-Vis reflectance and CID systems three squares of the red 'Flirty B52' colour swatch were used (Figure 4.5). These discs were not visually distinguishable, though differences could be observed between the discs with CID measurement. Observation of 10 repeat measurements taken using diffuse reflectance, specular reflectance and CID colorimetry showed that each swatch was discernable using each technique, except with diffuse reflectance at 630nm. Results from these measurements are shown in Table 4.1, with the CID results adjusted to percent of maximum luminosity (255) to allow a more direct comparison of results and precision. It can be seen that the uncertainties of both reflectance and CID techniques were similar, with an average RSD of 0.1% in each technique. Diffuse and specular reflectance measurements were taken at 630, 570 and 450nm to provide comparison to the R, G and B channels of the CID system, as these wavelengths are representative of red, green and blue LEDs [16].

However, as shown by Table 4.1, even with wavelengths chosen to coincide with LED emission, the results of the two techniques were not similar. In general CID results provided higher values and showed an inversion of the results for B and G channels when compared to the 450 nm and 570 nm results, with CID showing 'blue' higher than 'green' and UV-Vis the opposite. Examination of the reflectance spectrum shown in Figure 4.5 indicates that this was not due to the wavelength selected for reflectance analysis, as there were no significant UV-Vis features under 550 nm, but another factor. A difference was also apparent in the analysis of the B and C discs, in which C was observed to have a lower luminosity than B in the R channel, and yet, with reflectance, C was higher in all cases. The differences

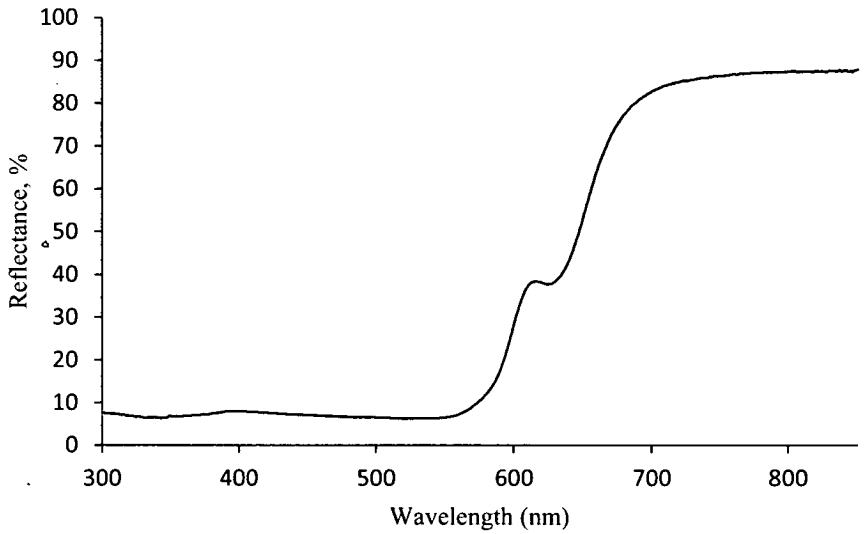

Figure 4.5 – Reflectance spectrum (specular) for 'Flirty B52' red colour swatch.

may be explained by the broader peak width at half height with the CID system, typically in the order of 30 nm [16], leading to an examination of a larger portion of the visible spectrum than with UV-Vis studies. This may have been due to a post measurement algorithm applied to the data, such as those used to correct for metamerism [15,23]. As these algorithms are more complex than those used for other reflectance models, for instance Kubelka-Munk theory [24], and were assumed to be proprietary intellectual property, information on the scanner-specific correction was not found.

As useable results were obtained after the application of these corrections these algorithms were not seen to affect performance. Observation of the error involved shows that the CID technique is comparable in precision to UV-Vis reflectance spectrophotometry, but that the differences observed in response between the techniques does not allow direct comparison of results. As such, the CID system

Table 4.1 – Results of 10 repeat scans of three red colour paint swatches, A, B and C. 100% reflectance/luminosity was taken by measurement of bleached white printer paper. Mean reflectance values are used, and R, G and B percentage values were obtained from mean luminosity divided by 255 (maximum luminosity), error values are ± one standard deviation.

		CID	Diffuse	Specular
		(% luminosity)	(% reflectance)	(% reflectance)
	A	67.11 ± 0.03	44.03 ± 0.02	44.27 ± 0.04
R/630nm	B	66.94 ± 0.03	44.02 ± 0.03	43.82 ± 0.02
	C	66.84 ± 0.02	44.66 ± 0.02	44.37 ± 0.03
	A	19.63 ± 0.03	10.82 ± 0.01	10.54 ± 0.01
G/570nm	B	19.76 ± 0.02	10.67 ± 0.01	10.11 ± 0.01
	C	20.05 ± 0.02	10.75 ± 0.01	10.26 ± 0.02
	A	23.18 ± 0.02	8.45 ± 0.01	8.09 ± 0.01
B/450nm	B	23.26 ± 0.02	8.35 ± 0.02	7.67 ± 0.01
	C	23.50 ± 0.02	8.40 ± 0.01	7.81 ± 0.01

requires its own calibration, rather than being able to adapt the UV-Vis calibration, but otherwise functions comparably to the UV-Vis reflectance system in terms of analytical quality.

4.4 – Analysis of MTB(10) Discs

4.4.1 – CID Analysis of Homogeneous MTB(10) Discs

Homogenously coloured methylthymol blue (MTB) discs, where dye had been immobilised at pH 10 [MTB(10)], were used to ascertain the ability of CID to quantify Cu(II) loading. Discs that had previously been analysed by UV-Vis reflectance were used, allowing direct comparison between the calibrations of these two techniques. Figure 4.6, below, shows the R, G and B channel responses to Cu(II) loading, with metal loading obtained by acid extraction and ICP-MS analysis as described in Chapter 3. The largest response, in terms of luminosity change per mass of complexed Cu(II), can be seen in the G channel. This is to be expected as the wavelength of maximum sensitivity observed with UV-Vis analysis was in the 555 to 570 nm range and typical green LEDs have their peak emission close to this wavelength [17]. Responses are also seen in the R (630-660 nm) and B (470-430 nm) channels but are less substantial, as expected from the UV-Vis spectrum (Figure 3.8). B channel response is inverted compared to that of the R and G channels, and this can be understood when the UV-Vis reflectance spectrum of the MTB complexes is considered (Figure 3.8). In the UV-Vis spectrum the reflectance is seen to decrease below 490 nm with an increasing Cu(II) loading, where the blue LED's peak emission lies. Reflectance response is seen to increase with Cu(II) loading above 490 nm, where the peak emissions of green and red LEDs lie. In this way the CID response can be considered as proportional to the reflectance response at certain, discreet, wavelengths corresponding to the LED peak emission wavelengths.

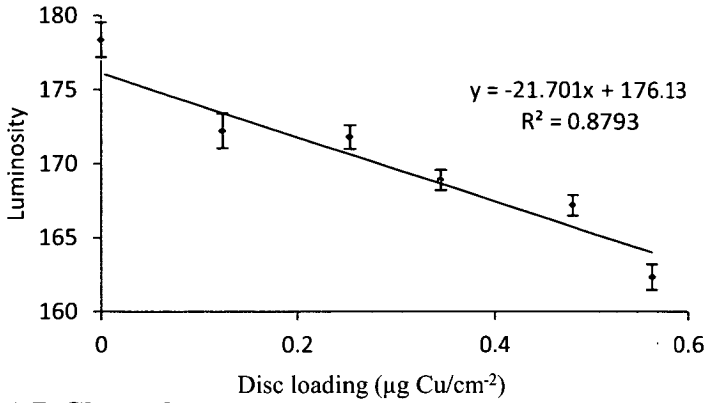

a) R Channel

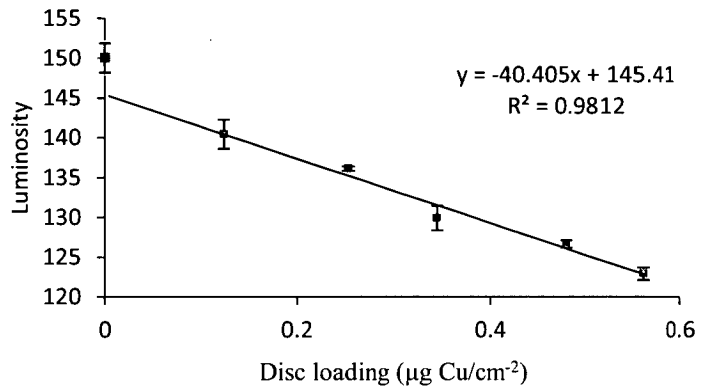

b) G Channel

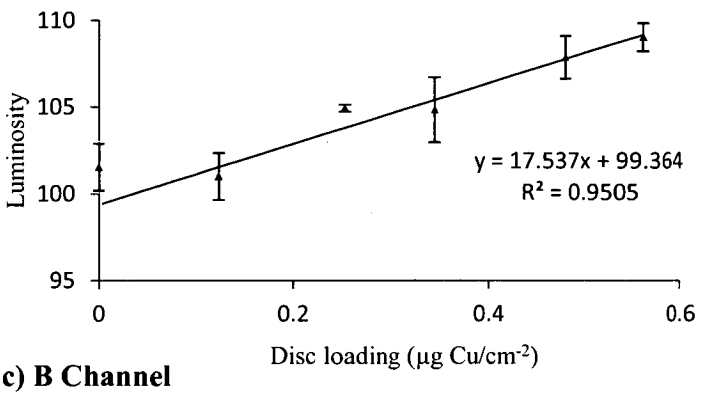

c) B Channel

Figure 4.6 –CID luminosity channel responses of homogenously coloured MTB(10) discs to Cu(II) adsorption.

Variation within triplicates for CID was significantly less than for UV-Vis analysis, with average relative standard deviations being 0.8 % for CID and 2.1 % for UV-Vis diffuse reflectance measurements, showing a more precise measurement of Cu(II) loading with CID. Variation was greater than CID measurement error (0.1 % RSD), obtained from repeated scans of the same disc and, as such, the majority of error is still thought to be due to disc manufacture and deployment as discussed in Chapter 3. An increased luminosity of the blanks, relative to the other data points, was observed with CID, similar to the increased blank observed with UV-Vis reflectance. In Figure 4.6 the blanks have been considered outliers, with the change believed to be due to the NO_3^- effect discussed in Chapter 3. As such the lines of best fit seen in Figure 4.6 were chosen without the blanks, justified further as they were observed to be lighter than the outer portion of discs, where Cu(II) had not bound, deployed in $NaNO_3$ solutions with Cu(II) present.

As colour within any single portion of the disc surface would be related directly to Cu(II) loading, then inhomogeneous areas of lower than average colouration should be corrected for by areas of larger than average colouration, and an accurate measurement of inhomogeneously coloured discs could be obtained. CID allows for this by analysing all areas effectively simultaneously and equally, whereas reflectance analysis was limited to an assessable area of ca. 1 cm^2 in the centre of the disc. However, this means that in order to obtain an accurate assessment of loading, it is necessary to select the entire exposed area without selecting any of the un-exposed regions as they would bias the result towards a lower loading.

This proved to be technically difficult, partially due to selection methods discussed in Section 4.3.2, and partially due to the nature of exposure. Warnken et al. [10]

discuss that lateral diffusion within a typical 0.08 cm thick diffusive layer increases the radius of the exposed area by up to 8%, potentially increasing the exposed area by 17%. This effect was partially accounted for with CID by selection of the coloured area, but accurate selection of the perimeter was made difficult by the diffusely coloured nature of the border. As manual selection of the exposed area was necessary for each disc, border discrimination became increasingly difficult for lower loadings due to less contrast between the exposed and unexposed portions. In practice, a relatively consistent level of variation within triplicates was observed by selecting as close to the border as possible, but while remaining inside the border. Therefore, this issue is not expected to be significant if a consistent approach is used when selecting the area to be analysed. In the case of discs with a low Cu(II) loading, the majority of response is due to the uncomplexed MTB and inclusion of excess uncomplexed MTB by selection of area outside the exposure border was not seen to have a significant impact on results or RSD values. Effectively, the method in which CID provides results, i.e. in terms of loading per pixel, also allowed for correction of some spatial error as each of the several thousand pixels analysed acted as a discrete sampler, with the average loading across the disc obtained from the average luminosity of all measured pixels.

This can be seen as an array of micro samplers being deployed, allowing a high spatial resolution which may be of benefit to 2 dimensional studies such as in sediment heterogeneity studies like those performed by Teasdale et al. [1]. As an average of 1,500 pixels was present in 1 cm^2 at the scanning resolution used (100dpi) this allows for a high degree of spatial discrimination. Several groups have studied the applicability of the CID method to investigating these heterogeneities

[1,25,26] and have found it to be quite suitable for the technique, as sectioning of the gel before analysis is not required [27]. Resolution is significantly improved over sectioning, as obtaining 1 mm^2 resolution traditionally requires digestion of 1 mm^2 gel portions and can be very difficult, whereas with CID 1 mm^2 contains 15 pixels at 100dpi and, therefore, has improved resolution over this fine gel sectioning work by default. In comparison the relatively expensive, time-consuming and destructive laser ablation technique has a resolution of approximately 100 samples per mm^2 [28].

4.4.2 – Analysis of Inhomogeneous MTB(10) Discs

The ability to analyse a larger, more well defined, area of the disc, and to compensate for fluctuations in colour meant that CID analysis may be applicable to the analysis of inhomogenously coloured discs obtained from direct Cu(II) uptake studies (see section 3.3.4.2). In the case of inhomogeneous discs, the average relative standard deviation of triplicate discs was reduced from 3.8% to 2%, and standard deviations were consistent between sample sets. Figure 4.7 compares CID to UV-Vis reflectance using data collected from 'inhomogeneous' discs, where Cu(II) had been complexed directly from solution, i.e. without the aid of a diffusive layer. These discs contained substantial perimeter colouration at lower loadings, with weaker colour in the centre of the disc. As mentioned, this caused analysis problems with reflectance as it was only able to measure the central portion of the disc, whereas CID was capable of assessing the entire exposed area of the disc at once and the reduced error was clearly seen.

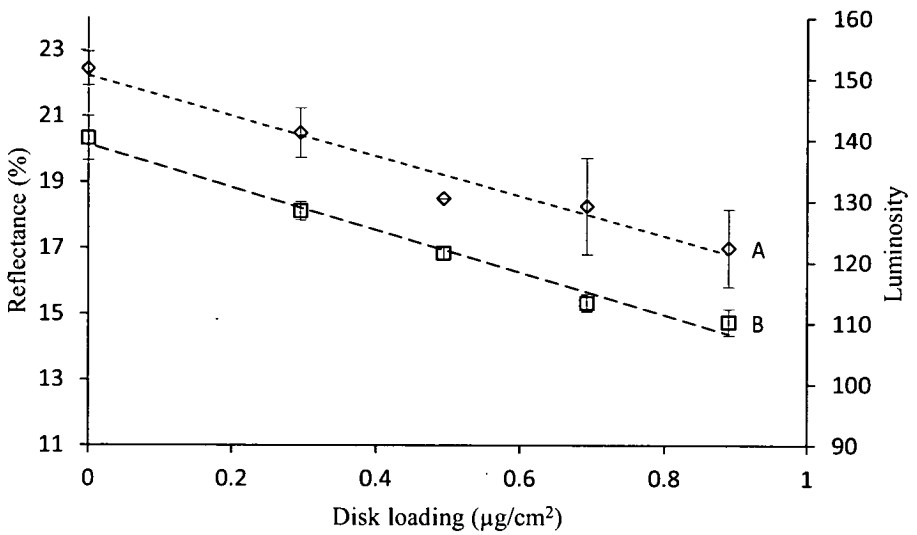

Figure 4.7 – Comparison of diffuse reflectance (A, top) and CID (B, bottom) techniques for analysis of inhomogeneous MTB discs. Note the significantly larger error associated with reflectance.

The reduced complexity of the direct uptake system meant that it was possible to easily perform loading tests over a greater range, as the use of nitrate and reliance on predicted Cu(II) loadings from DGT-type calibrations were omitted. Figure 4.8 shows R, G and B channel responses across a 90% complexed MTB loading test. The highest response was seen with the G channel at 34.8 luminosity units per µg Cu(II) cm^{-2}, as compared to 29.5 for the R channel and 10.0 for the B channel. A substantial difference was not observed between the G and R channels and, as the green channel was seen to lose linearity at loadings over ca. 1 µg cm^{-2}, the R channel would provide better analysis at these higher loadings. However, as discussed previously and mentioned also by Ouyang and Pawliszyn [31], a maximum loading for DGT use of 50% is advised. The B channel maintained a linear calibration, but with a significantly lower response than the other 2 channels. When compared to the

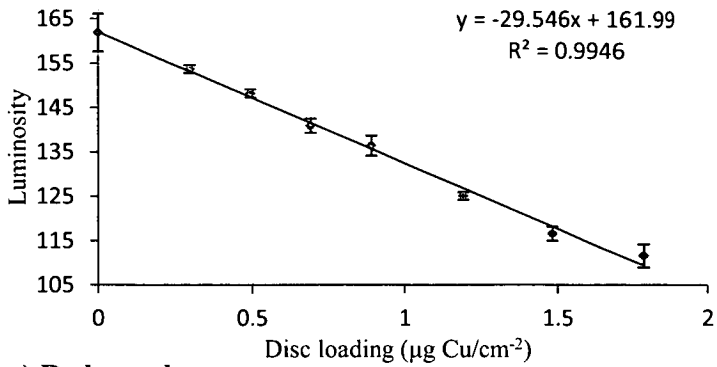

a) R channel

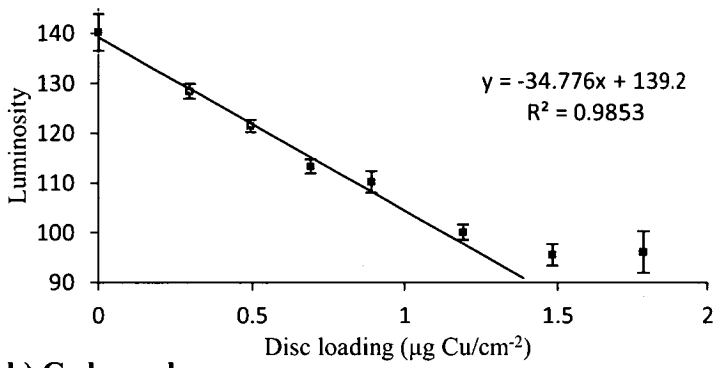

b) G channel

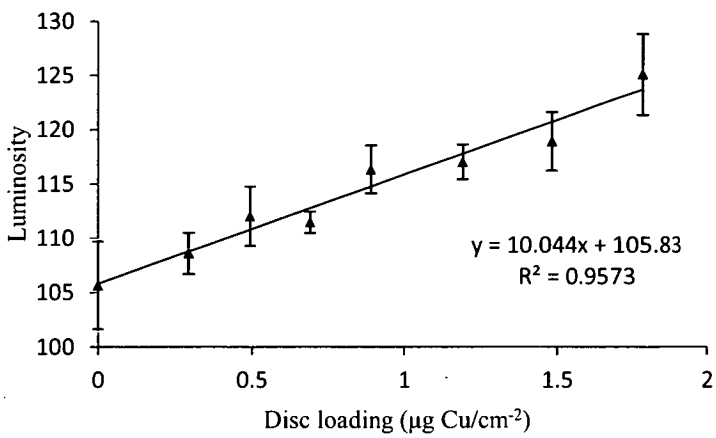

c) B channel

Figure 4.8 – R(a), G(b) and B(c) channel response of inhomogenously coloured MTB(10) discs to Cu(II) adsorption with a maximum loading of 90% (1.8 µg cm^{-2})

homogenous calibrations (Figure 4.6) a lower response was seen in the G and B channels. This is likely to be due to the NO_3^- effect on un-bound MTB improving the homogenous response by lightening the background proportionally more at lower loadings, as seen by the significantly high blanks with nitrate-exposed Cu(II) uptake tests.

The main point of interest in these data was the loss of response at high loadings for the G channel. As the R channel remained linear, this does not appear to be a chemical effect, but rather due to the analysis methods employed. The UV-Vis absorbance of homogenously coloured MTB(10) at various loadings (see Figure 3.10) may explain this, with a shift in the absorbance spectrum in the G channel range (550-570 nm) seen. Visual observation of the discs showed no obvious variation and an apparent uniform purple colour present on all the disks. As such, this loss of response and increase in variation may be due to a slight hypsochromic shift of a feature resulting in a changed response with the CID system as the shift is seen in the UV-Vis reflectance of MTB resin. This may also show the previously discussed lack of ability to effectively analyse colour changes in a dye where the principal wavelength lies between or outside the LED emission ranges. This is of concern, as in the situation of a colour change where the changes in the UV-Vis spectrum lie entirely between or outside the LED emission ranges, insufficient light would be reflected from the sensitive area of the spectrum and no response would be obtained.

This 'out-of-range' metameric failure is the primary drawback of the contact image sensor (CIS) based CID method. The use of three base LED colours significantly reduces the light reflected over a large portion of the visible spectrum, leading to a

greatly reduced response if the principal wavelength of a dye-metal interaction falls outside of the emission peaks. The use of a charge-coupled device (CCD)-based scanner may correct for some of this error, as the light source used is a fluorescent tube with a much broader emission spectrum. However, CCD-based devices still suffer from limited measurable wavelengths, as the colour filters used over the light collection capacitors would reduce or negate response in the blocked wavelength ranges. In light of this discussion, it must be noted that in visible solid-phase spectroscopy it is unusual to find a feature providing a visible colour change that would not cover a range wide enough to include one of these wavelengths, and the CID technique would be expected to provide a usable response in the majority of cases with either scanner type.

4.4.3 – Understanding CID Response

Teasdale et al. [1] and Jezequel et. al [25] have developed colorimetric diffusion-based passive sampling methods, and both use digital methods for analyte quantification. Linearity of response was not discussed directly by Jezequel, who used a second gel layer for post-exposure development of colour rather than in-situ colour development. Jezequel et al.'s system, therefore, differs from the one described in this chapter to an extent where it cannot be directly compared. Teasdale and co-workers did not observe a linear response, either, and their system also differed in the details of the analysis method, and the method of colour development. Their colour, effectively a black-white system referred to as optical

density, was obtained through the reaction of an AgI crystal with S^{2-} to produce black Ag_2S.

Their non-linearity was initially assumed to be due to the colour development occurring on the 'back' of particles, after the scanner-facing side had already accumulated sulfide, or change occurring on particles obscured by darkened particles where luminosity change may not be observable. Teasdale and co-workers (Robertson et al., [30]) expand on this and ascribe this lack of linearity to the non-linear relationship between transmission and optical density, the latter of which is equivalent to absorbance in Beer's Law. They state that the pixels of a digital imaging device are designed for a linear response to light transmission, and as such, the non-linearity observed with these optical density studies is due to the transmission-optical density relationship. It seems reasonable that further factors would also affect linearity in this system. For instance, development of Ag_2S crystals could cause a loss of linearity, as larger crystals would have a proportionally smaller cross-section due to surface-area to volume considerations. The use of a scanner, which is constructed for reflected light quantification [14], may also impact on linearity when it is considered that transmission is occurring though the gel in concert with reflection of transmitted light from the inner scanner lid surface. As such, the complexity of the gel-scanner system limits comparison to the primarily disc-surface reflection based system described in this chapter.

Another difference between the gel and disc based methods is that the concentration of coloured species does not change, and the system used here is defined by two limiting optical parameters, namely the luminosity of the uncomplexed dye and the luminosity of the complexed dye. A linear response is observed in the R and B

channels over a 90% Cu(II) loading range (see Figure 8) with the MTB work presented earlier, where Cu(II) loading remains below 100%. A simple model of CID colour analysis could be constructed to represent this. The 0 and 100% loading of a MTB disc are represented in an individual channel by two luminosity values, which essentially represent the reflectance of light in a small wavelength range from the uncomplexed and from the complexed dye, respectively. As a single pixel, which can be considered the sensing unit in CID work, will contain a certain number of MTB molecules, the overall luminosity of that pixel will be the ratio of complexed to uncomplexed MTB molecules, with respect to their luminosities, such that:

$$U + C = \text{total adsorbed dye}$$

where U represents the quantity of uncomplexed MTB molecules, in moles, and C represents the complexed molecules, in moles, and:

$$U / (\text{total adsorbed dye}) * L_U + C / (\text{total adsorbed dye}) * L_C = L_O$$

where L_U and L_C are the respective luminosity values of the uncomplexed and complexed MTB molecules, with L_O being the observed luminosity. As such, any point where the MTB molecules contributing to the pixel consist of both complexed and uncomplexed dye, the luminosity of the pixel will be proportionally between these two extreme luminosity values. Therefore, provided that the wavelength of

maximum response did not undergo a chromatic shift during complexation, a linear range should be expected between the 0 and 100% loadings of a coloured disc in a CID system, even if scanner response is not necessarily linear across the range. If a chromatic shift were to occur, then a non-linear calibration would be observed due to a change in sensor signal. This would be caused by a shift of the UV-Vis spectrum within, or outside of, the CID assessable range. A chromatic shift occurred with MTB in the G channel area of the spectrum, as discussed in Section 3.3.4.2. This is believed to have led to the loss of linearity observed with G-channel CID work during MTB Cu(II) complexation, as seen earlier.

While this model may account for the observed linearity in the calibration of the MTB-Cu(II) complex when compared to the non-linear calibrations observed in the optical density methods previously used, it would require a robust and simple colour system to verify. While this would certainly be possible, it is outside the scope of this work as the necessity was to provide a functioning colorimetric analysis system for Cu(II), which was achieved to the practical 50% DGT limit [31] in all channels.

4.5 – Conclusion

The CID analysis system assessed in this chapter was shown to function well for analysis of visible colour changes in the adsorbed MTB system. Accuracy and precision of the CID technique were typically better than those obtainable using UV-Vis diffuse reflectance, and CID had the added advantages of being cheaper, faster and more user-friendly than a UV-Vis system. However, the CID system was shown to have some limitations for general use, particularly in the limited range of the visible spectrum that is assessed by a scanner and this may potentially limit the application of this system to novel dyes. For MTB(10) this was not a significant issue and it is not anticipated to be a problem for the majority of dye substances available due to the broad nature of UV-Visible spectrum features.

Application of the system to quantification of MTB(10) complexed Cu(II) showed improved performance over the UV-Vis diffuse reflectance technique, and provided linear calibration plots. A brief theoretical model was discussed for explaining the linearity observed and that such linearity is likely to be expected for most analyses of this type.

In light of these results the CID system was considered more appropriate for quantification of colorimetric DGT binding phases than the UV-Vis system and is recommended for use in similar work.

References

[1] P.R. Teasdale, S. Hayward, W. Davison, Analytical Chemistry, 71 (1999) 2186.

[2] developed at the U.S. National Institutes of Health and available on the Internet at http://rsb.info.nih.gov/nih-image/

[3] S. Abrahamsson, Journal of Scientitic Instruments, 43 (1966) 931.

[4] J.F.W. Mallet, J.N. Champness, A.R. Faruqi, T.H. Gossling, Journal of Physics E: Scientific Instruments, 10 (1977) 351.

[5] C. Goocheer, W. Rasband, L. Sokoloff, Annals of Neurology, 7 (1980) 359.

[6] N.L. Anderson, J. Taylor, A.E. Scandora, B.P. Coulter, N.G. Anderson, Clinical Chemistry, 27 (1981) 1807.

[7] D.B. Masters, C.T. Griggs, C.B. Berde, Biotechniques, 12 (1992) 902.

[8] T.B. Shea, Biotechniques, 16 (1994) 684.

[9] C.D. Fermin, M.A. Gerber, J.R. Torrebueno, Journal of Microscopy, 167 (1992) 85.

[10] L. Byrne, J. Barker, G. Pennarun-Thomas, D. Diamond, Trends in Analytical Chemistry, 19 (2000) 517.

[11] S.P. Mustoe, D. McCrossen, Chromatographia Supplement, 53 (2001) S474.

[12] S.E. Umbaugh, Computer imaging : digital image analysis and processing, CRC Press, Boca Raton, Florida, 2005.

[13] J. Farrell, D. Sherman, B. Wandell, IS&T's Tenth International Congresson Advances in Non-Impact Printing Technologies, 1994.

[14] M. Vrhel, et al. IEEE Signal Processing Magazine, 22 (2005) 23.

[15] P. Urban, R.-R. Grigat, Signal, Image and Video Processing, 3 (2008) 171.

[16] LEDtronics, Discrete & SMT Rating and Characteristic Curves. 1999.

[17] I. Moreno, U. Contreras, Optics Express, 15 (2007) 3607.

[18] W.S. Rasband, ImageJ, U. S. National Institute of Health

[19] S.E. Umbaugh, Computer Imaging: digital image analysis and processing, CRC Press, Boca Raton, 2005.

[20] K.W. Warnken, H. Zhang, W. Davison, Analytical Chemistry, 78 (2006) 3780.

[21] C. Huh, W.J. Schaff, L.F. Eastman, S.-J. Park, IEEE Electron Device Letters, 25 (2004) 61.

[22] McGraw-Hill, McGraw-Hill Encyclopedia of Science and Technology, McGraw-Hill, 1997, p. 402.

[23] H.S. Fairman, J.L. Armitage, Color Reasearch & Application, 12 (1986) 261.

[24] P. Kubelka, F. Munk, Zeitschrift fur Physik, 12 (1931) 593.

[25] D. Jezequel, etal., Estuarine, Coastal and Shelf Science, 72 (2007) 420.

[26] N.J. Rogers, S.C. Apte, Environmental Science and Technology, 38 (2004) 5134.

[27] P. Divis, M. Leermakers, H. Docekalova, Y. Gao, Analytical and Bioanalytical Chemistry, 382 (2005) 1715.

[28] K.W. Warnken, W. Davison, H. Zhang, Analytical Chemistry, 76 (2004) 6077.

[29] B. Vrana, et al., Trends in Analytical Chemistry, 24 (2005) 845.

[30] D. Robertson, P.R. Teasdale, D.T. Welsh, Limnology and Oceanography: Methods, 6 (2008) 502.

[31] G. Ouyang, J. Pawliszyn, Journal of Chromatography A, 1168 (2007) 226

Chapter 5

Exploration of Alternative Dyes

Enhancing the application of the colorimetric DGT binding phase

5.1 – Consideration of Other Dyes

The colorimetric binding phase system described in Chapters 2 to 4 has been shown to provide effective quantification of Cu(II). This system was designed so that its analytical capabilities could be expanded through the use of other colorimetric chelating agents. The use of a commonly available indicator dye (MTB, discussed in Chapters 3 and 4) allowed for an inexpensive binding phase to be created and characterised, with 1 gram of dye being sufficient for creation of over 110 g of resin at a dye loading of 10 μmol per gram of resin (10 μmol g^{-1}).

In general, indicator dyes, while inexpensive and readily available, may not be ideally suited to DGT binding phase use as their selectivity is typically poor. This selectivity issue is highlighted by the buffering that is usually required to obtain reasonable metal response, and the common use of co-reagents, such as masking agents [1]. An example of this is that, for the use of MTB as an aqueous metallochromic indicator, it is recommended to maintain the solution's pH at approximately 12 for Zn(II) analysis and between 4 and 5 for Cu(II) analysis. In addition to the buffering of analytical solutions, for Cu(II) analysis it may be also be necessary to add 1,10-phenanthroline as an Fe(III) masking agent. With resin-adsorbed dyes this is difficult to achieve, as the addition of masking agents to the binding phase may not be possible, and may not provide the same utility as in aqueous solution. Furthermore, the pH and oxidative conditions of a DGT deployment will be determined by the environment, meaning control of these factors may not be possible. Ideally the chosen colorimetric chelating reagent will not rely

on masking agents or precise buffering for colorimetric, selective response in environmental matrices.

Considering that solution conditions cannot be directly controlled, and masking agents may not be possible to add, an exploration of commercially available metal-selective reagents was of interest. Ideally, the discovery of reagents that did not require co-reagents, and are applicable over a range of environmental conditions, would allow for the most useful binding phases. While this may be possible with some indicator dyes, it was thought that another class of compounds may better meet the necessary criteria. When examining these reagents the primary criteria were those of colorimetric response, stability, selectivity, and cost. A further important factor was the ability of a reagent to function after adsorption onto resin. An ideal situation would see the selection of analyte-specific chromogenic ionophores which could be immobilised and were stable under typical environmental conditions for periods of at least several days and, preferably, several months.

The analytes of primary interest in this study were Cu(II), Zn(II), Pb(II), and Cd(II), and reagents specific for these metals were examined as a priority. Unfortunately, the ability of reagents to interact with aqueous metals at near-neutral environmental pH is not easily predictable [2] and experimental studies would likely be necessary to examine any potential chromogenic ionophores. Also, as noted for MTB in Chapter 3, the interaction of chromogenic reagents with metals in aqueous solutions was not indicative of the metal-dye reactions observed once adsorbed onto the resin.

A group of promising reagents are crown ether compounds, described by Pederson in 1967 [3], which have been shown to be excellent metal-specific agents. The

process for metal chelation in a crown ether is not fully understood, but they have been noted to have particularly high selectivity for individual metal ions, and have been used for this reason in many processes [4,5]. Crown ethers are part of the large class of macrocycle compounds, including crown amines, cyclic molecules containing a mixture of heteroatoms (typically oxygen and nitrogen) and calixarenes, all which can have highly metal-selective behavior. Costs for these vary from less than $1 per gram to many thousands of dollars per gram, with synthesis varying similarly in that some compounds are easily synthesised from inexpensive materials, and some require many weeks of laboratory work with low yields. Unfortunately, few of the studies into these compounds discuss colorimetric reactions and testing for such would therefore have to be performed in-house.

The stability of these compounds is not commonly discussed, although the application of many for use in ion selective electrodes (ISE) suggests that stability is not a major concern in some situations [6-9]. Unfortunately, ISE use requires different chemical properties, in that the exchange between free and complexed analyte forms should be fast to facilitate transport across the membrane [4]. This property makes the compounds used in ISE work unsuitable for DGT use as they would not be strong chelating agents. Of the studies discussing macrocycles specific to the analytes of interest for this project, none were found which were noted to have high formation constants. This is likely due to the cost of many specialist compounds limiting their application to the type of single-use projects where irreversible binding would be employed. As significant work would need to be performed in assessing a wide range of compounds, macrocycles were not

considered a suitable class to examine at this point for application to a colorimetric DGT binding phase.

Fluorescent ionophores were considered as an alternative to chromogenic reagents, particularly as many have been noted to have selective Zn(II) reactions [10,11] and, less commonly, reactions with other analytes [12,13]. In general, fluorescence reactions are highly specific as they rely on a particular metal-moiety interaction rather than the ability of the compound to specifically bind the analyte. However, Fluorescent ionophores have not been used in similar circumstances to DGT binding phases and their applicability to DGT deployment could not be guaranteed. Further to this, the requirement of a fluorimeter for analysis has not been examined for this work, and fluorescence is not considered to be as user-friendly or flexible as computer imaging densitometry (CID). As such, fluorescent methods were not explored.

These two classes appeared to be the most promising methods for obtaining selectivity, but neither was seen to have the desired properties reported. While it is likely that some compounds from these classes may prove suitable, significant laboratory work would need to be undertaken to assess potential compounds.

As indicator dye compounds were readily available, and had been applied to DGT use through MTB, they were therefore considered the most appropriate class of compounds to screen. In particular, well-established reagents, such as those highlighted in the CRC Handbook of Organic Analytical Reagents [1], were of interest for further study. To this end a selection of readily available indicator dyes was chosen, and immobilisation of these dyes was performed using PSDVB resins

(Chapter 2). The dyes were then calibrated using a similar method to MTB (Chapter3), with CID analysis (Chapter 4) used where quantitative results could be obtained without metameric issues.

5.2 – Experimental

5.2.1 – Typical Chemicals

Metal salts of analytical grade were used for metal exposure tests. The salts used were $CuSO_4$, $CdCl_2$, $MnCl_2$, $PbNO_3$ (Ajax Chemicals, Sydney, Australia); $FeSO_4$ and $ZnSO_4$ (BDH, Melbourne, Australia). Ultra high quality (UHQ) water was sourced from a Barnstead water purifier (Thermo Scientific, Waltham, USA) with a conductivity of 18 ± 1 MΩ cm^{-1}. Phosphate buffers were made using Riedel-de Haën low-metal phosphate (p.a. grade Na_2HPO_4 and NaH_2PO_4, Seelze, Germany). $NaNO_3$ was obtained from ChemSupply, (99%+ AR Grade, Gillman, Australia). Equipment was acid washed using a 10% v/v HNO_3 bath.

5.2.2 – UV-Vis Absorbance Studies

Dye solutions were prepared at 1 mmol L^{-1} by dissolution in UHQ water, AR grade methanol (BDH, Melbourne, Australia), or AR grade acetone (BDH, Melbourne, Australia) as required (see Appendix 1). Metal solutions of 100 mg L^{-1} were made in UHQ water for exposure to the dye solutions as discussed in Chapter 2, section 2.2.1. Absorbance studies were undertaken using a Cary 1E spectrophotometer (Varian, Melbourne, Australia) with 1 cm path length quartz cuvettes (Starna, Baulkham Hills, Australia). Where absorbance was greater than 2, solutions were diluted in 1:1 steps to obtain dye absorbance values close to, but below, one.

5.2.3 – Resin Immobilisation of Dyes

For the purpose of immobilisation dyes were dissolved at 1 mmol L^{-1} in the appropriate solvent. Dyes used and their purities are noted in Appendix 1, along with dye immobilisation conditions. An overview of the dye immobilisation methods is provided below.

Immobilisation onto Dowex 1x8 was by exposure of a weighed quantity of vacuum dried resin to approximately 50 mL of dye solution containing the dye required for the intended loading. For instance, for a gram of resin with a loading of 10 μmol g^{-1}: 1.00 gram of dry Dowex 1x8 was immersed in 40 mL of UHQ water and 10.0 mL of 1.00 mmol L^{-1} (10.0 μmol) dye was added. The pH was adjusted after resin addition, but before dye addition, with 98% H_2SO_4 (AnalaR, BDH, Kilsyth, Australia) and 1 mol L^{-1} NaOH (AnalaR, BDH, Melbounre, Australia). This pH adjustment was measured using an Orion model 720A pH meter with a GPH Electroder pH probe. This solution was shaken for 24 h at or above 100 rpm on a Lab Line Orbit shaker before the resin was collected by vacuum filtration onto Whatman #54 filter paper and air dried. Dye uptake completion was confirmed visually, possible as visible dyes were observable at concentrations of 2 μmol L^{-1}, and uptake solution dye concentration was typically 200 μmol L^{-1}. This allowed uptake to be confirmed as 99% or greater, and uptake was verified by observation of resin coloration. In the case of non visible dyes, UV-Vis absorbance was used to examine the supernatant in the UV region to confirm dye adsorption.

Immobilisation of dyes onto Amberchrom CG-300c resin (Rohm and Haas, Bellefonte, USA) was from acetone (99% AR grade, Ajax Finechem, Sydney,

Australia), isopropyl alcohol (IPA, 99% minimum LC grade, Waters Associates, Milford, USA) or ethanol (96% GPR, BDH, Melbourne, Australia) depending on dye solvent as described in Appendix 1. After 24 h shaking, the resin was vacuum filtered onto Whatman #54 paper and air dried for more than 24 h.

Air dried resin was adhered to 2.54 cm diameter Esselte 'Quik Stik' adhesive paper label discs (Stamford, Connecticut, USA) by removing backing material and pushing the adhesive side of the disc into the resin. Discs were cut using a stainless steel circle punch with the plastic backing contacting the metal. Resin was then spread over the disc and lightly pressed on using nitrile gloves, with discs then tapped to remove excess resin. Once resin-discs were made, equilibration of the resin was performed by immersing discs in UHQ water containing a pH 6.8 phosphate buffer. CG-300c based discs were pre-wet with isopropyl alcohol before immersion in solution. After immersion in the equilibration solution for more than one hour, discs were removed and rinsed with deionised water to remove excess resin before being air dried.

5.2.4 – Quantitative Metal Interaction Tests

In order to determine which metals a dye would interact with, dyes were adsorbed onto resin as stated in Appendix 1 and quantitative tests were performed on the resulting resin-dye, without paper label immobilisation. The adsorbed dyes were exposed to equimolar and twice equimolar metal concentrations for 24 h, to ensure colour development was complete. Comparison of the colour developed during the equimolar and twice equimolar tests allowed determination of whether greater than

equimolar metal quantities would be needed for calibration, if so, less colouration would have been seen with the equimolar tests.

5.2.5 – Disc Metal Capacity Tests

To determine dye metal capacity, individual discs were immersed in 20 mL of UHQ water with 20.0 μg of Cu(II) present in a 70 mL plastic container (Sarsteadt, Ingle Farm, Australia). After shaking for 4 h in this solution, the discs were removed, rinsed briefly three times using UHQ water and transferred to another 70 mL container. Those dyes adsorbed onto CG-300c resin were wet with ethanol prior to the transfer. To this container 10.0 mL of 2.0 mol L^{-1} HNO_3 was added and the discs were shaken for 24 h, with noted colour change in all discs. Acid extract solutions were analysed on a SpectrAA 800 (Varian, Melbourne, Australia) AAS with GTA-95 graphite furnace attachment and autosampler. Volumes were determined by weighing the containers at each step to ± 1 mg.

5.2.6 – Calibration of Binding Phases

Homogeneous colouration during binding phase calibration was achieved using acid-washed aqueous DGT sampling devices (DGT Research Ltd., Lancaster, UK) with 0.82 mm polyacrylamide diffusive gels (DGT Research Ltd., Lancaster, UK) and two vinyl spacers (0.33 mm each). Samplers were assembled immediately before exposure, after wetting with 0.01 mol L^{-1} pH 6.8 phosphate buffer, and placed in 200 mL polycarbonate containers (Sarsteadt, Ingle Farm, Australia).

Exposure solutions contained 0.1 mol L^{-1} $NaNO_3$ and 0.01 mol L^{-1} PO_4^{3-} buffer, cleaned by exposure to 5 g of Chelex 100 (Sigma, Munich, Germany) per litre to remove transition metals. Test lengths were either 24 h or 4 h. Cu(II) concentrations of 355, 710, 1065, 1420 or 1775 μg L^{-1} were added for 24 hour tests, and of 53.4, 108, 162.8, 217.1 or 270.8 μg L^{-1} were added for 12 hour tests. Extra exposures at times of twice and thrice this length were performed at the lowest concentration used. The concentrations required were calculated using the DGT equation [14] using the constants given earlier along with D = 5.42 x10^{-6} cm^2 s^{-1} and a = 3.14 cm^2. After shaking on a Lab Line Orbit shaker at 100 rpm, solutions were discarded and binding phases recovered for colorimetric analysis and extraction.

The shorter 4 h deployment time was used to reduce testing time and was not believed to impact on DGT accuracy, as 4 h has been used by Warnken et al. [15] in their thorough DGT study. Warnken et al. discussed that 4 h was considered sufficient, as the primary effect of time on accuracy is believed to be due to establishment of the diffusion gradient, which is thought to be obtained in under 10 min when the work of Zhang et al. [16] is considered. This assumption is confirmed by the linear uptake over time seen in Figure 5.1.

5.2.7 – Complex Matrix Tests

Seawater exposure tests used 3 μm-filtered natural seawater obtained from the Australian Maritime College National Centre for Marine Conservation and Resource Sustainability's Aquatic Key Centre (Newnham Campus, University of Tasmania, Australia) and further cleaned by exposure to Chelex 100 (Sigma, Germany) resin at

5 g of resin per litre of seawater. DGT exposure was performed as above, with samplers wetted with the cleaned seawater during assembly to ensure no trapped air was present. Cu(II) concentrations of 176.6, 353.2, 529.8, 706.4 and 883 $\mu g\ L^{-1}$ were used to assess Cu(II) uptake. Cu(II) solutions were added in stock concentrations providing that the analyte solution volume was less than 3% of the seawater volume to ensure that seawater concentration was not substantially affected.

5.2.8 – Metal Extraction and AAS-GF Analysis of Dye Extracts

Metal extraction was performed by placing dried, exposed resin discs in a 70 mL polycarbonate container (Sarsteadt, Melbourne, Australia) and adding 10.00 mL of 1 mol L^{-1} HNO_3 (from 65% w/v Suprapur, Merck, Darmstadt, Germany, and UHQ water). Weights were recorded at each step to obtain accurate volumes. Extraction solutions were shaken for 24 h on a Lab Line Orbit shaker before supernatants had 40 mL of UHQ water added for analysis. Extraction efficiency tests were performed by repeating this process on extracted discs of the highest metal loading.

Cu(II) analysis was performed using a SpectrAA 800 (Varian, Melbounre, Australia) AAS with GTA-95 graphite furnace attachment (AAS-GF) and autosampler. Sampling conditions were standard for Cu(II) at a 324.8 nm wavelength. Calibration was by prepared standard Cu(II) solutions auto-mixed to provide an equivalent matrix.

5.2.9 – Colorimetric Analysis – UV-Vis Reflectance and CID

Diffuse reflectance spectrophotometry was performed on a Cary 1E spectrophotometer (Varian, Melbourne, Australia) using Varian SpectrAA software (version 1.3) with a Labsphere DRA-CA-30I attachment (North Sutton, USA) utilising the 0° diffuse wedge. Baseline spectra were taken using the Spectraflect (AS-01158-060, USRS-99-010-0B69A) reflectance standard. To avoid variation in spectra caused by resin moisture, discs were analysed wet. Interference due to water on the disc surface was minimised by blotting discs with lint-free tissue paper and analysing within 5 min of this water removal. Discs were supported using a glass plate to help maintain a flat surface.

As with UV-Vis analysis, scanner-assessed (CID) discs were measured immediately after blotting to remove excess water while ensuring complete resin hydration. A consistent position on the scanner was maintained by marking the inside of the lid. Scans were collected in the Gimp 2.2.17 software package (maintained by Michael Natterer and Sven Neumann at http://www.gimp.org/) using TWAIN acquisition through the default Canon software. CID analysis of discs was performed by using the elliptical tool to select the exposed area while avoiding unexposed resin outside this area. In the case of scratched disks the area without resin was de-selected using the 'select hand-drawn regions' tool. Mean R, G and B values of the selected area were recorded from the histogram tool and stored in Microsoft Excel 2003.

5.3 – Results and Discussion

5.3.1 – Screening of Potential Dyes

A variety of readily available metal and pH indicating dyes were selected (see Appendix 1) for initial screening. A list of the acronyms used can be found in the Glossary before the Table of Contents. Aqueous solutions of these dyes were exposed to 100 mg L^{-1} solutions of Fe(II), Cd(II), Cu(II), Zn(II), Pb(II) and Mn(II) in order to determine if the interaction with these metals resulted in a solution colour change, which would indicate both metal interaction and colorimetric potential. When examined using UV-Vis absorbance, those solutions that showed colour change were selected for further study. This method did not provide ideal discrimination as the metal interactions with resin-adsorbed dyes differed substantially from the aqueous interactions, as was observed with MTB (Chapter 3).

For this reason, dyes that were seen to have a usable response in aqueous spectra, or that were known through the literature to be potentially useful, were immobilised on the polystyrene-divinylbenzene matrix resins Dowex 1x8 (anion-exchanger) or Amberchrom CG-300c (neutral). The resin used for each dye is listed in Appendix 1. The adsorbed dyes were then used for qualitative visual metal interaction studies, discussed later, with those showing significant interactions being examined as per MTB, focusing on verification of DGT performance and CID analysis.

The resin used for dye immobilisation was selected based on the structure of the dye. If no ionic moieties were present on the colorimetric reagent, the non-ionic Amberchrom CG-300c was used. Where anionic moieties were present Dowex 1x8

was chosen. In some cases ionic dyes were considered suitably aromatic to be immobilised on CG-300c, these cases and the conditions under which this occurred are covered in Appendix 1. No cationic moieties were present on dyes selected for this examination and, as such, no cation-exchange resin was used.

Adsorption pH was controlled based on published pK_a values, with the intention of keeping the molecule in either a protonated, non-ionised, form for adsorption onto the non-ionic CG-300c, or minimally ionised for Dowex 1x8. Minimal ionization was typically the best achievable, as many dyes had sulfonic acid groups which are not readily protonated. As well as this, minimal ionisation could be preferable as it has been noted that while the adsorption of most ionic and non-ionic dyes on to resins are primarily due to pi-pi interactions, ion-exchange is a prominent secondary effect [17]. Therefore, it was considered pertinent to have dyes in their least ionic form for adsorption to encourage pi-pi interaction, but to allow ion-exchange where possible. Dyes were adsorbed over 24 h, at a pH less than the most acidic chelating group pH, or at a pH suitable to protonate ionic sites, as noted [1]. MTB is excluded as it has been discussed sufficiently in other chapters.

The resin loading of the above dyes was typically assessed by visual observation of the adsorption solutions. All visible dyes were apparent at concentrations of 2 μmol L^{-1} or less. As uptake was typically performed at a concentration of 0.2 to 0.5 mmol L^{-1}, a lack of visible colouration assured 99% or greater uptake.

In the case of non-visible dyes, such as bathophenanthroline and the DTC-based dyes, solutions were examined with UV-Vis to ascertain whether the concentrations could be assessed. In the case of DMG, bathophenanthroline and oCPC, UV-Vis

examination of the adsorption solution spectra showed weak, or non-existent, UV-Vis absorption at these low concentrations. To determine whether some response could be assessed with these dyes, resin was added to dye solutions and stirred for 24 h. The resin was then filtered off and exposed to solutions of the 6 metal ions tested for at individual metal concentrations of 10 mg L^{-1}. No colour change was noted within 24 h of this exposure, and work with these dyes was abandoned as the lack of change indicated either no colorimetric reaction or the lack of dye adsorption using this technique.

Qualitative metal response was assessed by exposing ca. 0.1 g of dye-adsorbed resins to large excesses (molar ratio of 10-100) of the metal ions of interest. If a change in colour was observed then more detailed testing was performed. After adsorption to their respective resins, colour changes were observed at pH 6.8 for Zincon, EBT, DDTC, PAN, oCPC, DPCO, DPCI, TAN and XO. In all cases Cu(II) was seen to provide a colour change, with a few dyes also providing a coloured response to Fe(II) (oCPC, XO, EBT) and Zn(II) (PAN, TAN, oCPC, EBT).

Once coloured reactions were determined, tests were performed with each metal seen to provide a response at equimolar and twice equimolar (to dye quantity) metal quantities. The resulting coloured resins were examined using UV-Vis absorbance spectroscopy in 0.1 cm path length quartz cuvettes. This test showed that the maximum metal to dye ratio was 1:1, observed in all cases by observation of complete colouration (no heterogeneity) in the equimolar case and equivalent coloration in the twice equimolar case.

As Fe(II) was not considered a metal of interest, but rather an interference, further examination of Fe(II)-responding dyes was not performed. Cu(II) provided a common analyte for examination of dyes, as all dyes with a colorimetric response had a visual Cu(II) response. Zn(II) response was examined briefly for comparison but suffered from substantial interference issues. These Zn(II) tests were not considered as important as the Cu(II) tests for this study, and were not repeated. However, as the Zn(II) results are of interest they are discussed in Appendix 2.

Of those dyes showing Cu(II) responses mentioned above, oCPC, DPCI, DPCO and DDTC were not chosen for further examination. DPCI, DPCO and DDTC were not chosen due to particularly weak and unstable colorimetric responses. For these dyes, the colour developed over the first 24 h of metal exposure was lost over a continued immersion in water of one week. As such, these dyes were considered unsuitable for DGT use as long-term colour stability is an important criterion and colour loss may indicate a loss of complexed metal. In the case of oCPC a strong colour was developed for Cu(II) and Fe(II), however visual colour development took more than a week. This long colour development time would preclude the use of this dye for most deployments. This also indicates that metal complexation would be inappropriately slow for DGT use, where effectively instant complexation times are important for maintenance of the concentration gradient [15].

5.3.2 – Cu(II) Response in XO, EBT, PAN and TAN

Of the dyes examined, five showed promising response to Cu(II), those five being Zincon, xylenol orange (XO), eriochrome black T (EBT), 1-(2-pyridylazo)-2-

naphthol (PAN), and 1-(2-thiazolylazo)-2-naphthol (TAN). Zincon's selectivity for Cu(II) warranted extra examination and is discussed later, in Section 5.3.3. The remaining four dyes were examined for DGT suitability by assessing the complexation of Cu(II) from bulk solution when used as a DGT binding phase. Their colorimetric properties were then assessed by CID examination of the colour change.

During this stage of disc testing it was thought pertinent to examine whether the backing paper accumulated Cu(II). To this end, resin with the dyes listed above adsorbed was immobilised on 5.07 cm^2 labels and these were exposed to 20 μg of Cu(II). This was performed as in the equimolar and twice-equimolar tests, and extracted after a very brief rinse with UHQ water to remove solution sitting on the disc surface. The results of this experiment, listed in Table 5.1, showed that a consistent amount of Cu(II) was accumulated by each disc regardless of dye loading. In all cases 90% of the available Cu(II) was removed from solution, showing that each disc had accumulated more than 10 μg of Cu(II). This was more than a 1:1 loading, or more than a 10:1 loading in the case of EBT, and was not thought to be due to the dye complexation. This was also seen in the 'blank' discs, where Dowex 1x8 resin was used without adsorbed dye and, therefore, demonstrated that the resin and/or label were accumulating Cu(II). This had not been seen in the MTB work, where a more thorough rinsing procedure was used and Cu(II) loadings were sub-equimolar.

Due to the lack of excess Cu(II) seen in the work performed with MTB it is recommended that three good rinses of each disc with UHQ water are performed before analysis. These results show that it may be possible to use these discs as DGT

Table 5.1 – Cu(II) accumulation by dye adsorbed resin discs, from a stirred solution, containing 20.0 μg of Cu(II) over 4 h. Dye 'none' refers to discs with immobilised Dowex 1x8 but without adsorbed dye. Results were obtained by AAS-GF analysis of extract solutions.

Dye	**Extracted Cu(II)** (μg)	**Cu(II) remaining in solution** (μg)
None	13 ± 1	2.1 ± 0.5
XO	13 ± 2	1.3 ± 0.2
EBT	13 ± 1	1.7 ± 0.2
TAN	14 ± 2	1.4 ± <0.1
PAN	9.5 ± 0.9	1.8 ± <0.1
Zincon	14.2 ± 0.3	2 ± 0.3

binding phases past the capacity of their adsorbed dye to complex the analyte while maintaining a concentration gradient suitable for DGT work, as analyte may bind to the paper label. However, this is not useful as analyte bound to the paper will not be colorimetrically assessable. It does mean that, potentially, multiple dyes could be used on a single disc without the chance that one analyte reaching its capacity would interfere with the other analytes.

In order to test the DGT function of the resin-adsorbed dyes, discs were used as binding phases and calibrated in a simulated DGT deployment, as with MTB in Chapters 3 and 4. Discs were calibrated using varying Cu(II) concentrations over 4 or 24 h, and DGT function was further assessed by using a constant Cu(II) concentration over 12 h, or 72 h. These discs were assessed by CID, discussed later, and to observe actual metal loadings they were acid-extracted and analysed by AAS-GF, providing the results shown in Figure 5.1.

A clear linear trend can be seen between increasing concentration and Cu(II) loading for the 10 μmol g^{-1} dyes, up to 1 μg cm^{-2}, or approximately 50%. A linear trend is also observed for the entire explored range with EBT. These trends show that these dyes function to complex Cu(II), up to a 1 μg cm^{-2} loading with XO, PAN and TAN. Furthermore, the linear trends observed over time reinforces that these dyes are functioning correctly as DGT binding phases.

After a 1 μg cm^{-2} Cu(II) loading is reached, this linearity is suddenly lost with PAN and XO, accompanied by an increase in the RSDs of the triplicate discs at each concentration. This loss of linearity was quite pronounced, and was effectively a complete loss of response which could be explained by the maximum loading being reached. A maximum loading at these points would indicate a Cu(II) to dye ratio of1:2, which has been noted to occur close to a pH of 6.8 with Cu(II) using XO [1], and with TAN when a non-polar solvent is used [1]. Therefore, it is reasonable to expect that 1:2 metal to dye complexes are being formed with these dyes, resulting in the resin capacity being reached at approximately 50%, or 1 μg cm^{-2} loading. The relatively high standard deviations observed after a Cu(II) loading of 1 μg cm^{-2} was

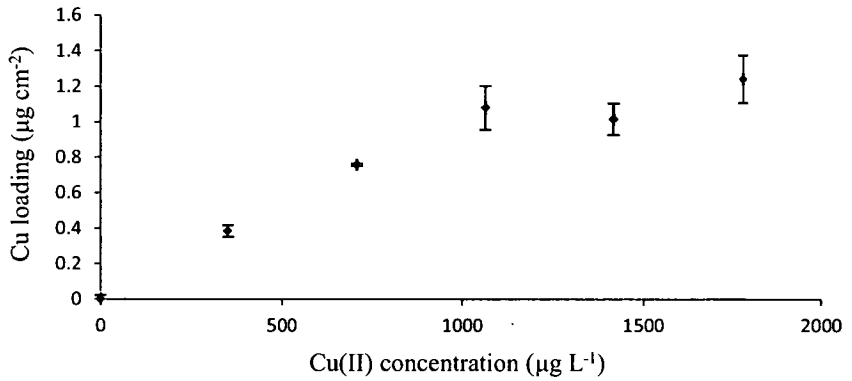

a) XO - Cu(II) uptake vs. conc.

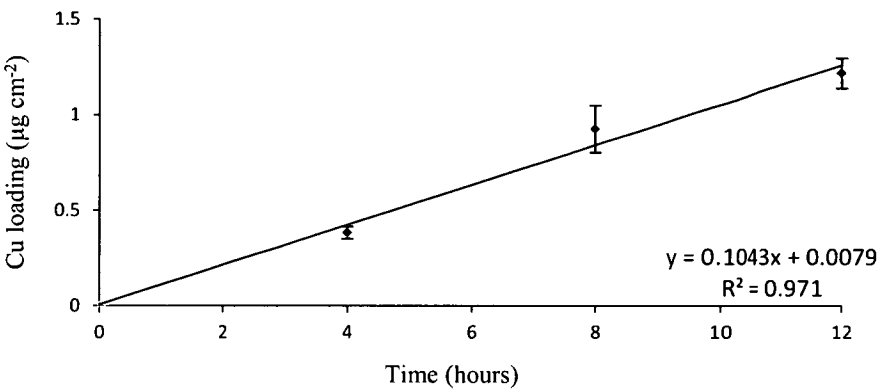

b) XO - Cu(II) uptake vs. time

Figure 5.1 a and b – AAS-GF observed Cu(II) quantities extracted from triplicate binding phases made of XO and Dowex 1x8. Deployments on the left were performed over 4 h at 355, 710, 1065, 1420 and 1775 µg L^{-1} of Cu(II), or at 355 µg L^{-1} over 4, 8 and 12 h.

Figure 1 continues overleaf

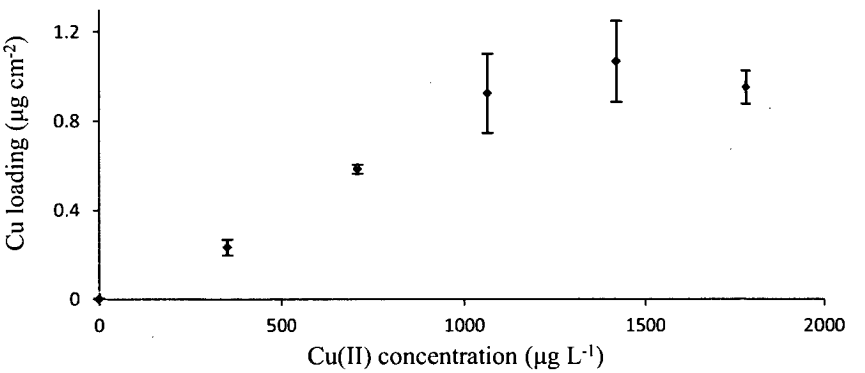

c) PAN - Cu(II) uptake vs. conc.

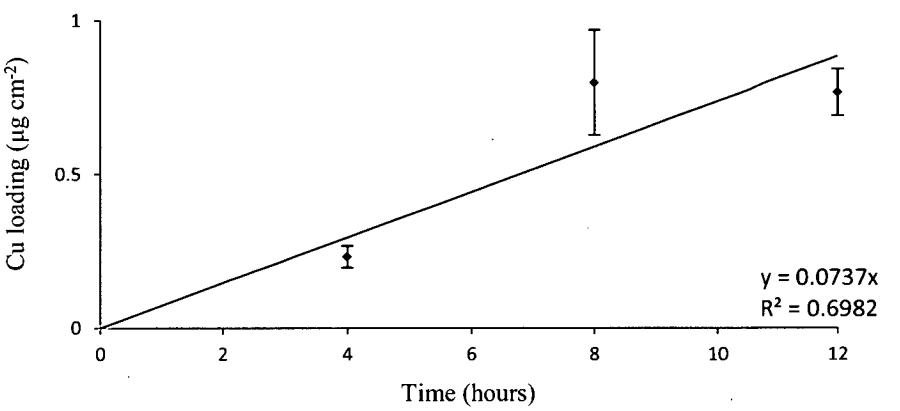

d) PAN - Cu(II) uptake vs. time

Figure 5.1 c and d – AAS-GF observed Cu(II) quantities extracted from triplicate binding phases made of PAN and CG-300c. Deployments were performed over 4 h at 355, 710, 1065, 1420 and 1775 µg L^{-1} of Cu(II), or at 355 µg L^{-1} over 4, 8 and 12 h.

Figure 1 continues overleaf

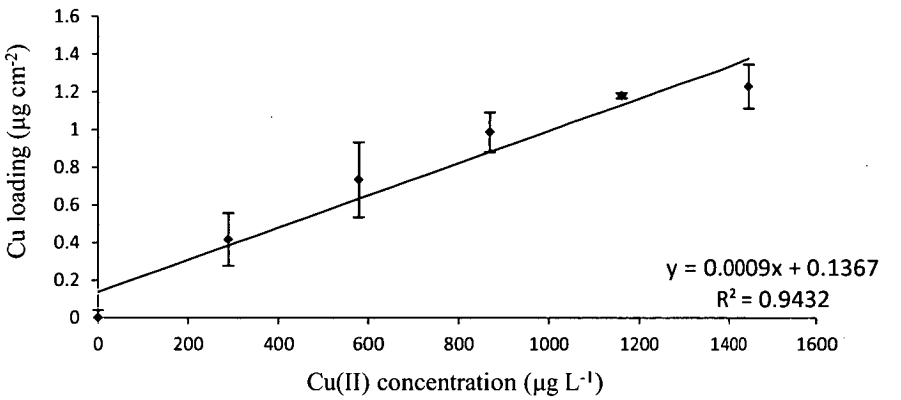

e) TAN - Cu(II) uptake vs. conc.

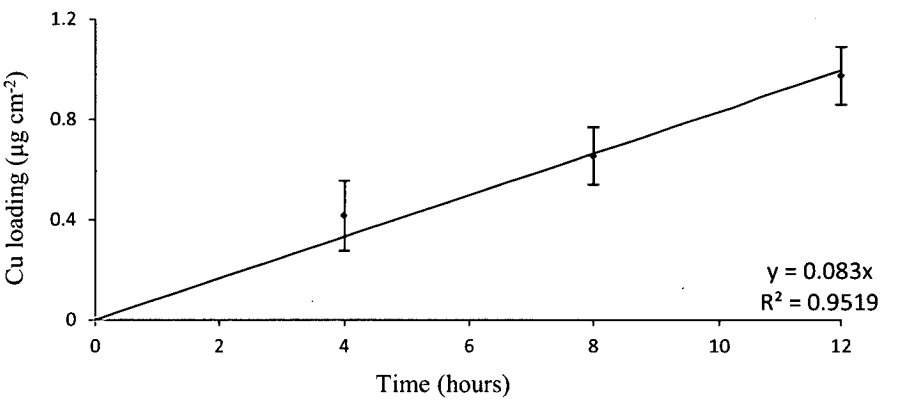

f) TAN - Cu(II) uptake vs. time

Figure 5.1 e and f – AAS-GF observed Cu(II) quantities extracted from triplicate binding phases made of TAN and CG-300c. Deployments were performed over 4 h at 355, 710, 1065, 1420 and 1775 µg L^{-1} of Cu(II), or at 355 µg L^{-1} over 4, 8 and 12 h.

Figure 1 continues overleaf

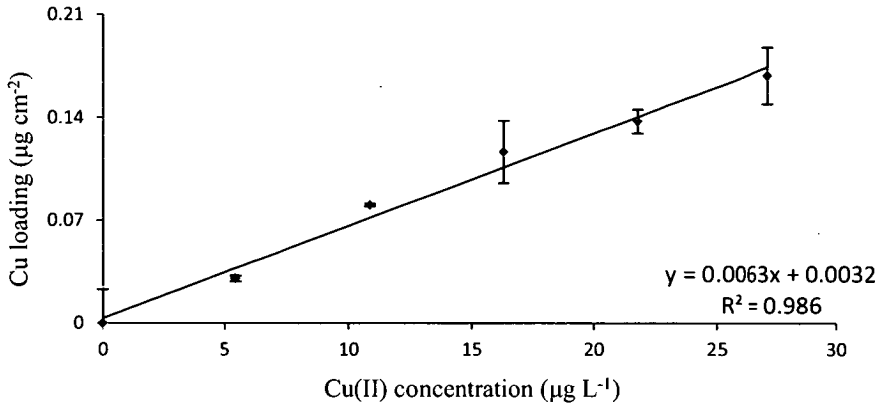

g) EBT - Cu(II) uptake vs. conc.

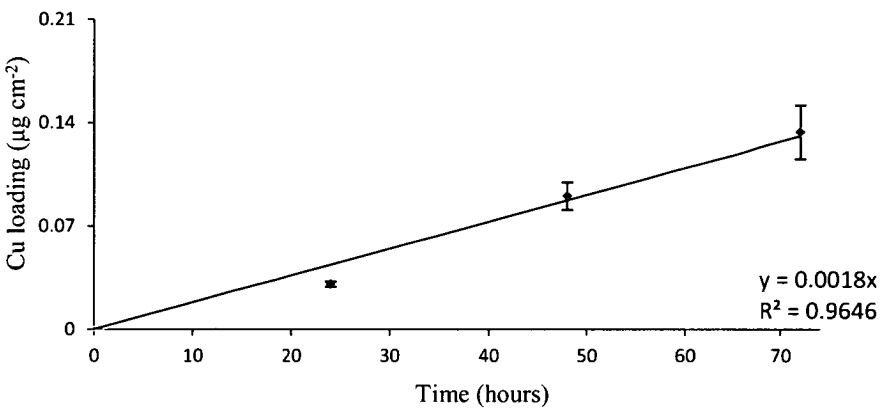

h) EBT - Cu(II) uptake vs. time

Figure 5.1 g and h – AAS-GF observed Cu(II) quantities extracted from triplicate binding phases made of EBT and Dowex 1x8. Deployments were performed over 24 h at Cu(II) concentrations of 5.34, 10.8, 16.3, 21.7 and 27.1 µg L^{-1}. Deployments were also performed at 5.43 µg L^{-1} of Cu(II) over 72 h.

reached are likely due to the variation in disc manufacture, and hence dye loading, providing a wide range of maximum Cu(II) complexation quantities. Further to this, in these cases the paper labels may contain Cu(II) due to the metal being able to diffuse past the resin layer, which may not be completely removed by rinsing. This would add to the increased RSD values from disc manufacture.

Linearity is maintained in the EBT and TAN cases, although some loss appears to be occurring with TAN after Cu(II) complexation of 1 $\mu g\ cm^{-2}$. The increasing loadings here show that the capacity of these resins has not been reached during these deployments. Considering the qualitative test results in Section 5.3.2, that indicate that 1:2 metal to dye ratios and greater are not occurring, the metal to dye ratio is likely 1:1. Results over time are linear, showing that the binding phases are functioning well as DGT binding phases.

5.3.3 – Colorimetric Response in XO, EBT, PAN and TAN

The colorimetric response of these binding phases was assessed using CID. The discs used for metal uptake tests, above, had their luminosity measured, giving the results presented in Figure 5.2. Luminosity was related to Cu(II) loading in a linear fashion in all cases, consistent with the theory presented at the end of Chapter 4.

Response, in terms of units of luminosity units per $\mu g\ cm^{-2}$ of complexed Cu(II), was high for TAN and PAN. The response of PAN, a maximum -98 luminosity units per $\mu g\ cm^{-2}$ of Cu(II) in the G channel, was the most precise seen with an RSD of

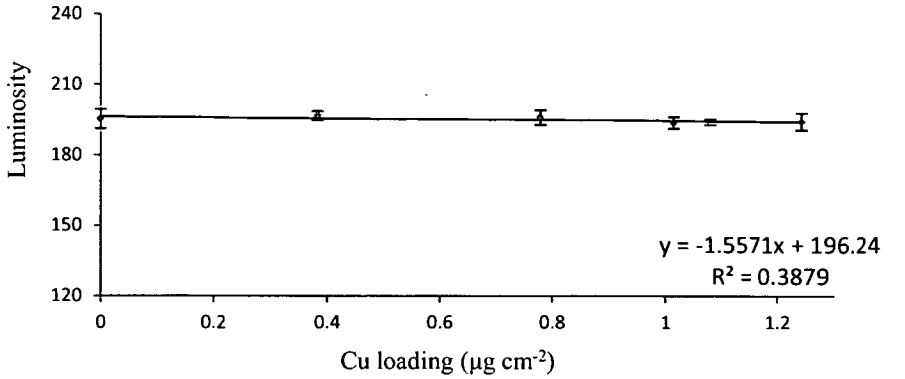

a) XO - R channel

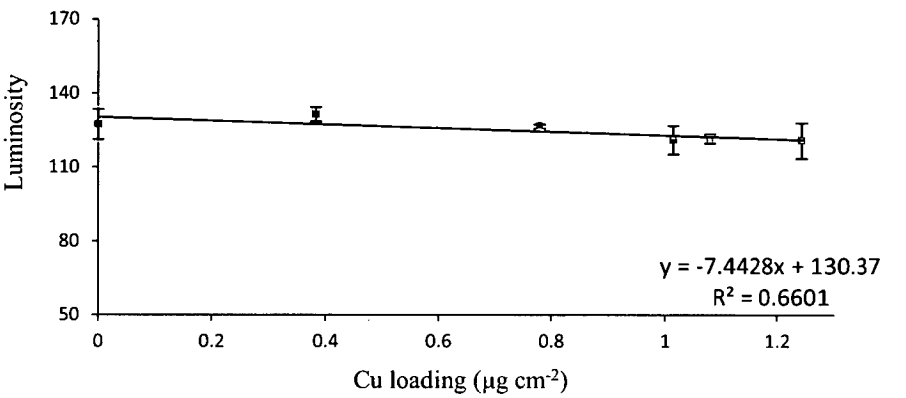

b) XO - G channel

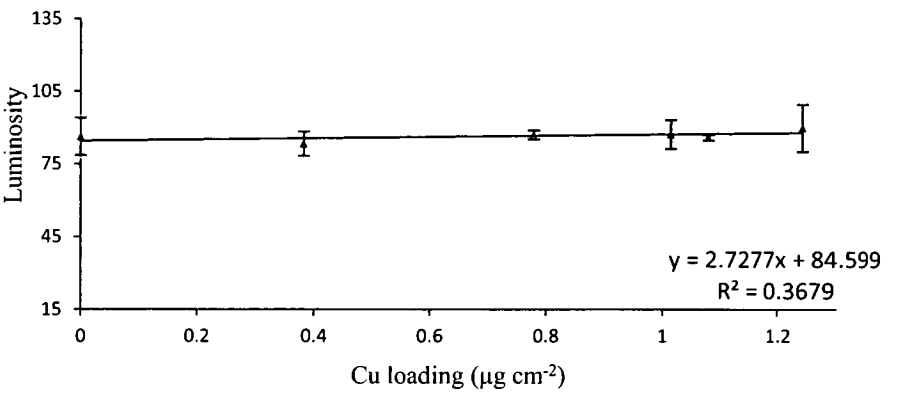

c) XO - B channel

Figure 5.2 a, b and c – CID analysis of XO binding phases. The range of luminosity values on the y-axis are consistently 120 to allow comparison of response. Loadings on the x-axis are AAS-GF observed, per disc.

Figure 2 continues overleaf

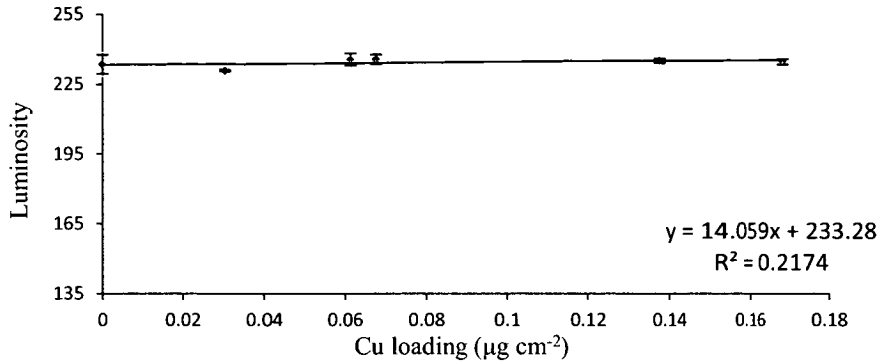

d) EBT - R channel

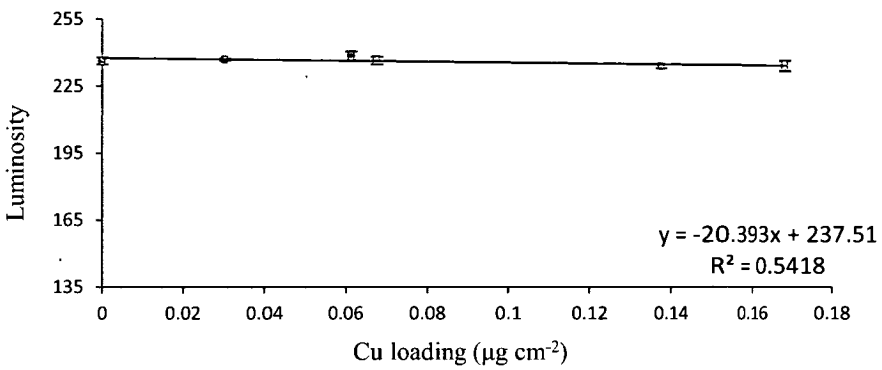

e) EBT - G channel

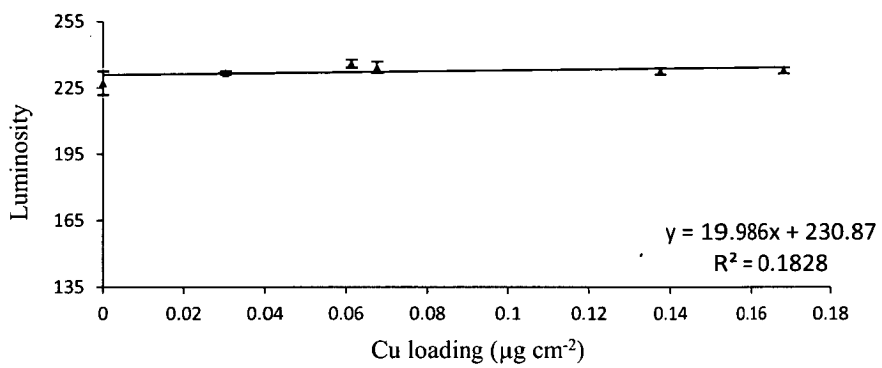

f) EBT - R channel

Figure 5.2 d, e and f – CID analysis of EBT binding phases. The range of luminosity values on the y-axis are consistently 120 to allow comparison of response. Loadings on the x-axis are AAS-GF observed, per disc. Note EBT loading is $1/10^{th}$ other dyes.

Figure 2 continues overleaf

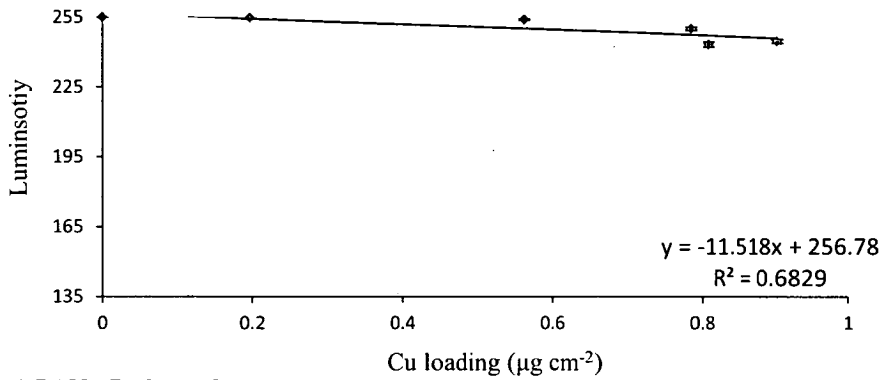

g) PAN - R channel

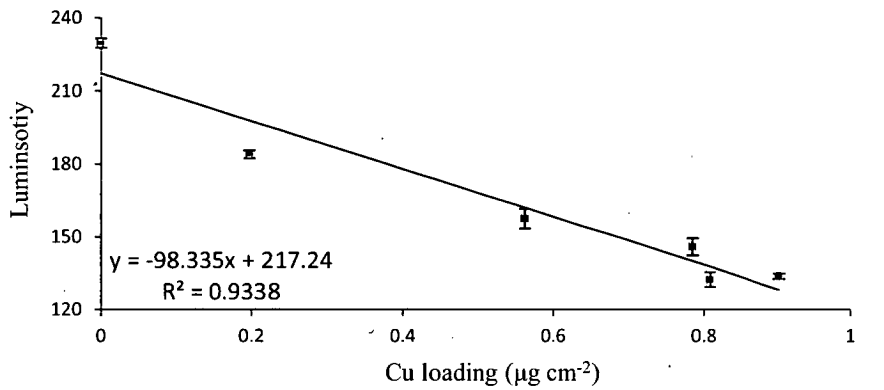

h) PAN - G channel

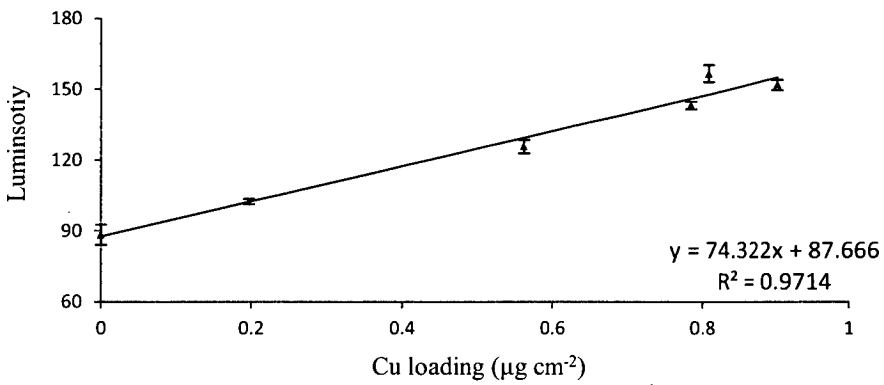

i) PAN - B channel

Figure 5.2 g, h and i – CID analysis of PAN binding phases. The range of luminosity values on the y-axis are consistently 120 to allow comparison of response. Loadings on the x-axis are AAS-GF observed, per disc.

Figure 2 continues overleaf

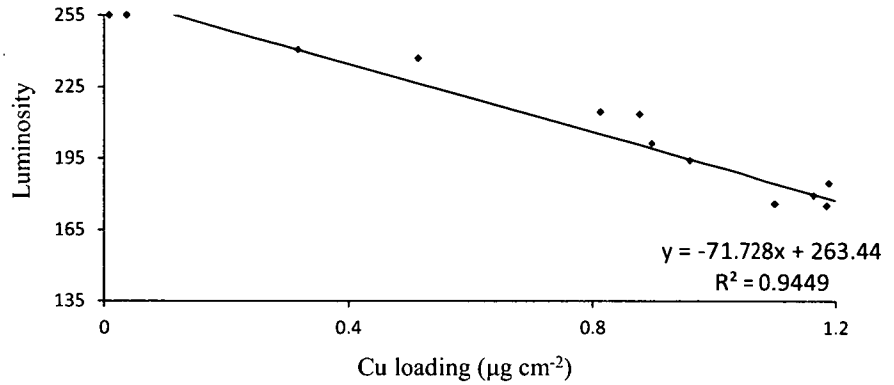

j) TAN - R channel

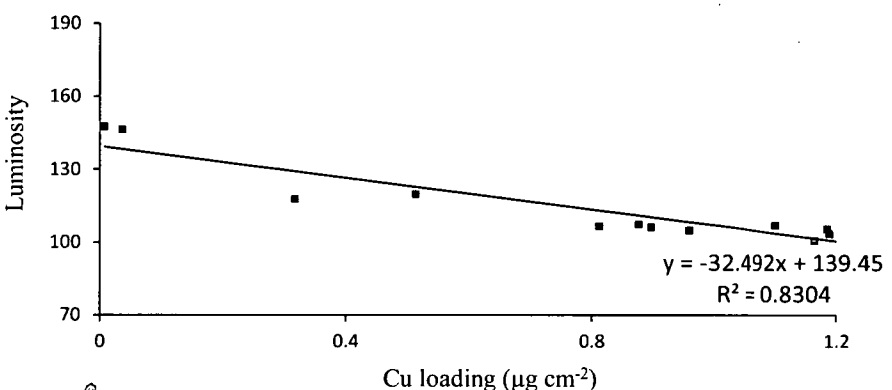

k) TAN - G channel

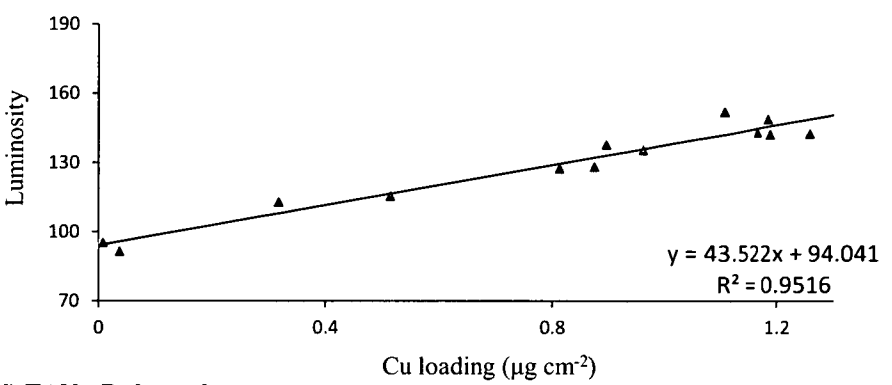

l) TAN - B channel

Figure 5.2 j, k and l – CID analysis of TAN binding phases. The range of luminosity values on the y-axis are consistently 120 to allow comparison of response. Loadings on the x-axis are AAS-GF observed, per disc.

2.6%. Results for TAN were similar, with a maximum response of -72 luminosity units per μg cm^{-2} of Cu(II) in the R channel.

Colorimetric results obtained using EBT provided linear relationships with regard to the extracted metal quantities, but with significantly lower responses. The maximum response seen with this dye of -20 luminosity units per μg cm^{-2} of Cu(II), in the G channel, would allow reasonable quantification considering an RSD of 13%, although in order to reliably accumulate a μg of Cu(II) the dye loading would need to be increased to 10 μmol g^{-1}. However, this response was less than that observed with PAN or TAN, or Zincon as discussed later, and as such EBT was not considered as suitable for use as a DGT binding phase as the other dyes examined.

The use of XO did not provide acceptable CID results in any channel, with a maximum response of -7 luminosity units per μg cm^{-2} of Cu(II) in the G channel and an RSD of over 50%. As such, XO binding phases would not be suitable for CID quantification. However, a clear visual change was seen when Cu(II) was complexed, so to further explore the response of XO the UV-Vis spectrum of these discs was examined. Using UV-Vis reflectance spectroscopy a maximum absorbance at 505 nm was found. It was thought that this was the reason that CID was not showing colour response, as this wavelength lies between the G and B channel wavelengths of approximately 570 nm and 450 nm, respectively [19]. When results at 505 nm were examined using UV-Vis reflectance the data in Figure 5.3 were obtained. These results show better quantitative ability, with a response of 2.2% reflectance per μg cm^{-2} of complexed Cu(II) and an average RSD of 18%, but are still not as precise as those displayed by other dyes.

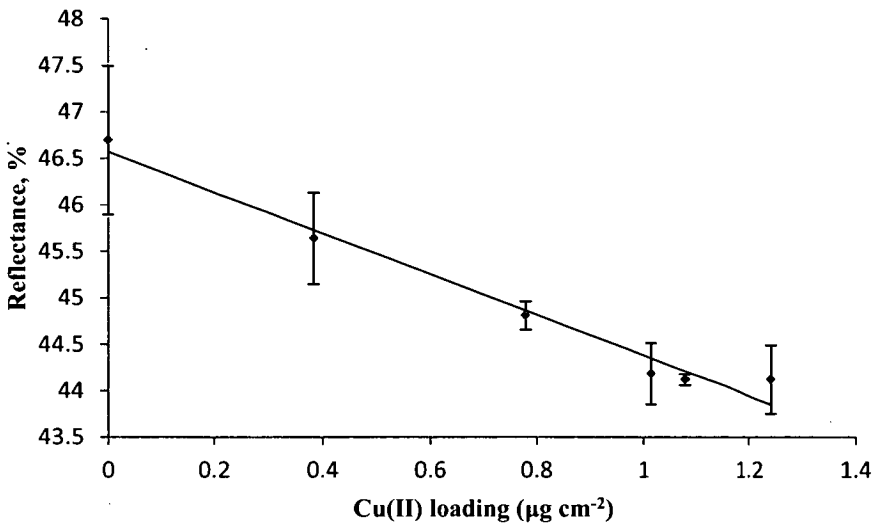

Figure 5.3 – UV-Vis reflectance colorimetry, at 505 nm, results of XO adsorbed binding phases exposed to Cu(II) solutions. Cu(II) loadings were determined from triplicate discs using AAS-GF.

The CID results for XO show the metameric failure situation that was discussed towards the end of Chapter 4. In this situation, the ability of the scanner to analyse the colour change was limited by the lack of light emitted in the frequency affected by Cu(II) complexation. By using diffuse reflectance, light of a correct wavelength could be employed, which made these discs assessable. As discussed in Chapter 4, it is unlikely that this will be a common failure when using visibly responding dyes; but this may be corrected through the use of CCD type scanners, or even other manufacturers' scanners which may employ LEDs of differing spectral properties.

The examination of these four dyes showed promising results with PAN and TAN. PAN showed interference from Zn(II), which is discussed in Appendix 2, but also showed the best Cu(II) response of all the dyes examined in this project. However,

these dyes were not further explored due to the use of CG-300c resin to create the binding phase. While this resin provided a plain white background, which is ideal for colorimetric work, the resin was not compatible with the polyacrylamide diffusive gel. During disassembly the binding phases were adhered to the diffusive gels, making removal of the diffusive gels before analysis very difficult. Further to this, removal of the diffusive gel typically resulted in damage to the binding phase, and this damage was responsible for the lack of combined triplicate data when TAN was assessed. This may be avoided by using a non-polyacrylamide diffusive layer, such as the paper layers assessed by Larner and Seen [20].

Another concern with the CG-300c based binding phases was that it was necessary to wet the resin with ethanol to allow water to interact with the dye. This led to a concern that leaching of ethanol during deployment would reduce the complexation abilities of the binding phase during deployment. As such, the CG-300c based binding phases had limitations in their ability to be used with DGT sampling.

5.3.4 – Exploring Zincon Performance

Zincon had shown selectivity towards Cu(II) in qualitative tests, during which none of the metals exposed to it had provided a colour change at a pH of 6.8, with the exception of Cu(II). Due to this, and that Zincon used Dowex 1x8 resin for adsorption, it was assessed in greater depth than the other dyes. Discs were made using Zincon adsorbed on to Dowex 1x8 resin, and triplicate discs were exposed to a Cu(II) concentration of 53.4 $\mu g\ L^{-1}$ over 24, 48, and 72 h. Further triplicate 24 hour exposures at Cu(II) concentrations of 108, 163, 217 and 271 $\mu g\ L^{-1}$ were also

performed. After exposure the discs were extracted and the extracts analysed using AAS-GF. The results for the varying concentrations over 24 h are shown in Figure 5.4a and results for the 72 hour period are shown in Figure 5.4b. Extraction efficiency was determined to be >99%, as the initial extract contained 7.58 μg of Cu(II) and no Cu(II) was observed in a secondary extract, where the detection limit would have allowed for quantities less than 0.05 μg to be observed.

Accumulated Cu(II) quantities were seen to increase in a linear fashion with increasing concentrations, and a good linear fit was obtained for metal uptake over time, providing an R^2 of over 0.95. These results show that the Zincon based binding phase was functioning well in simulated DGT deployment, even past a 50% molar loading of Cu(II) (at approximately 1 μg cm^{-2}).

The extracted metal loadings seen were 80% of those expected by use of the DGT equation, at the mean uptake temperature of 23.4°C (see Table 2, [21]; and [22]). While not as substantial as the reduction seen with MTB resin, the consistency of the decrease over the various tests shows this reduction was significant. A likely explanation for this is the swelling of the diffusive gel observed after cleaning the diffusive gels. These gels were not designed for repeated use, and a process of rinsing in 1 mol L^{-1} HCl and UHQ water was employed to ensure no trace metals remained within the gels after use so that they could be re-used. It was seen that this process, after approximately 10 cleaning cycles, resulted in an increased gel thickness, to over 1.1 mm. As this test was performed after several rinsing cycles it is reasonable to assume that this swelling accounted for the decrease in binding

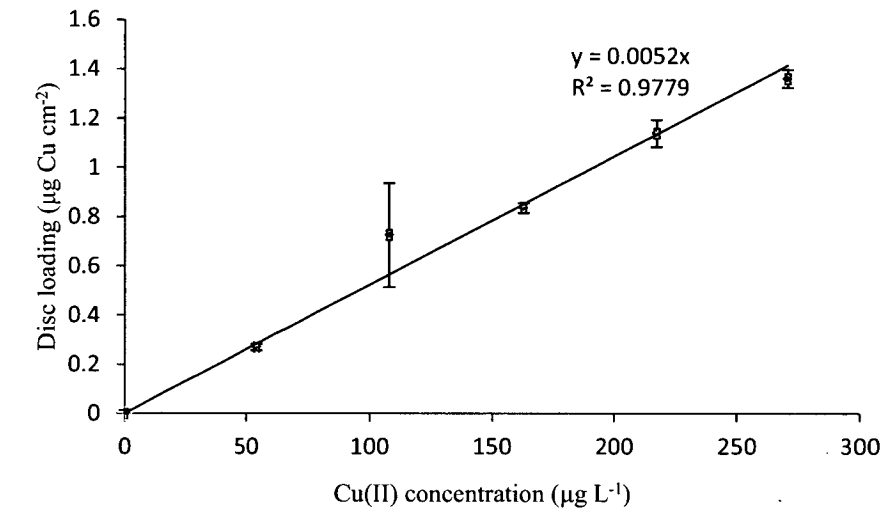

a) Cu(II) uptake vs. solution concentration

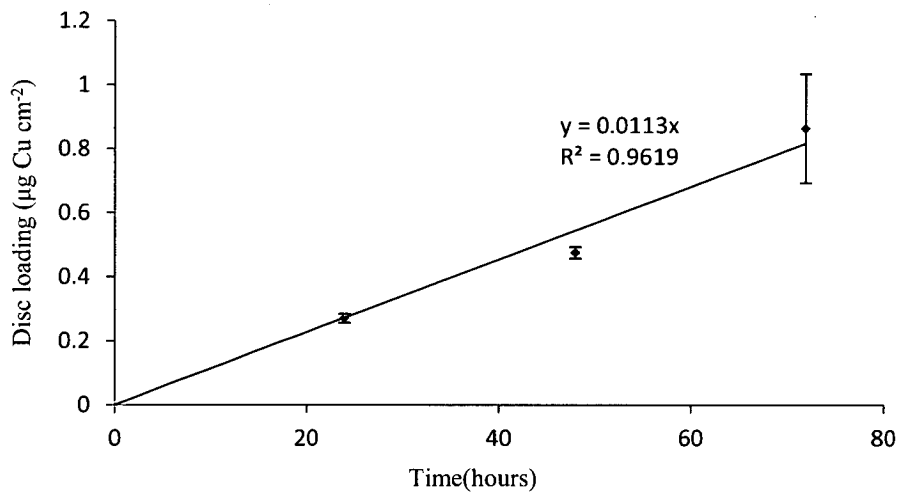

b) Cu(II) uptake vs. time

Figure 5.4 – Cu(II) uptake using discs of 10µmol g^{-1} Zincon dye immobilised on Dowex 1x8 resin. Cu(II) uptake over a concentration range is shown in (a), and Cu(II) uptake over three days is shown in (b).

phase Cu(II) uptake, as this 1.1 mm thickness observed would cause an apparent decrease in uptake of nearly 40%. The interaction of PO_4^{3-} with Cu(II) was not considered likely, as it had not been observed when PO_4^{3-} was examined with MTB (Chapter 3).

Figure 5.5 shows that the CID response of Zincon to Cu(II) was linear in all channels, with the largest response observed in the R channel. Above a loading of 1 μg cm^{-2} some loss of linearity was observed in the R channel, though sampling was not recommended beyond that loading due to the previously discussed concerns about the performance of kinetic-uptake passive sampling. As such it is further recommended that these samplers are not deployed past this loading of 1 μg cm^{-2} [18]. Luminosity response in the G and B channels followed a similar trend, with a smaller response in terms of luminosity units per μg cm^{-2}. The lowest average standard deviation of 1 luminosity unit was also observed using the R channel, with 3 and 2 units observed in the G and B channels, respectively. As such, analysis of Cu(II) adsorbed Zincon discs by CID was best performed using the R channel luminosity values, as this gave the least error at a RSD of 2% and the greatest response, being -55.9 luminosity units per μg cm^{-2} over the initial 1 μg cm^{-2}.

As Zincon based binding phases had shown promising Cu(II) selectivity they were examined further in order to assess the suitability of these discs for environmental deployment. The ability of the Zincon binding phases to sequester Cu(II) from seawater was assessed first, using 3 μm filtered natural seawater cleaned of metal contaminants by exposure to Chelex resin over 24 h. This water was used without ionic or pH buffering and with 177 μg L^{-1} of Cu(II) added for exposure over 24, 48,

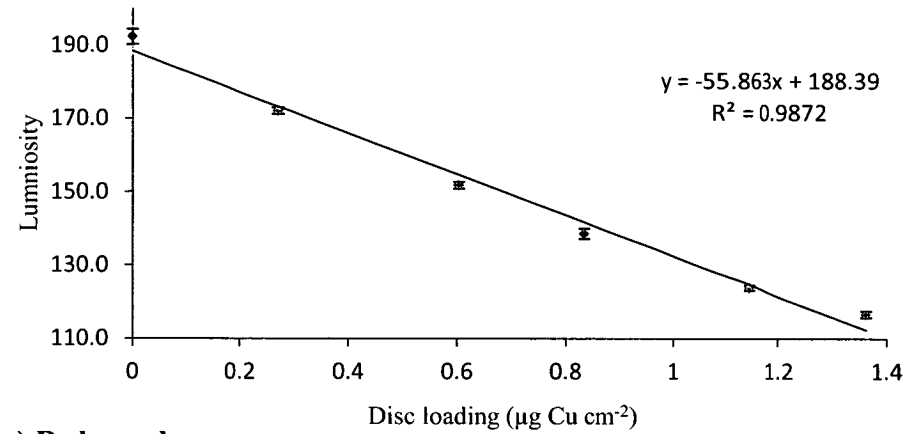

a) R channel

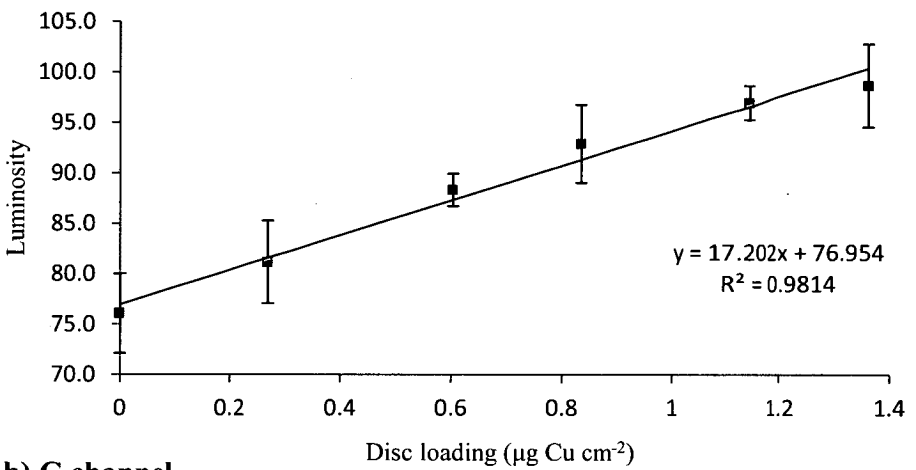

b) G channel

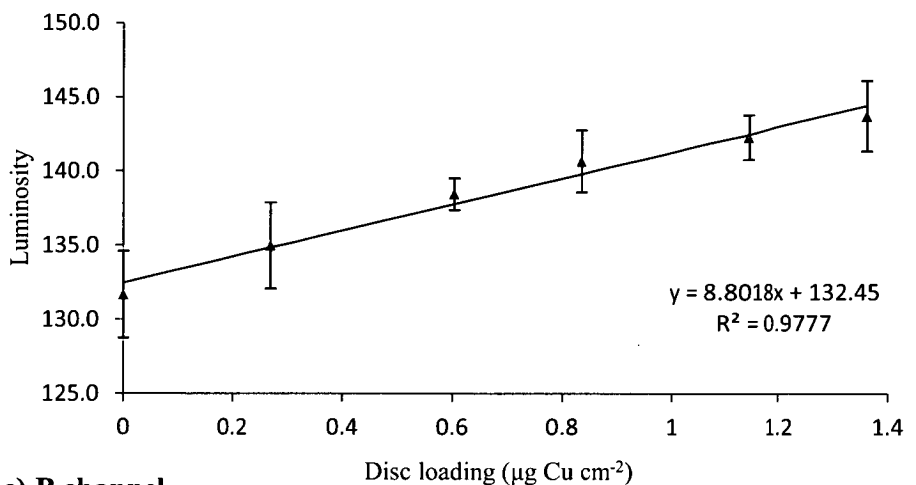

c) B channel

Figure 5.5 – Zincon luminosity response in the R, G and B channels after disc exposure to Cu(II).

and 72 h, with further 12 hour exposures at Cu(II) concentrations of 353, 530, 707 and 883 μg L^{-1}. Figure 5.6a shows that uptake of Cu(II) in the DGT binding phase was linear to solution concentration. Figure 5.6b shows linear uptake over time, and together Figures 5.6a and 5.6b show the required DGT performance.

Complexed Cu(II) quantities were 80% of that observed in the previous Zincon deployment, where loadings were also below expected, and hence the seawater Cu(II) quantities were 64% of those expected from the DGT equation. Due to this it appears that seawater is having an effect on the DGT accumulation of Cu(II) into a Zincon binding phase. The cause of this reduction may either be a reduction in the available Cu(II) fraction, potentially caused by complexation of Cu(II) by substances in the seawater matrix, or direct inhibition of the binding phase due to competing cationic species binding to the Zincon. A constant accumulation rate was observed, as seen by the linear trends in Figure 5.6, and therefore DGT function is predictable. As linear trends were observed the deployment of these devices as DGT samplers is possible in seawater, and the changes seen could be corrected for by applying equivalent diffusion coefficients calculated from the above experiment.

Quantification of loaded Cu(II) by CID was possible, with the relationship between luminosity and complexed Cu(II) shown in Figure 5.7. When calibrated in controlled solutions made from UHQ water, $NaNO_3$, and PO_4^{3-}, the R channel was observed to provide the best Cu(II) response, and this was also observed for seawater tests with a similar loss of linearity past 1 μg cm^{-2}. Comparison of the luminosity response observed in seawater to that observed under the more stringently controlled conditions are favorable, with R channel response under conditions of pH 6.8 and0.1 mol L^{-1} $NaNO_3$ providing -55.9 luminosity units

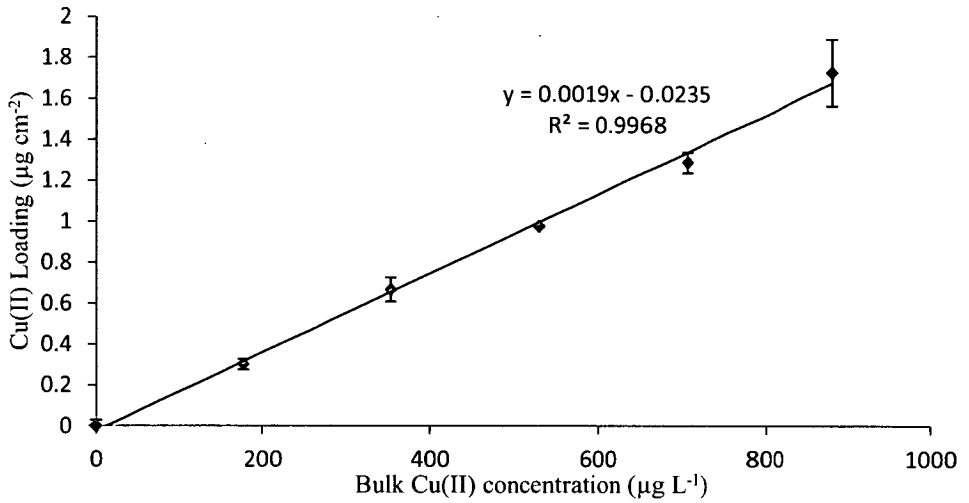

a) Cu(II) uptake vs. solution concentration

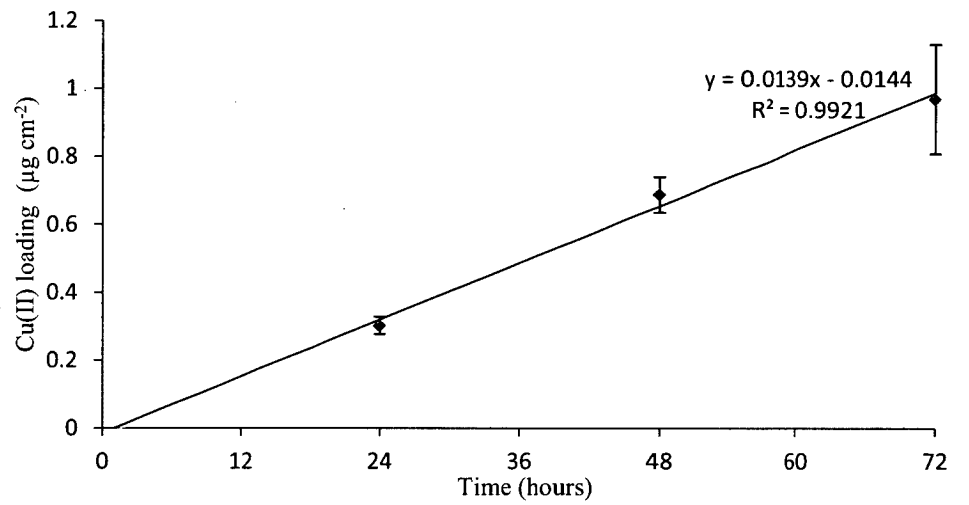

b) Cu(II) uptake vs. time

Figure 5.6 – Cu(II) uptake from seawater, using 10 µmol g^{-1} Zincon dye immobilised on Dowex 1x8 resin vs. time and solution Cu(II) concentration. The linear profiles show DGT performance is robust in a complex matrix. Cu(II) loadings are per disc, and were determined after 1 M HNO_3 extraction, using GF-AAS.

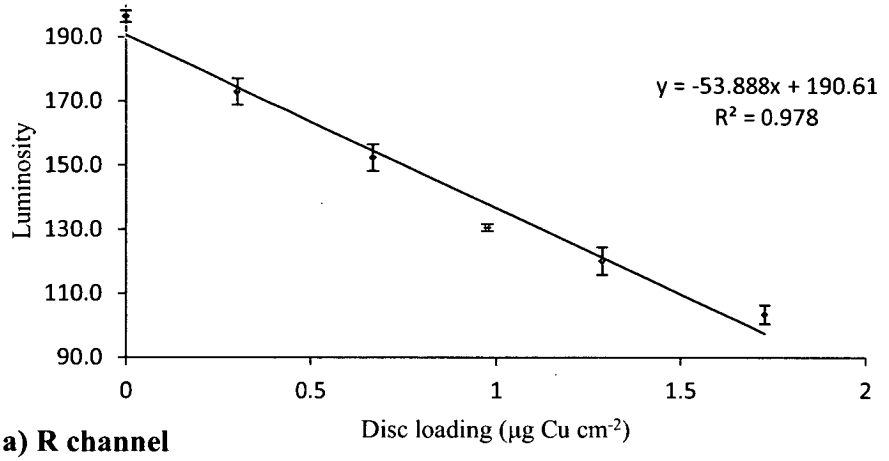

a) R channel

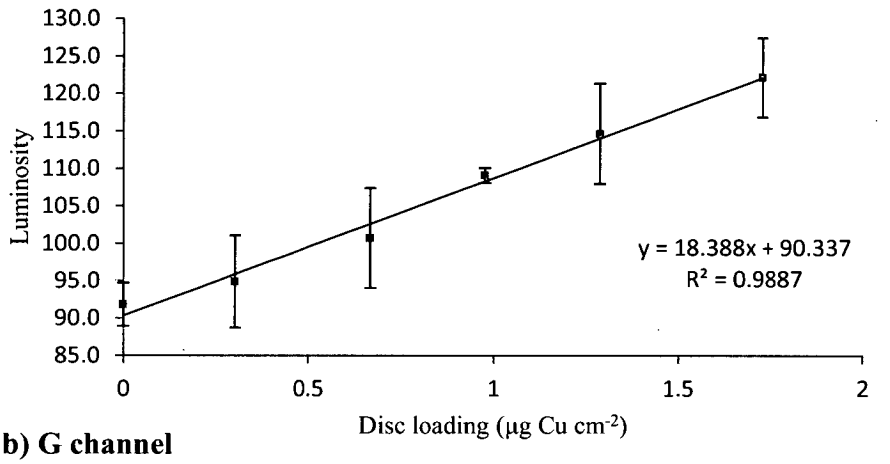

b) G channel

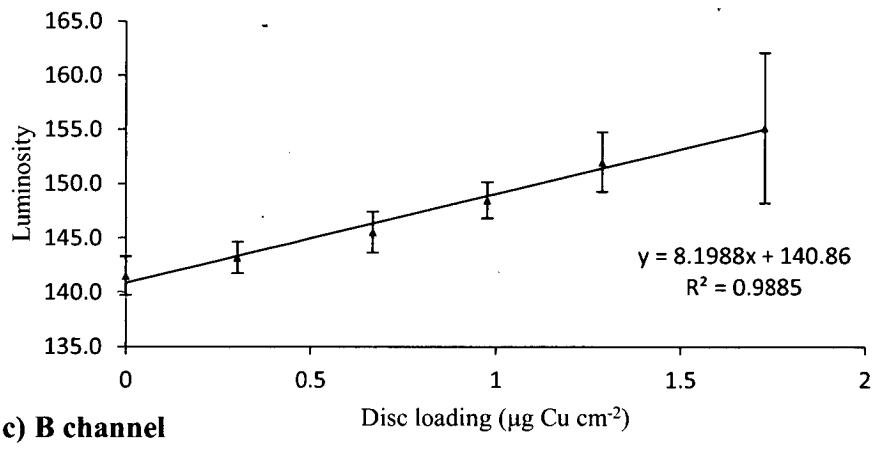

c) B channel

Figure 5.7 – CID response of Zincon discs to Cu(II) complexed from seawater.

per µg Cu(II), and seawater conditions providing -53.9 luminosity units per µg of Cu(II). In the B and G channels response varies by less than 10%, showing that the behavior of the colorimetric system in seawater is similar to that in a more controlled matrix, and, within reason, identical.

To test the applicability of this method, the UHQ water based calibration performed at first was used to quantify metal loadings on the seawater exposed discs, employing R channel values. These results were compared to the AAS-GF measured loadings from the seawater exposed discs, providing the data in Table 5.3. CID calculated loadings compared favorably with the AAS-GF observed loadings, both in terms of accuracy and precision. As such, even in a complex matrix such as seawater, Zincon discs were seen to perform well as colorimetric DGT binding phases for the quantification of Cu(II).

Considering the lack of a colorimetric change when exposed to the other metals tested, and the ability of Zincon binding phases to accumulate Cu(II), these discs are promising for environmental use. The selectivity tests performed were carried out at a pH of 6.8, and the seawater test was at an approximate pH of 7.5. The pH range represented here may well be exceeded during environmental deployment, and it is worth giving some consideration to the reported activity of Zincon across a broader pH range.

Richter et al. [23] studied Zincon immobilised on Sephadex A25 resin, an anion-exchange resin of cross-linked dextran matrix, employed for UV-Vis absorption

Table 5.3 – AAS-GF and CID loadings of Zincon binding phases exposed to Cu(II) in seawater.

Bulk Cu(II) conc. ($\mu g\ L^{-1}$)	176.6	353.2	529.8	706.4	883
AAS-GF loading ($\mu g\ cm^{-2}$)	0.30±0.03	0.67±0.06	0.976±0.003	1.28±0.05	1.7±0.2
CID 'R' loading ($\mu g\ cm^{-2}$)	0.27±0.03	0.64±0.03	1.03±0.03	1.22±0.05	1.5±0.1

analysis of Cu(II). They found that, at pH 7 and a wavelength of 621.5 nm, only Hg interfered with analysis of 50 $\mu g\ L^{-1}$ Cu(II), out of Hg, Cd, Ni, Zn, Fe and Pb at 100 $\mu g\ L^{-1}$ concentrations. At a lower pH of 5 Fe(II) was found to become an interference, and at a pH of 9 all the metals tested, with the exception of Fe, provided interference. Studies of Zincon immobilised in hydrophobic compounds other than resins have been performed, and have found that Cu(II) sensitivity remains a feature around neutral pHs [24,26]. However, in Oehme et al. [26] it was seen that Zn(II) does begin to provide a noticeable impact on the UV-Vis absorbance spectrum of this dye above 600 nm at a pH of 7.5. The spectrum below 600 nm remains unaffected, and as such Cu(II) analysis should still be possible at this wavelength using CID.

Zincon has shown Cu(II) selectivity at a pH of 6.8 and functions as a DGT binding phase in seawater matrices. Considering these points, and literature from studies similar to this one, it is believed that Zincon will provide a suitable colorimetric reagent for DGT binding phase use. By adsorption of Zincon onto Dowex 1x8 resin, and immobilisation of that resin using adhesive paper label discs, a cost-effective, selective, stable and precise binding phase can be created.

5.4 – Conclusion

A colorimetric reaction for Cu(II) has been shown to occur with a variety of metal indicating dyes after their adsorption onto a PSDVB based resin. This color response can be used to quantify metal loadings in a DGT system by employing the dye-adsorbed resins as a binding phase. Six dyes have been found to be approprtiate for this purpose out of the 19 assessed. Several dyes – DDTC, DPCO, DPCI and oCPC – were found to provide coloured responses that were unsuitable, due to either instability of the coloured complex or the long colour development period shown.

Of the dyes examined, Zincon was shown to provide good colorimetric response and also provided selectivity for Cu(II) at pH 6.8 in UHQ water based solutions. Zincon was shown to be suitable to quantify Cu(II) in seawater matricies, with the binding phase capable of colorimetrically quantifying Cu(II) concentration in seawater using an UHQ water calibration. As such, it is belived that a DGT system employing Zincon as a binding and colorimetiric reagent, and Dowex 1x8 as an immobilisation substrate, would be well suited to passive analysis of marine Cu(II) levels. The selectivity of this system may be of benefit where inteferences are present in high conentrations, as low Cu(II) concentrations could still be quantified. A further advantage is that the cost of this system, from raw materials to data collection, is substantially less expensive than the currently employed DGT methods.

References

[1] K. Ueno, T. Inamura, K.L. Cheng, Handbook of Organic Analytical Reagents, CRC Press, 1992.

[2] P. Thuery, M. Nierlich, V. Lamare, J. Dozol, Z. Asfari, J. Vincens, Journal of Inclusion Phenomena and Macrocyclic Chemistry, 36 (2000) 375.

[3] C.J. Pederson, Journal of the American Chemical Society, 89 (1967) 2495.

[4] E. Bakker, P. Buhlmann, E. Pretsch, Chemical Reviews, 97 (1997) 3083.

[5] G.W. Gokel, W.M. Leavey, M.E. Weber, Chemical Reviews, 104 (2004) 2723.

[6] M.R. Ganjali, H.A. Zamani, P. Norouzi, M. Adib, M. Rezapour, M. Aceedy, Bulletin of the Korean Chemical Society, 26 (2005) 579.

[7] M.H. Mashhadizadeh, I. Sheikhshoaie, S. Saeid-Nia, Electroanalysis, 17 (2005) 648.

[8] M. Shamsipur, M.H. Mashhadizadeh, Talanta, 53 (2001) 1065.

[9] M.A. Akl, A.K. Ghoneim, M.H. Abd El-Ziz, Electroanalysis, 18 (2006) 299.

[10] C.J. Farhni, T.V. O'Halloran, Journal of the American Chemical Society, 121 (1999) 11448.

[11] T. Gunnlaugsson, T.C. Lee, R. Parkesh, Organic and Biomolecular Chemistry, 1 (2003) 3265.

[12] K. Guzow, M. Milewska, D. Wrolewski, A. Gieldo, W. Wickz, Tetrahedron, 60 (2004) 11889.

[13] R. Maellet-Renault, A. Herault, J.J. Vachon, R.B. Pansu, S. Amigoni-Gerbier, C. Larpent, 5, 3 (2006).

[14] H. Zhang, W. Davison, Analytical Chemistry, 67 (1995) 3391.

[15] K.W. Warnken, H. Zhang, W. Davison, Analytical Chemistry, 77 (2005) 5440.

[16] H. Zhang, W. Davison, S. Miller, W. Tych, Geochimica et Cosmochimica Acta, 59 (1995) 4181.

[17] M.L. Marina, V. Gonzalez, A.R. Rodriguez, Mircochemical Journal, 33 (1986) 275.

[18] G. Ouyang, J. Pawliszyn, Journal of Chromatography A, 1168 (2007) 226.

[19] LEDtronics, Discrete & SMT Rating and Characteristic Curves. 1999.

[20] B.L. Larner, A.J. Seen, Analytica Chimica Acta, 539 (2005) 349.

[21] H. Zhang, DGT summary. DGT Research Ltd. 2003.

[22] W. Davison, H. Zhang, Nature, 367 (1994) 546.

[23] P. Richter, M.I. Toral, H. Castro, Analytical Letters, 35 (2002) 635.

[24] I. Oehme, B. Prokes, I. Murkovic, T. Werner, I. Klimant, O.S. Wolfbeis, Fresenius Journal of Analytical Chemistry, 350 (1994) 563.

[25] DGT Research, DGT –for measurements in waters, soils and sediments. 2003.

[26] I. Oehme, S. Prattes, O.S. Wolfbeis, G.J. Mohr, Talanta, 47 (1998) 595.

Conclusion

Through the application of colorimetric chelating agents it has been possible to construct a DGT binding phase that is capable of accurately assessing Cu(II) concentrations in complex matrices through colour change alone. In order to make this binding phase function correctly it was necessary to first immobilise the reagent, then to craft the immobilised reagent into a binding phase, and then to assess the ability of the newly minted binding phase to perform in a DGT device. Once function was understood colorimetric methods were examined, followed by an expansion of the technique through examination of a wider range of reagents.

Immobilisation of the reagent was examined using adsorption, ion-exchange, and chemical grafting techniques. Literature review and laboratory tests showed that the adsorption of the reagent onto an ion-exchange resin with a hydrophobic matrix was most suitable. This immobilisation method could be reinforced by ion-exchange occurring between ionic reagents and the ion-exchange groups of these resins. Further to this, the ion-exchange groups allowed for effective wetting of the binding phase, necessary for interaction of the reagent with the bulk solution. A binding phase could then be created from this resin-adsorbed reagent by adhering the resin to commercial paper labels. These labels were robust in water and provided a highly reflective background, which was ideal for colorimetric work.

The use of MTB, a readily available colorimetric metal indicating dye, allowed for the prototyping of the binding phase system for analysis of Cu(II). Using this dye Cu(II) was seen to bind in a 1:1 ratio to MTB, with Zn(II) and Fe(II) also being seen to bind. Function as a DGT binding phase was assessed by examining metal

complexation from bulk solution over a range of concentrations during a fixed period of time, and over several time periods at a fixed concentration.

Colorimetric ability was assessed through the use of UV-Vis reflectance as a colour change, and hence bound metal, quantification method. This provided acceptable results and detection limits of less than a μg of bound Cu(II) per disc. The application of CID, involving a commercial flat-bed scanner and photo manipulation software, to colour analysis provided more consistent results than UV-Vis analysis. CID also proved more flexible than UV-Vis reflectance, requiring only a small scanner and a laptop for data collection. Due to these factors CID was considered a more suitable method than UV-Vis reflectance for colorimetric analysis.

A selection of indicator dyes (Appendix 1) was then trialed, as well as a hydrophobic resin without ion-exchange groups. As no classes of colorimetric metal chelating reagents were considered to be as appropriate as indicator dyes no other reagents were trialed. The majority of dyes trialed were seen to have Cu(II) responses, and several were also seen to have Zn(II) and/or Fe(II) response. Of these dyes Zincon was found to have a high selectivity towards Cu(II) at neutral pHs, and also performed well in a seawater matrix.

As such, the use of indicator dyes as colorimetric reagents for use in DGT binding phases has been shown to be possible, with quantification using either UV-Vis reflectance or CID analysis. Further studies into Cu(II) analysis using this technique would be recommended to use Zincon immobilised onto Dowex 1x8 resin. An examination of further indicator dye compounds could provide dyes with selectivity towards other analytes of interest. Expanding of the tested reagents to include

calixarene or fluorometric compounds may yield highly selective compounds to be employed in the above fashion, but as the majority of these compounds have not been examined in the context of colorimetric response and/or long-term stability this would be a substantial project.

In summary, the use of colorimetric binding phases is capable of providing DGT results comparable to those obtained through the current extraction and physical analysis methods, but in less time and at less expense.

Appendix 1 – Dyes Examined

APDTC

Ammonium pyrrolidine dithiocarbamate

LR Grade, BDH, Poole, England
Solution in Acetone

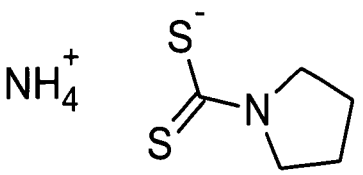

Adsorption details:

Solvent:	Acetone
Solvent pH:	N/A
Resin:	CG-300c

BPhen

Bathophenanthroline

Purissa p.a. 99%+, Fluka, Buchs, Switzerland
Solution in iso-propyl alcohol

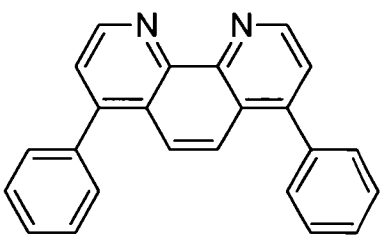

Adsorption details:

Solvent:	Isopropyl alcohol
Solvent pH:	N/A
Resin:	CG-300c

Cadion

Grade not stated, Hopkin & Williams, Chadwell Heath, England

Solution in water

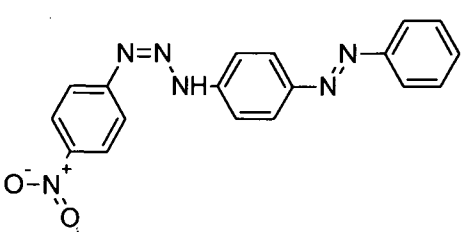

Adsorption details:

Solvent:	Water
Solvent pH:	not adjusted
Resin:	Dowex 1x8

CAS

Chrome azurol S

Indicator Grade, 65% +, Aldrich, Milwaukee, U.S.A.
Solution in water

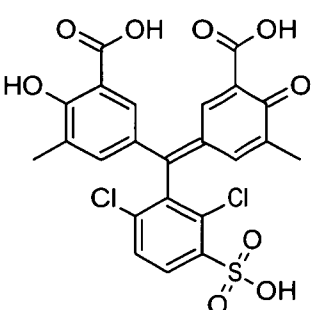

Adsorption details:

Solvent:	Water
Solvent pH:	not adjusted
Resin:	Dowex 1x8

Cupferron

AnalaR, Sigma, St. Louis, U.S.A.
Solution in water

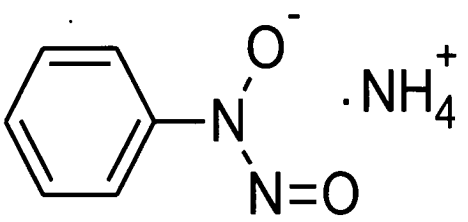

Adsorption details:

Solvent:	Water
Solvent pH:	2
Resin:	Dowex 1x8

DeDDTC

Diethylamino diethyldithiocarbamate

GPR Reagent, BDH, Poole, England
Solution in water

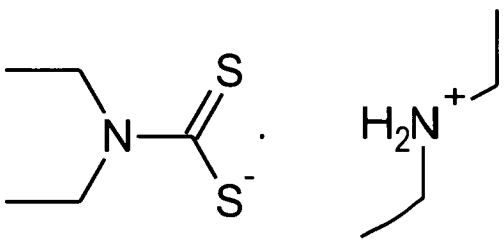

Adsorption details:

Solvent:	Water
Solvent pH:	4-7
Resin:	Dowex 1x8

DMG

Dimethyl glyoxime

AnalaR, 98% +, BDH, Poole, England
Solution in Ethanol

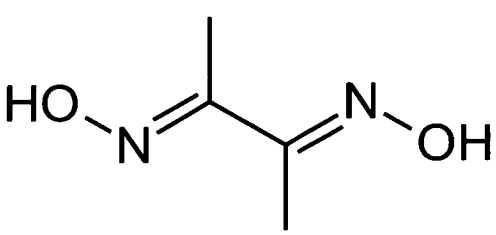

Adsorption details:

Solvent:	Ethanol
Solvent pH:	N/A
Resin:	CG-300c

DPCI

Diphenyl carbazide

Grade not stated, Hopkins & Williams, Chadwell Heath, England
Solution in ethanol

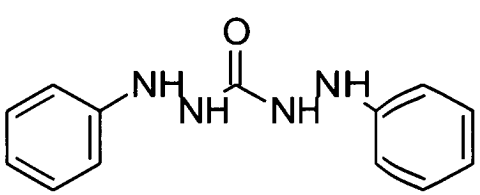

Adsorption details:

Solvent:	Ethanol
Solvent pH:	N/A
Resin:	CG-300c

DPCO

Diphenyl carabazone

Grade not stated, 5mg per tablet, Hopkins & Williams, Chadwell Heath, England

Solution in ethanol

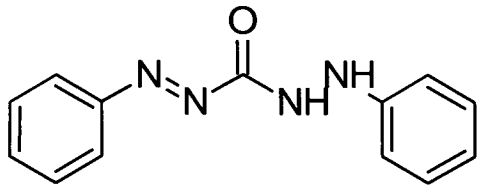

Adsorption details:

Solvent:	Ethanol
Solvent pH:	N/A
Resin:	CG-300c

DT

Dithizone

AR Grade, 99%, BDH, Poole, England
Solution in acetone

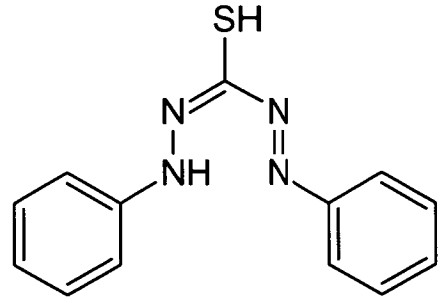

Adsorption details:

Solvent:	20%Acetone / 80% IPA
Solvent pH:	N/A
Resin:	CG-300c

EBT

Eriochrome Black T

Grade not stated, Sigma, St. Louis, U.S.A.
Solution in water

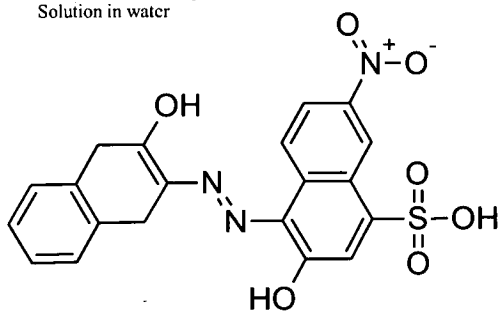

Adsorption details:

Solvent:	Water
Solvent pH:	9
Resin:	Dowex 1x8

MTB

Methylthymol Blue

Indicator grade, Riedel-de Haën, Seelze, Germany
Solution in water

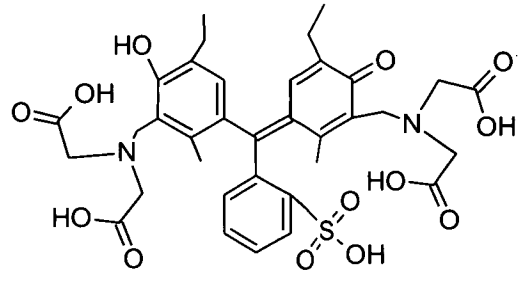

Adsorption details:

Solvent:	Water
Solvent pH:	2 or 10
Resin:	Dowex 1x8

oCPC

ortho-cresolphthaline complexone

LR Grade, Aldrich, Milwaukee, U.S.A.
Solution in water

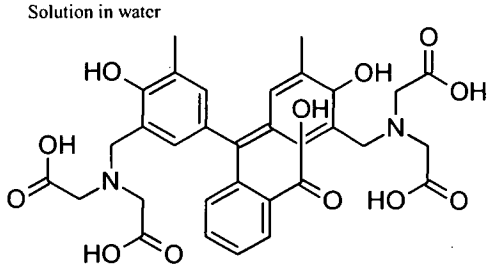

Adsorption details:

Solvent:	Water
Solvent pH:	1
Resin:	Dowex 1x8

Alternate Adsorption details:

Solvent:	Isopropyl alcohol
Solvent pH:	N/A
Resin:	CG-300c

PAN

1-(2-pyridylazo)-2-naphthol

LR Grade, BDH, Poole, England
Solution in ethanol

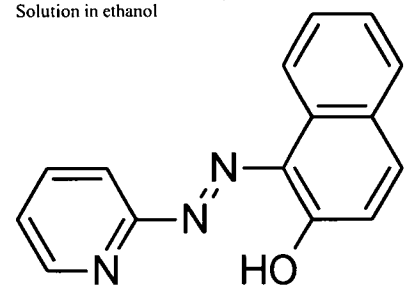

Adsorption details:

Solvent:	Ethanol
Solvent pH:	N/A
Resin:	CG-300c

TAN

1-(2-thiazolylazo)-2-naphthol

Purissa p.a. 99%+, Fluka, Japan
Solution in ethanol

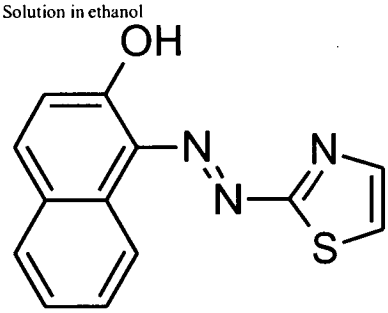

Adsorption details:

Solvent:	Acetone
Solvent pH:	N/A
Resin:	CG-300c

XO

Xylenol Orange

LR Grade, BDH, Poole, England
Solution in water

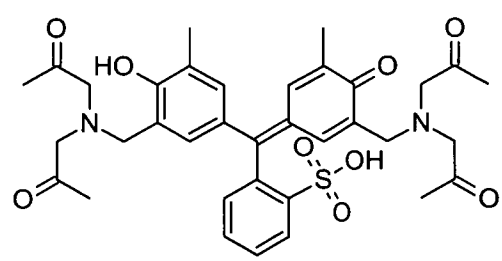

Adsorption details:

Solvent:	Water
Solvent pH:	2
Resin:	Dowex 1x8

PCV

Pyrocatechol Violet

Indicator Grade, 90%+, Aldrich, Milwaukee, USA
Solution in water

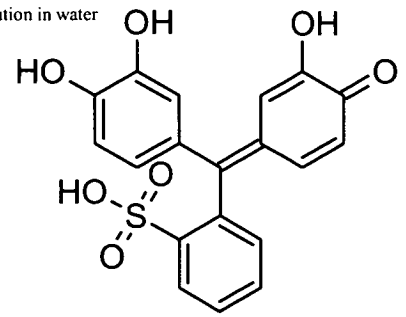

Adsorption details:

Solvent:	Water
Solvent pH:	2
Resin:	Dowex 1x8

Zincon

Grade not stated, Sigma, St. Louis, U.S.A.
Solution in water

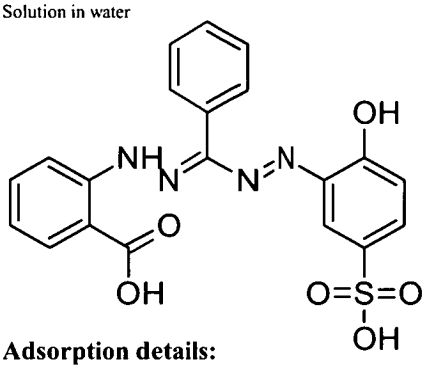

Adsorption details:

Solvent:	Water
Solvent pH:	2
Resin:	Dowex 1x8

Appendix 2 – Zinc response in PAN and XO

Experimental

The resin immobilisation of PAN and XO is covered in the Chapter 5 experimental section. Homogeneous colouration was achieved using acid-washed aqueous DGT sampling devices (DGT Research Ltd., Lancaster, UK) with 0.82 mm polyacrylamide diffusive gels (DGT Research Ltd., Lancaster, UK) and two vinyl spacers (0.3 mm). Samplers were assembled immediately before exposure while wet with 0.01M phosphate buffer and placed in 200 ml polycarbonate containers (Sarsteadt, Ingle Farm, Australia). Exposure solutions contained 0.1 M $NaNO_3$ and 0.01 M phosphate buffer of pH 6.8 cleaned with Chelex 100 (Sigma, Munich, Germany) to remove transition metals, along with Zn(II) concentrations of 290, 580, 870, 1160 and 1450 $\mu g\ L^{-1}$ for 4 hour exposures, and 290 $\mu g\ L^{-1}$ for the 8 and 12 h exposures.

After exposure the discs were removed from the sampler, and in the case of PAN discs were wet with ethanol before having the diffusive gels removed. Discs were scanned and luminosity values collected before being extracted. Metal extraction was performed by placing dried, exposed resin discs in a 70 mL polycarbonate container (Sarstedt, Ingle Farm, Australia) and adding 10.00 mL of 1 M HNO_3 (from 69% w/v Suprapur, Merck, Darmstadt, Germany). Weights were recorded at each step to obtain accurate volumes. Extraction solutions were shaken for 24 h on a Lab Line Orbit shaker before supernatants had 40 mL of ultrapure water added for analysis. Extraction efficiency tests were performed by repeating this process on extracted discs of the highest metal loading.

Initial Zn(II) analysis was performed using a SpectrAA 800 (Varian, Melbourne, Australia) AAS with GTA-95 graphite furnace attachment (AAS-GF) and autosampler. Sampling conditions used for Zn(II) were, in terms of temperature in °C(time in s): 85(5), 95(40), 120(10), 300(8), 1900(4.8) at 213.9 nm. Calibration was by prepared standard Zn(II) solutions auto-mixed to provide an equivalent matrix through a concentration range of 10 to 250 $\mu g\ L^{-1}$. Consistently high Zn(II) readings were obtained for the SpectraAA obtained results, and extracts were re-analysed on a GBC XplorAA instrument with a GF 3000 graphite furnace attachment and a PAL autosampler. A modified temperature profile: : 20(12), 90(10), 120(35), 600(15), 600(2, no gas), 1800(3.5, no gas), 1800(2) was used to obtain improved results, but high blanks were still observed along with highly variable replicate extracts.

Results and Discussion

Amongst those dyes tested both PAN and XO showed a colour change on exposure to zinc. Figure A1.1 shows discs scanned from an exposure test at increasing Zn(II) concentrations for both dyes. It can be seen that coloration of the exposed disc portion is increasing with an increasing solution concentration. This showed that the samplers were functioning correctly, but to confirm this function Zn(II) loadings were quantified. Extractions were undertaken but showed high Zn(II) levels in the blanks and highly variably replicate extracts, believed to be due to contamination. Due to time and equipment constraints these exposure tests were not repeated.

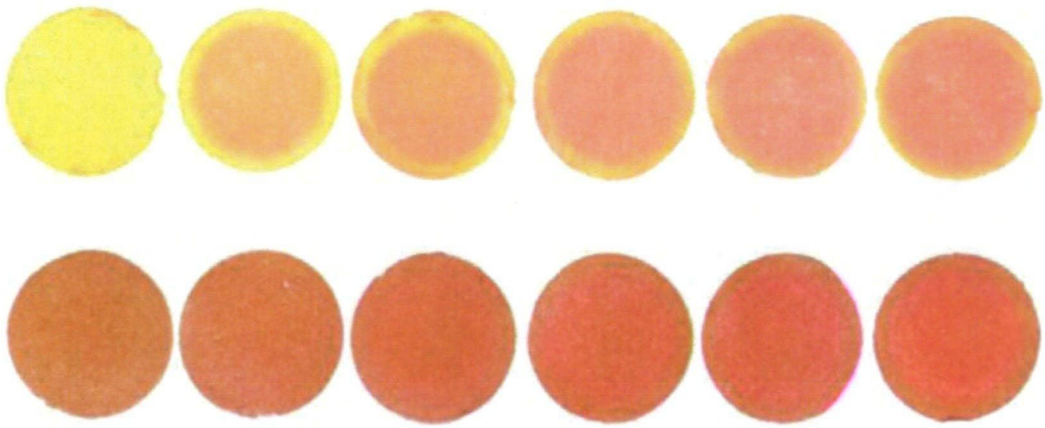

Figure A1.1 – PAN (upper) and XO (lower) discs after exposure to Zn(II) solutions in an aqueous DGT sampler with diffusive gels, Zn(II) concentration increasing to the right. Note the increasing coloration of the exposed area as Zn(II) concentration increases.

However, the results from CID measurement can be used to show the function of these binding phases, both chemically and in terms of DGT deployment. A comparison of the luminosity of these discs to solution Zn(II) concentration shows that some DGT performance was provided (Figure A2.2). A clear linear trend can be seen between G channel luminosity and solution concentration for XO, indicating that the discs were functioning appropriately as a DGT binding phase for the colorimetric detection of Zn(II). PAN shows a loss of linearity by 100 $\mu g\ L^{-1}$, which may be due to maximum loading being obtained, but this is not observable without extraction results. If so, this decrease would be due to effectively half-of-expected capacity resulting from the $Zn(PAN)_2$ complex being formed, which is noted in the *Handbook of Organic Analytical Reagents [1]* to be readily extracted from aqueous to non-polar solvents. Considering the non-polar resin being used it seems likely that

this compound would be formed on the resin surface. The $Zn(PAN)_2$ complex is noted as red-violet, fitting with observation of the discs, and is reported to have a wavelength of maximum absorbance of 555 nm. This fits well with the greater response seen in the G channel rather than the B channel.

However, due to the lack of extraction results the applicability of these binding phase to Zn(II) analysis cannot be determined thoroughly. However, these results do clearly show that, with correct dyes, the system is applicable to metals other than Cu(II).

[1] K. Ueno, T. Inamura, K.L. Cheng, Hanbook of Organic Analytical Reagents, CRC Press, 1992.

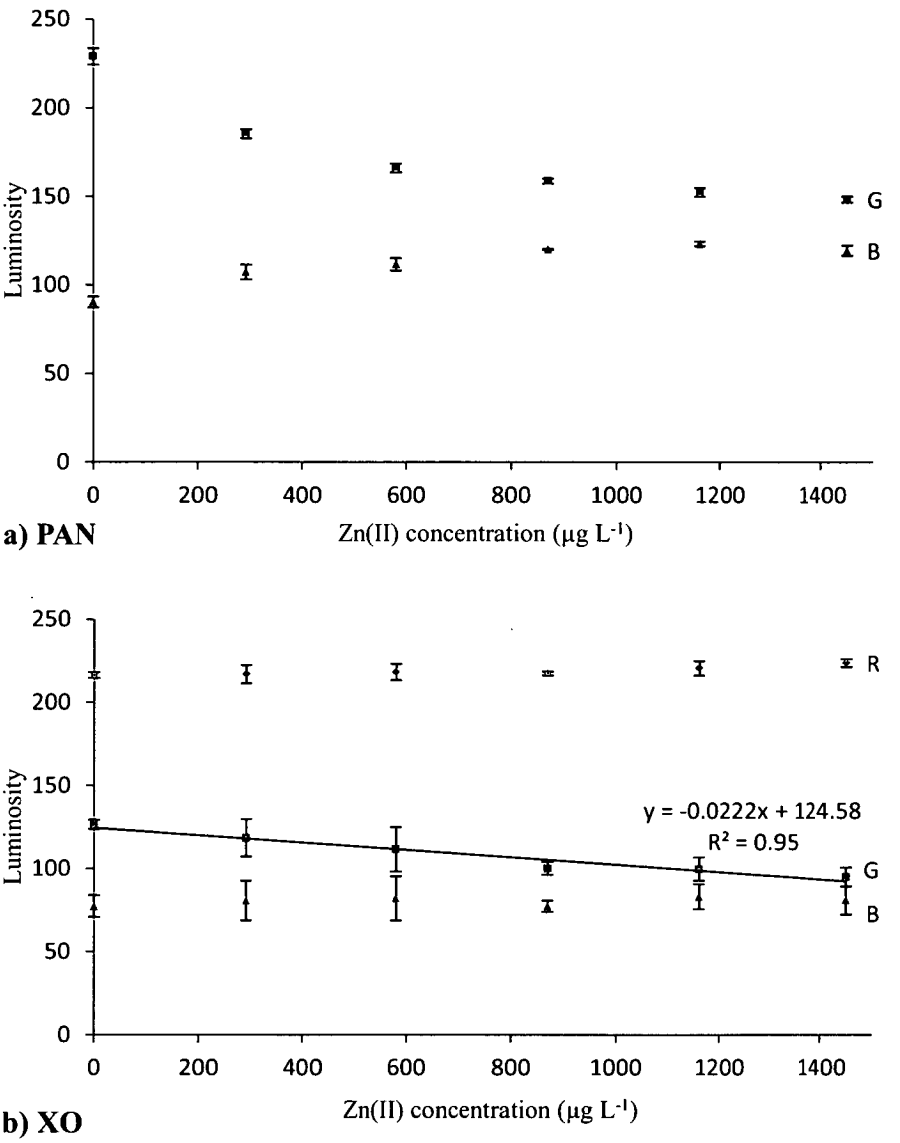

Figure A2.2 – Zn(II) CID results showing linearity of bulk concentration vs. luminosity for XO, and for the low concentrations using PAN. DGT function appears to be robust in XO when Zn(II) is assessed.